A Theoretical Model of the Kraft Pulping Process

by

Richard Roy Gustafson

A dissertation submitted in partial fulfillment
of the requirements for the degree of

Doctor of Philosophy

University of Washington

1982

Approved by _____
(Chairperson of Supervisory Committee)

Program Authorized
to Offer Degree Chemical Engineering

Date 6/28/82

University of Washington

Abstract

A THEORETICAL MODEL OF THE KRAFT PULPING PROCESS

By Richard Roy Gustafson

Chairperson of the Supervisory Committee: Charles A. Sleicher

Department of Chemical Engineering

A theoretical model of a batch kraft pulp digester is developed that predicts, a priori, the lignin content distribution, the carbohydrate content distribution, and the effective alkali concentration distribution within pulp chips as a function of cooking time. From this information the kappa number, yield, screen rejects, and kappa number distribution of the pulp are calculated. The model also predicts the bulk phase effective alkali concentration as a function of cooking time. Input to the model are the initial hydroxyl concentration and sulfide concentration, the chip-thickness distribution, the temperature history of the cook, and the chemical composition and density of the species of wood to be pulped.

Model predictions are compared with data from pulping experiments in which the reaction rates are kinetically controlled and with experiments in which the diffusion rate restricts the overall reaction rates. In both cases the comparison is good.

Model results show that the normalized second moment of the lignin content is a better predictor of rejects than the fiber liberation point. Results also show that in indirect heated batch digesters the inter-chip mass transfer resistence is negligible.

The pulping model is coupled with an optimization scheme to find the optimum pulping conditions. One result of the optimization is that an increase in productivity of 19 % can be obtained by optimization of the effective alkali concentration in a kraft cook.

The effect of digester temperature gradients on the lignin content distribution of a pulp is shown to be significant, but the effect on screen rejects is negligible. Stratifying the chip by thickness to take advantage of temperature gradients is found to narrow the lignin content distribution, but has no effect on the screen rejects of a cook.

Doctoral Disseration

In presenting this disseration in partial fulfillment of the requirements for the Doctoral degree at the University of Washington, I agree that the Library shall make its copies freely available for inspection. I further agree that extensive copying of this disseration is allowable only for scholarly purposes, consistent with "fair use" as prescribed in the U.S. Copyright Law. Requests for copying or reproduction of this dissertation may be referred to University Microfilms, 300 North Zeeb Road, Ann Arbor, Michigan 48106, to whom the author has granted "the right to reproduce and sell (a) copies of the manuscript in microform and/or (b) printed copies of the manuscript made from microform."

Signature_____

Date_____

TABLE OF CONTENTS

LIST OF FIGURES

LIST OF TABLES

ACKNOWLEDGMENTS

I wish to express my appreciation to Professors Sleicher, McKean, Finlayson, Sarkanen, and Ricker for their help and guidance in this project. In addition, special thanks to Dr. Amar Neogi of the Weyerhaeuser Co. for the financial support and technical assistance for this project. Finally, I wish to thank my wife, Cheryl, for her patience, understanding, and support throughout our graduate studies.

CHAPTER 1

PURPOSE OF THE PROJECT

The kraft pulping process, introduced in 1879, is the dominant pulping process today and is to likely remain so for the near future. Approximately 35 million tons of kraft pulp (Pulp and Paper International, 1982) are produced in the United States alone. Despite its age and wide spread use, the production of kraft pulp is still very much an art. This dissertation describes a study done to improve the science of kraft pulping.

1.1 Purpose and scope of the project

Throughout the chemical industry, theoretical, physically realistic models are used to aid in the design and operation of reactors. In the pulp industry, reactor designs and operation policies generally are based on the experience of the designer and

the current popularity of a given design, with little regard for the specifics of the mill being built. If a model is used in a digester design, it is an empirical one based on data from laboratory scale experiments. In the great majority of these experiments the digesters are well stirred and the chips uniform in size and composition.

Commercial digesters are neither well stirred, nor are commercial chips uniform in size and composition; therefore, extrapolating laboratory scale results to a commercial scale is tenuous. Because running experiments on commercial scale units is impractical, a model is needed to combine the laboratory data with transport equations to simulate the commercial batch digester. As will be discussed in Section 2.3, current digester models are indequate for this purpose.

The primary purpose of this project, therefore, is to develop and apply a theoretical model of a batch kraft pulp digester that may be used as a rational basis for designing new digesters, and setting operating policies. The model will combine kinetic and transport equations to predict, a priori, the chemical composition of the chip phase and bulk liquid phase as functions of cooking time. From the chemical compositions, the kappa number, yield, screen rejects, screened yield, and kappa distribution of the pulp may be calculated, as well as the residual alkali concentration. It

should be noted that the knowledge of kraft pulping chemistry and transport properties in wood are insufficient to permit development of a model that predicts quantitatively the properties of a pulp produced from any wood species with any cooking conditions. The model will, however, accurately predict trends in pulp properties, and provide a framework in which specific equations for a given species and digester may be input to simulate quantitatively that system over a wider range of operating conditions than could be done with an empirical model. Discussion of the model development and the verification of the model is given in Chapters 3 - 5.

One good way to use the model in designing digesters and setting operating conditions is to couple the model with an optimization scheme. A discussion of how this is done and the results of two specific optimizations, one the maximization of productivity and the other the minimization of screen rejects, is given in Chapter 6.

A good digester model should predict the uniformity of a pulp. Pulp non-uniformities increase operating costs of the entire paper making process, and reduce the quality of the final paper. Pulp non-uniformity results from non-uniformities in the raw material input to the mill, and non-uniformities in the pulping process itself. Little can be done to reduce the effect of raw material non-uniformity. Sources of pulp non-uniformity in the pulping

process include over-sized chips, digester temperature gradients, liquor channeling, and variation in operating conditions from cook to cook. Much has been said qualitatively about pulp non-uniformity; however, more quantitative information on the sources and extent of pulp non-uniformity is needed.

The secondary purpose of this project, therefore, is to investigate the extent and nature of pulp non-uniformity. Specifically, the two sources of non-uniformity studied are over-sized chips and digester temperature gradients. The two measures of non-uniformity used in the study are the screen rejects and lignin content, or kappa, distribution of the pulp. Results of the investigation on the effect of over-sized chips on screen rejects are given in Section 5.3. Results of the investigation on the effect of digester temperature gradients on screen rejects and the lignin content distribution are given in Chapter 7.

The other chapters in the dissertation are Chapter 2, which provides background on kraft pulping and a review of previous kraft pulping models, and Chapter 8, which summarizes the major conclusions of this research and recommends future work.

CHAPTER 2

BACKGROUND AND LITERATURE SURVEY

To understand the modeling results presented in later chapters, some knowledge of the kraft pulping process is neccesary. In this chapter wood anatomy, wood composition, the kraft pulping process, and pertinent properties of the pulp are briefly reviewed.

Because the great majority of pulp produced comes from coniferous wood, and because their pulping characteristics are better understood than those of the hardwoods; the kraft pulping model was developed to simulate the cooking of coniferous woods only. Throughout this dissertation, comments on wood anatomy, wood composition, and kraft pulping chemistry apply to softwoods only, unless otherwise stated.

A review of previous kraft pulping models is also presented in this chapter.

2.1 Wood anatomy and composition

Wood is a fiber reinforced matrix. The fibers, called trachieds in softwoods, not only hold up the tree, but they also conduct fluids from the roots to leaves. A simple sketch of wood structure is shown in Figure 2.1. At the center of the trachied is the lumen, which is the void volume in the fibers used for fluid conduction.

Next is the secondary wall, which gives the fiber its strength and stiffness. In the secondary wall the cellulose occurs as crystalline bundles called micelles. The micelles are grouped to form fibrils, which are bound in a lignin matrix. The secondary wall contains the majority of the lignin and polysaccharides in the fiber. Following the secondary wall is the primary wall and the middle lamella. The middle lamella consists mainly of lignin and is the structure that holds the fibers together. The object in chemical pulping is to remove enough lignin for the wood to be separated easily into individual fibers.

Wood is an orthotropic material. The longitudinal direction is parallel to the fibers, the radial direction is from the edge of the tree to the center, and the tangential direction is orthonormal to the other two. The orthotropic nature of the wood has important consequences in chipping and in the wood transport properties, both

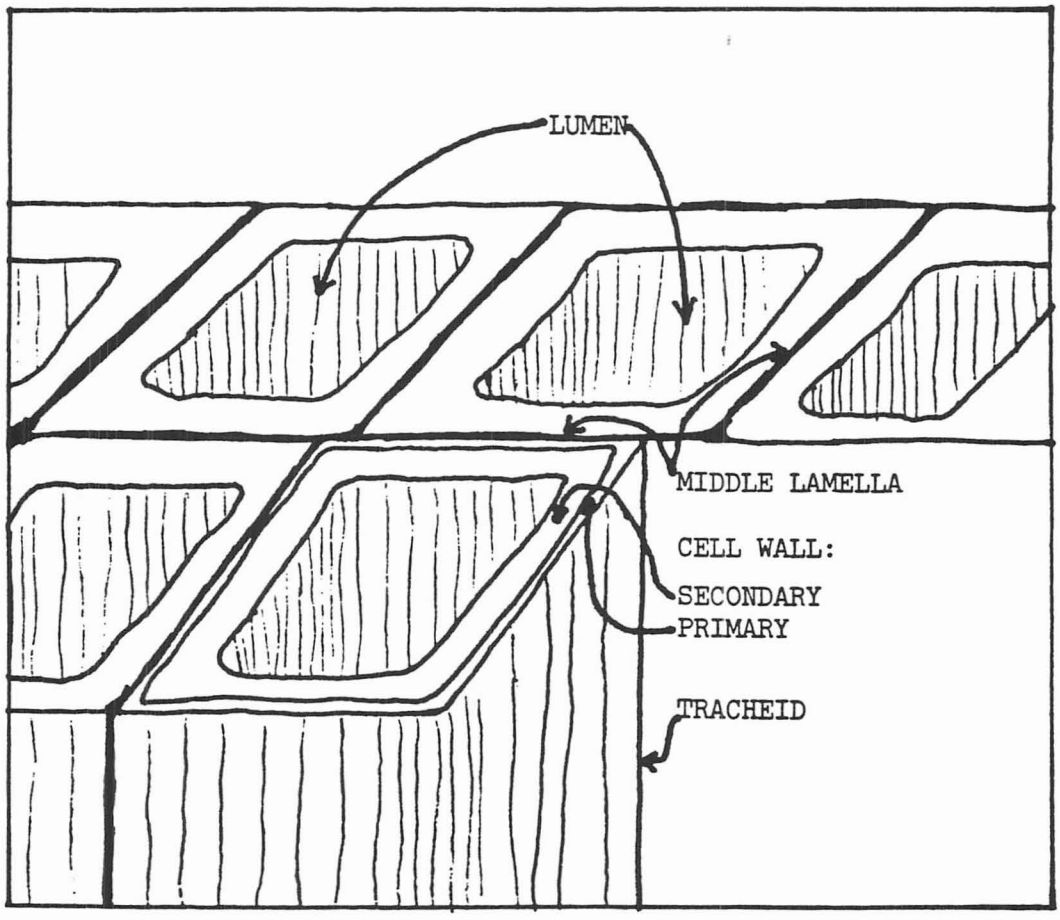

Figure 2.1. Structure of coniferous wood.

of which will be discussed later.

The chemical composition of coniferous wood varies among species and among the geographic region the trees are grown. The primary constituents of wood are lignin, cellulose, and hemi-cellulose. Lignin is a three dimensionmal polymer of phenolic groups linked with a variety of ether and carbon-carbon bonds. The lignin content in coniferous wood ranges from 27% - 33% on an extractive free basis. Cellulose is a linear polymer of β linked glucose molecules. The cellulose content in coniferous wood ranges from 41% - 44% on an extractive free basis. The hemi-celluloses comprise of the polysaccharides not in cellulose. The hemi-cellulose content in coniferous wood ranges from 25% - 30% on an extractive free basis. The hemi-celluloses may be broken down into glucomannan, arabinogalactan, and arbinoxylan. The content of these polymers in coniferous wood are about 15%, 2%, and 9% respectively. For details on the composition of various species see Rydholm (1965f).

2.2 The kraft pulping process

A schematic flow sheet of the kraft pulping process is shown in Figure 2.2. The primary sources of wood for a pulp mill are the forest and the lumber mill. Wood from these two sources are sent to

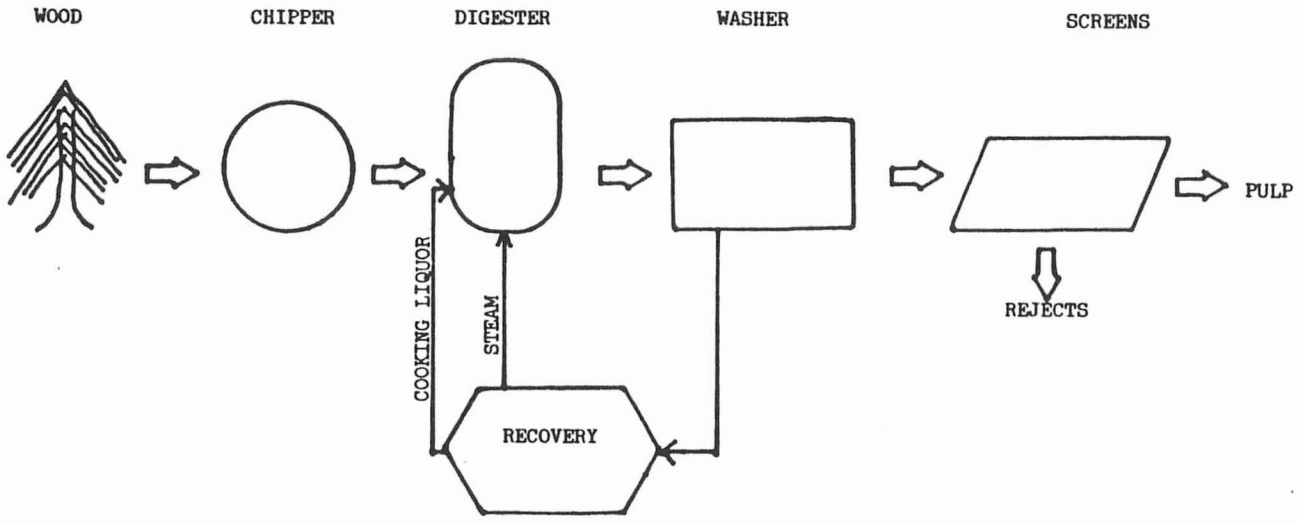

Figure 2.2. Schematic flow sheet of the kraft pulping process.

the pulp mill and cut up into chips. Wood chips used for pulping are 15 - 35 mm long and wide and 3 - 12 mm thick. The length of the chip is parallel to the longitudinal direction of the wood because the wood is weakest parallel to the grain. The chip-thickness and width are randomly oriented in the other two wood directions.

In kraft pulping, chip-thickness is the critical dimension. The first extensive work on the effect of chip-thickness was done by Hartler (Hartler and Ostberg, 1959, Hartler and Onisko, 1962). Using handcut pine heartwood chips, Hartler found that increasing the chip-thickness past three millimeters results in increased screenings accompanied by less delignification. Screenings at a given lignin content were also found to increase with cooking temperature for a given chip-thickness. Work done by Lightfoot (1962), Colombo et al. (1964), and Wahlman (1967) also show that the chip-thickness is the critical dimension in kraft pulping.

The best studies on the effect of chip dimensions on kraft pulp properties are those of Hatton and Keays (1973) and Akhtaruzzaman and Virkola (1979,1980). Both of the these authors conclude that increasing chip-thickness and chip length 'retard' pulping, and that the effect of chip-thickness is more pronounced than that of chip length. They also concluded that the maximum chip-thickness which gives no screenings ranges from 3 mm to 5 mm depending on the cooking conditions. Farkas (1965) also studied the effect of

chip-thickness, length, and width on pulp properties and found chip-thickness to be the critical dimension. The works of Hatton and Akhtaruzzaman will be discussed in more detail later as these are two of the studies used to check the digester model.

Not suprisingly, the mills have been slow to recognize the importance of chip thickness. In a 1967 survey (Borlew and Miller, 1970) of 26 mills in the U.S. and Canada only five considered chip-thickness to be the critical dimension in kraft pulping. In a 1975 survey (Helberg et al., 1975) it was found that only one of 125 continuous digesters in the U.S. and Canada made chip-thickness determinations.

In commercial digesters the chips are not all one thickness, but have a chip-thickness distribution. Chip-thickness distributions from various chipper designs and wood species have been published (Lightfoot and Premont, 1962; Colombo, et al.,1964; Akhtaruzzaman and Virkola, 1979, 1980). A typical chip-thickness distribution is shown Table 2.1. It can be seen from Table 2.1 that the delignification rate in the majority of the chips will be kinetically controlled; however, there is a sizable fraction of chips thicker than 5 mm in which there will be significant concentration gradients. It will be seen later that these thick chips are responsible for screen rejects and broadening of the pulp kappa distribution.

Chip -thickness (mm)	Weight fraction
3	0.4101
5	0.3847
7	0.1152
9	0.0247
12	0.0653

Table 2.1. Chip-thickness distribution used by Akhtaruzzaman and Virkola (1979, 1980).

After the chipper, the chips are mixed with the liquor in the digester. A typical batch digester is a cylinder about 15 meters tall and 4 meters in diameter. There are two broad categories of batch digesters: direct heated and indirect heated. In a direct heated digester, the chips and cooking liquor are heated by live steam blown in the bottom of the digester. In an indirect heated digester, the chips are heated by the cooking liquor which is steam heated in a heat exchanger and circulated through the chip bed. Significant temperature gradients have been reported in both indirect (Annergren, et al., 1973; Stephenson, 1950), and direct heated batch digesters (Bailey and Yawn, 1969). These temperature gradients have a large effect on pulp uniformity and will be discussed in detail in Chapter 7.

The primary chemicals in kraft liquor are sodium hydroxide and sodium sulfide. A typical liquor contains about 1 M NaOH and 0.2 M Na_2S. The active chemical species are the hydroxyl ion, OH^-, and the sulfide ion, S^{-2} or hydrosulfide ion, HS^-, which are equally reactive (McKean, 1968). To calculate the concentrations of these active species from the NaOH and Na_2S concentrations, the equilibrium behavior of Na_2S must be known. Sulfide ions react with water in the following sequence:

$$S^{-2} + H_2O = HS^- + OH^- \qquad (2.1)$$

$$HS^- + H_2O = H_2S + OH^- \qquad (2.2)$$

The exact pK_a of Reaction 2.1 is unknown, but it is believed to be around 13.5 (Rydholm, 1965a) The pK_a of Reaction 2.2 is about 7.0. At pulping concentrations, therefore, it has been found that Reaction 2.1 goes to completion and that Reaction 2.2 proceeds negligibly (Teder and Tormund, 1973). With this thermodynamic information it can be concluded that the effective alkali is the best measure of the alkali concentration. The effective alkali is defined as:

$$[NaOH] + 1/2\ [Na_2S] \qquad (2.3)$$

where the concentrations are in sodium equivalents. The other common alkali concentration is the active alkali which is defined as:

$$[NaOH] + [Na_2S] \qquad (2.4)$$

where again the concentrations are expressed in sodium equivalents. The active alkali is a poor measure of the hydroxyl concentration

because it is assumed that both reactions, Equations 2.1 and 2.2, go to completion.

The hydroxyl ion concentration used in the model is the effective alkali concentration expressed in moles per liter. The sulfide concentration used in the model is simply the molar sodium sulfide concentration. In the text, the effective alkali concentration may be expressed as percent on wood as NaOH, and the sulfide concentration as sulfidity. The former is the weight of effective alkali, as NaOH, divided by the intial oven dry (O.D.) weight of the wood. The sulfidity is defined in Equation 2.5.

$$[Na_2S]/([NaOH] + [Na_2S]) \tag{2.5}$$

where the concentrations are expressed in sodium equivalents.

The cooking liquor and the chips are heated in the digester to about 170 C. Typical heating times range from 30 minutes to 2 hours. The temperature is then held at the maximum level for a duration ranging from 30 minutes to 2 hours. The cooking conditions will depend, of course, upon the grade of pulp being produced and will vary from mill to mill. At the end of the cook the pressure is quickly released, providing the energy to separate the wood into

individual fibers. The pulp is then washed to remove the cooking chemicals and screened to remove the undefiberized shives.

The pulp properties of importance in this study are the lignin content, or kappa number, the carbohydrate content, the yield, the screen rejects, and the screen yield. The lignin content is the most important pulp property and is expressed in two ways. The first is the weight of lignin in the pulp divided by the intial oven dry (O.D.) weight of the wood times 100% (i.e. percent on wood). The second is the kappa number. The kappa is an indirect measure of the lignin content and can be calculated from the lignin content expressed in percent on wood by Equation 2.6.

$$\text{Kappa no.} = \text{lignin content}/(\text{yield}/100\% \times 0.15) \qquad (2.6)$$

The carbohydrate content of the pulp is the weight of all the carbohydrates in the pulp divided by the intial O.D. weight of the wood times 100%. The yield is defined as the total weight of pulp divided by the intial O.D. weight of the wood. The screen rejects is the weight of undefiberized material retained on the pulp screens divided by the intial O.D. weight of the wood. Finally, the screened yield is the difference between the yield and the screen rejects. The yield, screen rejects, and the screen yield are all expressed in percent.

2.3 Previous kraft pulping models

Kraft pulping models of varying complexity have been developed for control and design purposes. The simplest of these models are those that assume the pulping reaction rates are kinetically controlled. One of the earliest kinetic models was developed by Vroom (1957), who used an Arrhenius type expression for the reaction rate temperature dependence to derive the "H factor." The H factor, which combines the cooking temperature and cooking time into one variable, is at the heart of many control schemes today.

Many empirical models have been derived. Typical of these is Hatton's (1973) model which predicts the kappa number and yield for a variety of wood species with an equation of the form

$$Y \text{ or } K = \alpha - \beta\,[(\log H) \times (EA)^n) \qquad (2.7)$$

where

Y is the yield

K is the kappa number

α and β are adjustable parameters

H is the H factor

EA is the effective alkali concentration

These empirical models may be quite complex. For example, the model of Bailey et al. (1969) uses five variables in a twenty term polynomial to predict pulp kappa numbers.

Semi-theoretical kinetic models have been derived by Kerr (1970) and Smith (1975). In Kerr's model the form of the delignification rate equation is

$$dL/dt = -k \ OH \ L \qquad (2.8)$$

where

L is the lignin content
t is the cooking time
k is the rate constant
OH is the effective alkali concentration

The alkali consumption rate in Kerr's model is assumed to be a linear function of the delignification rate for each delignification period. (See Section 3.3.1 for a discussion of the three delignification periods). The H factor is used to account for the time-temperature behavior. Pulp kappa numbers are predicted with Kerr's model given the time-temperature behavior and the intial effective alkali concentration. In a later paper by Kerr and Uprichard (1976), Kerr's model is refined to incorporate,

empirically, the pulping variables sulfidity, chip size, chip moisture content, and liquor to wood ratio.

The most complex kinetic model is Smith's (1975), in which wood is divided into five species: high-reactivity lignin, low-reactivity lignin, cellulose, galactomannan, and arabinoxylan. The form of the kinetic equation Smith uses for each species is,

$$-dC/dt = (k_1 OH + k_2 OH\ S)C \qquad (2.9)$$

where

C is the wood species concentration
OH is the alkali concentration
S is the sulfide concentration
k_1 and k_2 are rate constants
t is the cooking time

Smith calculated the stoichiomentric coefficients relating the alkali and sulfide consumption to the lignin and carbohydrate degradation using chemical data from an industrial kraft cook. Smith also used these data to check the accuracy of his model.

Even the best kinetic models cannot predict the overall pulping rate in commercial chips. As stated in Section 2.2, there are chips

in commercial chip-thickness distributions in which the reaction rates are partially mass transfer limited, and that these chips are responsible for most of the rejects. An accurate pulping model, therefore, must incorporate the effect of chip-thickness either empirically or, better still, theoretically.

Empirical models describing the effect of chip dimensions on pulp properties were derived by Hatton and Keays (1973) and Akhtaruzzamn and Virkola (1979, 1980). Hatton and Keays derived a series of polynomial regression equations from their experimental data in which the screened yield, yield, screen rejects, kappa number, permanganate number, and effective alkali consumption are functions of chip length and chip-thickness. Hatton and Keays used only one pulping condition so their results are limited.

Akhtaruzzaman and Virkola pulped chips of varying dimensions under a variety of conditions. In their study a series of polynomial regression equations were derived from their experimental data and give the kappa number, yield, screened yield, rejects, effective alkali consumption, pulp viscosity, fiber length, and paper strength properties as a function of chip-thickness, chip length, intial effective alkali concentration and H factor.

Empirical models are only useful for interpolating between the experimental conditions used to generate the response surface. To

extrapolate from those experimental conditions, a theoretical model is needed. The model of Johnsson (1971) is a step in this direction; the effect of chip-thickness on pulp properties was theoretically modeled. Johnsson solved the differential equations describing the combined mass transfer and reaction kinetics in a pulp chip during a kraft cook.

Johnsson's model predicts reasonably well cumulative kappa number distributions of a pulp produced in an industrial continuous digester. Subsequent kinetic studies have shown, however, that the kinetic equations used by Johnsson are too simple to give acceptable results. For example, Johnsson uses one delignification rate equation for all three reaction periods. In this equation the delignification rate is first order in the alkali concentration and zero order in the sulfide concentration. Johnsson's equation is not consistent with experimental kinetic measurements (Norden and Teder, 1979), and his alkali consumption equation fails to predict the residual data of Aurell and Hartler (1965).

Johnsson's assumption that the diffusivity in wood is a function of temperature only is also incorrect. Results published by Hartler (1962) show that the diffusivity of a solute in wood is a strong function of pH and yield.

A semi-theoretical model was developed by Tyler (1981). Tyler

modeled the combined diffusion and kinetic problem for chips pulped in laboratory scale digesters. Only bulk period kinetics were used in Tyler's rate equations, and he also assumed that the diffusivity in wood is a function only of temperature. The model was empirically fit to the data of Hatton and Keays (1973) and Akhtaruzzaman and Virkola (1979,1980) by adjusting the alkali diffusivity and the reaction rate constants.

From this review it is evident that improvements in modeling the kraft pulping process may be made. Kinetic equations for all three reaction periods are available. The diffusivity in wood may be expressed as a function of temperature, pH, and yield. With good kinetic and diffusivity equations the lignin content, carbohydrate content, and alkali concentration may be predicted, a priori, at each point within a chip at any given time during a cook. With this information the kappa number, kappa number distribution, yield, screen rejects, and screen yield of a pulp may be predicted for a given set of cooking conditions. The following chapters describe the development and application of such a model.

CHAPTER 3

DEVELOPMENT OF THE MODEL

To predict the chemical composition within a wood chip as a function of cooking time for a given pulping condition, the equations for the simultaneous heat transfer, mass transfer, and reaction kinetics must be derived and solved for the chip phase and the bulk liquid phase. In this chapter the derivation of these equations are presented.

3.1 Assumptions

The kraft pulping of a wood chip is a very complex phenomenon; therefore, simplifying assumptions are needed to model the process mathematically. The assumptions that are made in the model development and their justification are the following:

1. The chip is completely filled with cooking liquor before the digester temperature reaches a level at which the pulping reaction rates are significant.

   This assumption is reasonable for typical heating rates because the liquor penetration is complete about the time the digester reaches 140 C (Hartler, 1962), and at this temperature the delignification rate is slow. This assumption is invalid for very fast heating times (i.e on the order of minutes) unless the chips are pre-impregnated or pre-steamed.

2. The chips are isothermal.

   The characteristic time for heat transfer is much less than other characteristic times of the pulping process. Furthermore, the heats of reaction of pulping reactions are essentially zero.

3. The pulp chips are one-dimensional.

   In Section 2.2, literature was presented that shows chip-thickness is the critical dimension. Pulp chips have an aspect ratio of about five. In alkaline pulping the diffusivities in the three primary directions are not significantly different (Stone,1957; Hartler, 1962). We anticipate, therfore, that chip-thickness is the critical dimension.

4. In laboratory scale digesters the bulk liquid phase is homogeneous and well stirred.

   The digester is modeled as a CSTR in which the mass transfer coefficient from the bulk phase to the chip phase is assumed to be infinite. These are good assumptions for modeling lab scale digesters because they are well agitated. The validity of these assumptions for commercial digesters is discussed in Chapter 7.

5. Wood is divided into lignin, carbohydrates, and acetyl. Combining the carbohydrates into one catagory is justified because in softwoods the relative amount of different carbohydrates are not significantly altered by normal changes in pulping conditions (Aurell and Hartler, 1965; Yllner et al., 1957). The acetyl groups are considered as a separate component (they are actually a component of the galactoglucomannans) because they consume a small, but significant, amount of alkali in a well characterized fashion (see Section 3.3.2). Their inclusion, therefore, improves the alkali consumption rate equation. The other major wood component, the extractives, are assumed to be dissolved out of the wood before pulping begins (Olm and Tistad, 1979).

6. Delignification reactions are irreversible.

The kraft delignification mechanisms presented by Gierer (1980) show this to be a good assumption. Condensation reactions, however, in which dissolved lignin condenses back on to the wood phase occur when the liquor lignin concentration is high and the alkali concentration is low (Hartler, 1978). Condensation reactions may occur, therefore, at the end of a cook, and at the center of thick chips. No accounting is made, in the model, for the condensation reactions because knowledge of the reactions is too limited. The effect of condensation reactions on the model predictions and on reject formation are discussed in Section 5.2 and 5.3 respectively.

With these assumptions , the pulping process is modeled as shown in Figure 3.1. At the beginning of the cook , diagram I, it is assumed that the chip phase is full of cooking liquor and the alkali and sulfide concentration are uniform throughout. As the digester heats up, pulping reactions begin, diagram II, that produce degradation products that neutralize alkali as they diffuse out of the wood. Alkali is transported from the bulk phase to the chip surface and then diffuses into the chip to replace the alkali consumed by the degradation products. The sulfide concentration is assumed to remain constant (see Section 3.3.2), and therefore, it does not diffuse into the chip. (Note that both the sulfide ions

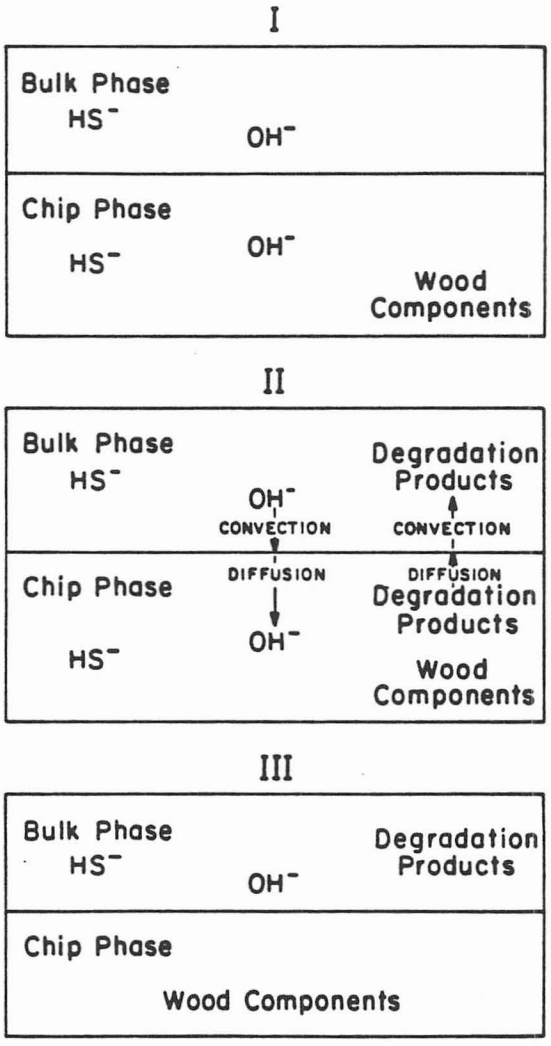

Figure 3.1. Schematic of kraft pulping of a single chip.

and hydrosulfide ions are regarded as the sulfide. This is done because S in the bulk delignification rate equation (Equation 3.17) is the total sulfide sulfur concentration (Lemon and Teder, 1973)). At the end of the cook, and after the pulp has been washed, diagram III, all that remains in the pulp is the bound wood components.

3.2 Differential equations

A mass balance on the chip, with the foregoing assumptions, gives the following equations.

$$\partial C_i / \partial t = (\partial/\partial x)(D_i \ \partial C_i / \partial x) - Ra_i \qquad (3.1)$$

$$\partial C_i / \partial x = 0 \qquad \text{chip center} \qquad (3.2)$$

$$D_i \ \partial C_i / \partial x = k_i \ (C_{i\ bulk} - C_i) \qquad \text{chip edge} \qquad (3.3)$$

$$C_i = C_{io} \qquad t=0 \qquad (3.4)$$

where

C_i is the concentration of i-th species.

C_{io} is the initial concentration of the i-th species.

$C_{i\ bulk}$ is the concentration of the i-th species in the bulk liquid phase.

D_i is the diffusivity of the i-th species.

k_i is the mass transfer coefficient of the i-th species.

Ra_i is the reaction rate of species i.

t is the time.

x is the distance from the chip center.

A mass balance on the bulk phase alkali gives the following equations.

$$dOH_{bulk}/dt = - D_{OH} \left. \partial OH/\partial x \right|_{chip\ edge} V_c/(CT\ V_b) \qquad (3.5)$$

$$OH_{bulk} = OH_{bulk\ o} \qquad t=0 \qquad (3.6)$$

where

OH_{bulk} is the bulk phase alkali concentration.

OH is the chip phase alkali concentration.

V_c is the volume of the chip.

V_b is the volume of the bulk liquid phase.

CT is one-half the chip-thickness.

$OH_{bulk\ o}$ is the initial bulk phase alkali concentration

x is the distance from the chip center

t is the time

D_{OH} is the diffusivity of the alkali

Expanding Equation 3.1 and non-dimensionalizing Equations 3.1 - 3.4 gives the following expressions.

$$\partial C_i^* / \partial t^* = \partial \alpha_i / \partial x^* \; \partial C_i^* / \partial x^* + \alpha_i \; \partial^2 C_i^* / \partial x^{*2} - Ra_i^* \qquad (3.7)$$

$$\partial C_i^* / \partial x = 0 \qquad x^* = 0 \qquad (3.8)$$

$$\partial C_i^* / \partial x^* = Bw_i \; (C_{i\,bulk}^* - C_i^*) \qquad x^* = 1 \qquad (3.9)$$

$$C_i^* = 1 \quad t^* = 0 \qquad (3.10)$$

where

C_i^* is C_i/C_{io}

$C_{i\,bulk}^*$ is $C_{i\,bulk}/C_{io}$

Ra_i^* is $Ra_i tf/C_{io}$

t^* is t/tf

tf is the total cooking time

x^* is x/CT

α_i is $D_i tf/CT^2$

Bw_i is $k_i CT/D_i$

Non-dimensionalizing Equations 3.5 and 3.6 gives the following expressions.

$$dOH_{bulk}^*/dt^* = \alpha_{OH}\, \partial OH^*/\partial x^* (V_c/V_b) \tag{3.11}$$

$$OH_{bulk}^* = 1 \qquad t=0 \tag{3.12}$$

where

OH_{bulk}^* is OH_{bulk}/OH_o

OH^* is OH/OH_o

To solve the differential equations, expressions for the kinetics and the diffusivities of the lignin, carbohydrate, acetyl,

hydroxyl, and sulfide are needed. For modeling the laboratory scale digester the Biot number, Bw_i in Equation 3.9, for the alkali is set equal to 10,000 to simulate the well stirred case. The value of the alkali Biot number in commercial digesters is discussed in Section 7.1.

3.3 Kinetics

The foundation of a pulping model is the kinetic equations. Many kraft pulping kinetic studies have been done, but few provide data from which kinetic equations may be derived. Often in these kinetic studies the cooks are non-isothermal, or the liquor to wood ratio is low so the effective alkali concentration changes throughout the cook, or the chips are unscreened so the reaction rates are partially diffusion controlled. The kinetic equations selected for the model are derived from the best available data and are generally of a form that is consistent with the wood chemistry of softwoods. The lignin, carbohydrate, and acetyl kinetics, are presented first and are followed by the alkali and sulfide kinetics.

3.3.1 Lignin, carbohydrate, and acetyl kinetics

The kinetics of kraft pulping can be divided into three periods: initial, bulk, and residual (Kleppe, 1970; Kleinert,

1966; Norden and Teder, 1979), see Figure 3.2. (Typically these three periods are referred to as phases, but to avoid confusion, we restrict the term phase to distinguish between the bulk liquid and the chip phase). The initial period is characterized by rapid delignification, significant hemicellulose degradation, and large alkali consumption. The only published study on initial period kinetics is the one recently carried out by Olm and Tistad (1979). (Further work on intial delignification is currently being done by Prof. K.V. Sarkanen at the University of Washington). The delignification expression derived from their data is given by Equation 3.13.

$$dL/dt = 36.2\ T^{1/2}\ e^{(-4807.69/T)}L \qquad (3.13)$$

where

L is the lignin content [=] (% on wood)

T is the temperature [=] (K)

t is the time [=] (min)

The lack of alkali or sulfide dependence in Equation 3.13 can be explained by the intial period chemistry. Intial period

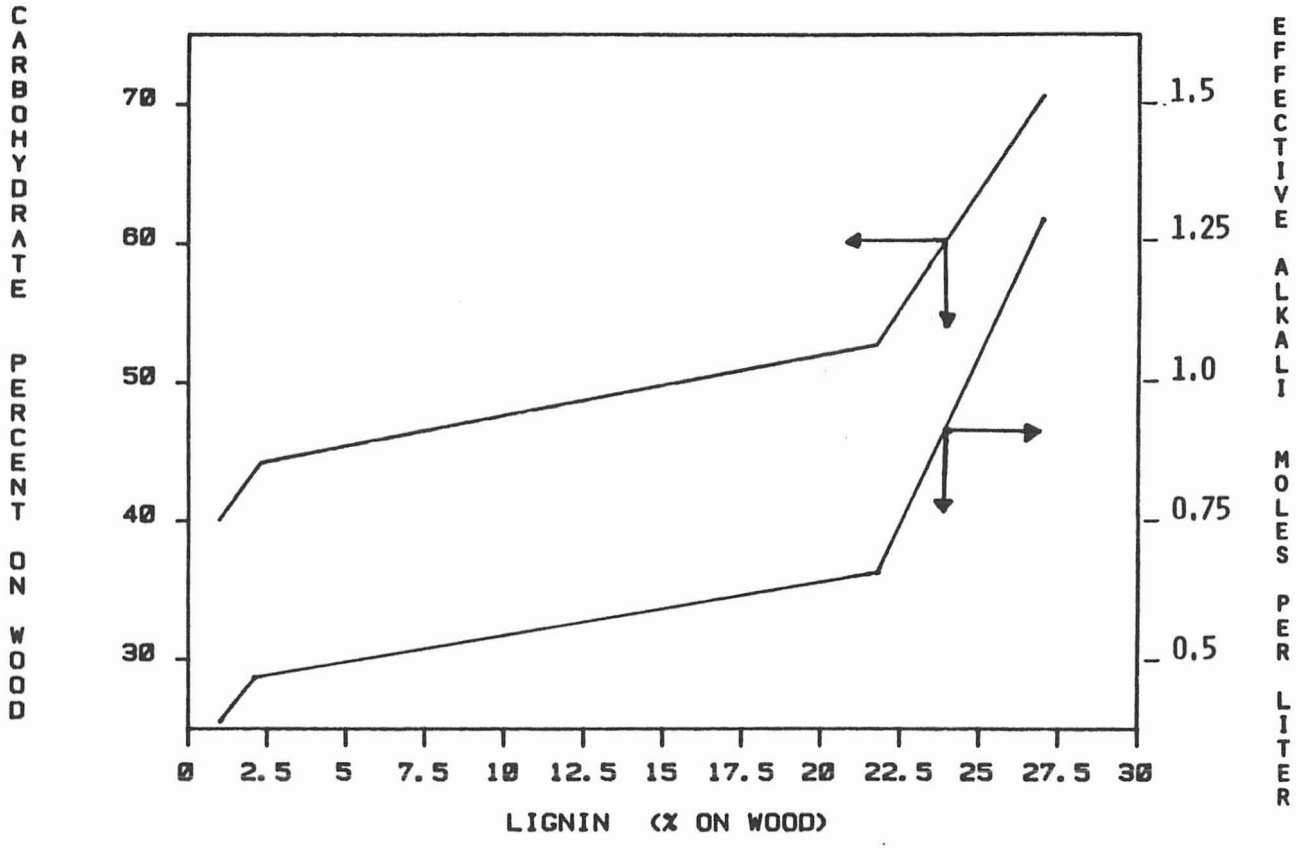

Figure 3.2. Change in effective alkali concentration and carbohydrate content with lignin content during a typical kraft cook (Rekunen et al., 1980).

delignification is attributed to the cleavage of phenolic α or β aryl-ether groups. Work with model compounds (Gierer, 1980) shows that this cleavage readily takes place at pulping temperatures provided the pH is above 12. The pH during a kraft cook will always be above 12 except, possibly, at the center of thick chips.

It can be seen in Figure 3.2 that the carbohydrate reaction rate for each period is a linear function of the lignin reaction rate (Aurell and Hartler, 1965; Kleinert, 1966; Olm and Tistad, 1979). This is attributed to the chemical links between the carbohydrates and the lignin (Kleinert, 1966; Eriksson et al., 1980)and the similarity of the reaction mechanism of carbohydrate peeling and lignin degradation (Gierer, 1980). Olm and Tistad (1979) show that the constant relating the lignin reaction rate and the carbohydrate reaction rate in the intial period is independent of the sulfide concentration but dependent upon the alkali concentration. From their data Equation 3.14 is derived for the initial period carbohydrate degradation rate.

$$dC/dt = 2.53\ (OH)^{0.11}\ dL/dt \qquad (3.14)$$

where

L is the lignin content [=] (% on wood)

C is the carbohydrate content [=] (% on wood)

OH is the effective alkali concentration [=] (mole/l)

t is the time [=] (min)

Finally, Olm and Tistad show that the acetyl groups are removed from the hemicellulose very quickly and are neutralized completely by the NaOH in the intial period.

The transition from the initial period to the bulk period takes place at a lignin content of about 22 % on wood and is independent of temperature, sulfide concentration, and alkali concentration (Olm and Tistad, 1979; Rekunen et al., 1980).

Most of the lignin is removed in the bulk period. Carbohydrate degradation continues in this period as well, although at a much slower rate than in the intial period. The bulk delignification kinetics have been the subject of many studies (Kleinert, 1966; Wilder and Daleski, 1965; Daleski, 1965; Lemon and Teder, 1973). The results of Wilder and Daleski's study (1965) and Lemon and Teder's study (1973) are used in the derivation of the bulk delignification kinetic equation for the model.

In the Wilder and Daleski study the bulk delignification rate

of Loblolly pine chips was measured at 142, 150, 160, and 170 C with liquor compositions ranging from 20 gm/l soda liquors to 60 gm/l active alkali, 100 % sulfidity kraft liquors. The form of the rate equation they assumed is given by Equation 3.15.

$$dL/dt = (k_1\ OH + k_2\ S^n)\ L \qquad (3.15)$$

where

L is the lignin content [=] (% on wood)

OH is the effective alkali concentration [=] (mole/l)

S is the sulfide sulfur concentration [=] (mole/l)

t is the time [=] (min)

k_1 and k_2 are rate constants

This form is incorrect because it does not predict a zero reaction rate as the alkali concentration approaches zero. Furthermore, the value of the constants k_1 and k_2 are such that at typical pulping conditions $k_2S^n > k_1OH$. This implies, incorrectly, that the reaction rate is more strongly dependent on the sulfide concentration than the alkali concentration.

Lemon and Teder measured the bulk period delignification rate of Scots pine at 170 C. The form of the rate equation they derived is

$$dL/dt = (k_1\ OH + k_2\ OH^{0.5}\ S^{0.4})\ L \qquad (3.16)$$

where

L is the lignin content [=] (% on wood)

OH is the effective alkali concentration [=] (mole/l)

S is the sulfide concentration [=] (mole/l)

t is the time [=] (min)

Equation 3.16 is used in this study. It predicts a zero reaction rate as the hydroxyl concentration goes to zero and reduces to the soda cooking rate as the sulfide concentration goes to zero. The dependence of Equation 3.16 upon the hydroxyl and sulfide concentration is consistent with the chemistry of non-phenolic β -o-aryl ether cleavage (Gierer, 1980).

The temperature dependence of the constants k_1 and k_2 in Equation 3.16 is taken from Wilder and Daleski's study. This is legitimate, provided the activation energies are not functions of the caustic or sulfide concentration, because the rate constants in the two studies are derived in the same way. With this correction the bulk delignification rate expression used in the model is:

$$dL/dt = [e^{(35.19 - 17200/T)}_{OH} + e^{(29.23 - 14400/T)}_{OH^{0.5}S^{0.4}}] L \quad (3.17)$$

where

L is the lignin content [=] (% on wood)

OH is the effective alkali concentration [=] (mole/l)

S is the sulfide concentration [=] (mole/l)

t is the time [=] (min)

T is the temperature [=] (K)

The carbohydrate reaction rate in the bulk period is proportional to the lignin reaction rate and the constant of proportionality is independent of cooking conditions (Kleinert, 1966; Aurell and Hartler, 1965; Yllner et al., 1957). The rate constant used in the model is taken from Rekunen's (1980) data, and the carbohydrate reaction rate is given by

$$dC/dt = 0.47\ dL/dt \quad (3.18)$$

where

L is the lignin content [=] (% on wood)

C is the carbohydrate content [=] (% on wood)

t is the time [=] (min)

The lignin content at the transition from the bulk period to the residual period is dependent upon temperature (Kleinert, 1966) and sulfidity (Norden and Teder, 1979), but the available data are insufficient to predict the transition point given the pulping conditions. The lignin content of the pulp at the transition point may vary from 2.5 % on wood (Rekunen et al.,1980) to 1.1 % on wood (Kleinert, 1966). The value used in the model is taken from experiments run at conditions closest to those being simulated. The value of the bulk to residual transition point is input to the model.

The residual period is characterized by very slow delignification, significant carbohydrate degradation, and significant alkali consumption. The form of the residual delignification rate equation is taken from Norden and Teder's (1979) paper and the value of the rate constant is calculated from Kleinert's (1966) data. The expression used in the model is

$$dL/dt = e^{(19.64 - 10804/T)}{}_{OH}{}^{0.7}{}_{L} \qquad (3.19)$$

where

L is the lignin content [=] (% on wood)

OH is the effective alkali concentration [=] (mole/l)

t is the time [=] (min)

T is the temperature [=] (K)

The carbohydrate reaction rate for the residual period is derived from Rekunen's (1980) data and is shown in Equation 3.20.

$$dC/dt = 2.19\ dL/dt \qquad (3.20)$$

where

L = lignin content (% on wood)

C = carbohydrate content (% on wood)

t = time (min)

The reaction rates presented above will not apply for all species, even among the softwoods, under all conditions. Both

Wilder and Daleski (1965) and Lemon and Teder (1973) found that the bulk delignification rate changes significantly with the conditions used in the initial period. The bulk delignification rate measured for spruce (Kleinert, 1966) is about 20 % higher than the value measured for pine (Wilder and Daleski, 1965; Lemon and Teder, 1973). Similar comments apply to the delignification rates in the other periods, and to the carbohydrate reaction rates as well. It is important to note that because the form of the rate equations are consistent with the wood chemistry for softwoods, differences in the kinetics between species may be accounted for by adjusting the rate constants. If the data are available the above kinetic equations will be modified to account for species differences. For the most part, however, the model results should be viewed as representative results rather than as predictions of specific behavior.

3.3.2 Alkali and sulfide consumption

A thorough study on the rate of consumption of alkali in kraft pulping has not been done. In fact, it is difficult to know the alkali concentration in kraft liquor. From the thermodynamic work that has been done on kraft liquors (Teder and Tormund, 1973), it is generally assumed that the effective alkali is the best measure of the alkali concentration. However, it is difficult to measure the true effective alkali concentration in the liquor because of the

organics in the liquor. Lemon and Teder (1973) show that quite different values for the effective alkali concentration in kraft liquor can be obtained by changing the titration end point, even with the addition of barium chloride.

Estimates of the amount of alkali consumed by reaction products have been made by Rydholm (1965b) and by Brauns and Grimes (1939). These estimates predict reasonable values for the total consumption of alkali, but cannot accurately predict the shape of the alkali concentration versus time curve.

To estimate the alkali reaction rate, it is assumed that the alkali consumption can be expressed as a linear function of the acetyl, lignin, and carbohydrate reaction rates. It is assumed that roughly one mole of alkali is consumed per mole of acetyl group liberated (Rydholm, 1965c). To calculate the amount of alkali consumed by the lignin and carbohydrate, the data of Rekunen et al. (1980) is used. Rekunen presents the carbohydrate content and the effective alkali concentration as linear functions of the lignin content for both the initial and bulk period during a kraft cook. This gives two linear equations that can be used to solve for the two unknowns; namely the moles of effective alkali consumed per gram of lignin and per gram of carbohydrate liberated from the chip. The alkali reaction rate calculated in this manner is

$$dOH/dt = (1.87X10^{-2}\ dAc/dt - 4.78X10^{-3}\ dL/dt + 1.81X10^{-2}\ dC/dt)\ \rho/\varepsilon \qquad (3.21)$$

where

L is the lignin content [=] (% on wood)

C is the carbohydrate content [=] (% on wood)

Ac is the acetyl content [=] (% on wood)

OH is the effective alkali concentration [=] (mole/l)

t is the time [=] (min)

ε is the void fraction in the chip

ρ is the wood density

It will be shown later that Equation 3.21 predicts the data well for a wide range of conditions, but it probably has little physical significance. Note, for example, the negative coefficient of the lignin term. Given the typical amounts of carbohydrate, lignin, and acetyl consumed in a kraft cook, equation 3.21 does predict the well known fact that most of the alkali is consumed in the neutralization of saccharinic acids.

The concentration of sulfide is assumed to be constant throughout the cook. Reactions that produce thiolignins and other

sulfur containing compounds consume approximately 5-10 g sulfur per Kg of wood (Rydholm, 1965d). Because of this low consumption of sulfur and because of the low delignification rate dependence on sulfur (see Equation 3.21), the assumption that the sulfide concentration is constant is a good one provided the initial concentration is above a value corresponding to about 20 % sulfidity.

3.4 Diffusion

The diffusivities of the carbohydrate and the lignin are zero since these species are bound in the wood. The diffusivity of the sulfide is unimportant because the sulfide concentration is held constant. The reaction products of delignification and carbohydrate peeling diffuse out of the wood, but we are not concerned with the diffusion rate because the pulping reactions are assumed to be irreversible (assumption 5) and because lignin and carbohydrate contents of the <u>washed</u> pulp are the variables of interest.

The diffusivity of the alkali in pulp chips has not been measured directly. Much work has been done on the diffusion of other solutes in wood, however, and a review of these works provides a means of estimating the alkaline diffusivity.

The diffusivity of a solute in wood is generally reported as D/Do where D and Do are the diffusivities of the solute in the wood phase and in the bulk phase, respectively. Experimentally, D/Do is determined either by measuring the diffusivity directly or by electrical conductivity measurements. In the conductivity studies the results are expressed as K/Ko where K and Ko are the conductivities of the solution with and without a wood chip, respectively. Generally, the ratio D/Do or K/Ko are referred to as the effective capillary cross-sectional area, or ECCSA. Results of some diffusion and conductivity studies are shown in Table 3.1. Not suprisingly, the diffusivity , or conductivity, is much larger in the longitudinal direction than in the radial or tangential directions. It is also seen that species with higher specific gravities have lower diffusivities. Behr's (1953) work with napthalene shows that large solute molecules have a very difficult time moving through wood in the tangential direction. It should be noted that the ECCSA provides a good approximation of how the diffusivity of a solute in a wood chip may vary with cooking conditions or yield; however, the ECCSA cannot be generally applied to give an accurate, quantitative value for the diffusivity of that solute.

Diffusivities in the tangential and radial directions are a strong functions of pH and yield (see Figures 3.3 and 3.4). Diffusivity in the longitudinal direction is independent of pH and

Researcher	Species	Sp. Gr.	Experimental Method	Solute	ECCSA Long.	Rad.	Tang.
Luner (1956)	Balsa	0.31	Diffusion	KCl	0.56		
	Spruce	0.45	"	"	0.51	0.028	0.034
Burr (1947)	W. Pine	0.35	Conductivity	KCl	0.54	0.032	0.031
	D.Fir	0.48	"	"	0.42	0.02	0.022
	Hemlock	0.42	"	"	0.47	0.029	0.024
Behr (1953)	S. Spruce	0.34	Diffusion	NaCl	0.59		0.0146
	D. Fir	0.45	"	"	0.47		0.011
	D. Fir sapwood	0.50	"	"	0.43		0.012
	W. Cedar	0.34	"	Napthalene in benzene	0.55		0.006
	W. Cedar	0.28	"	NaCl	0.64		0.016

Table 3.1. ECCSA of various solutes in wood.

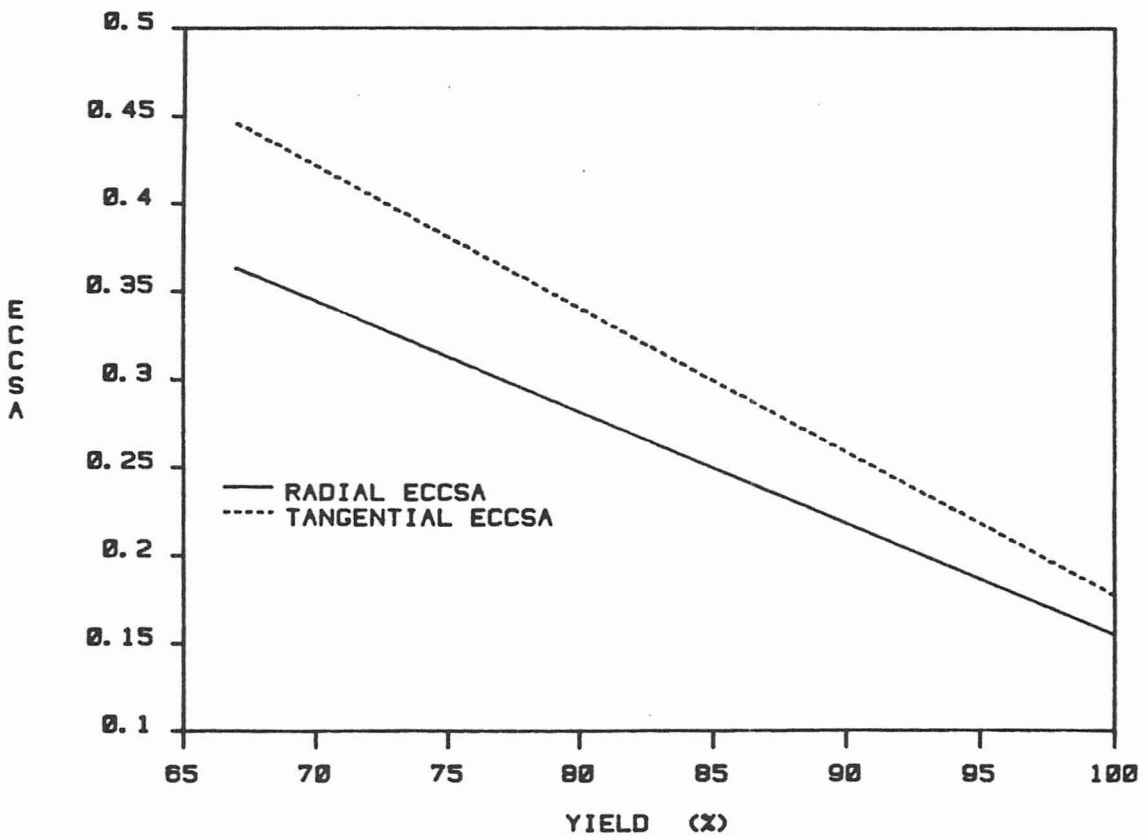

Figure 3.3. Change in ECCSA with yield at pH 13.2 (Hartler, 1962).

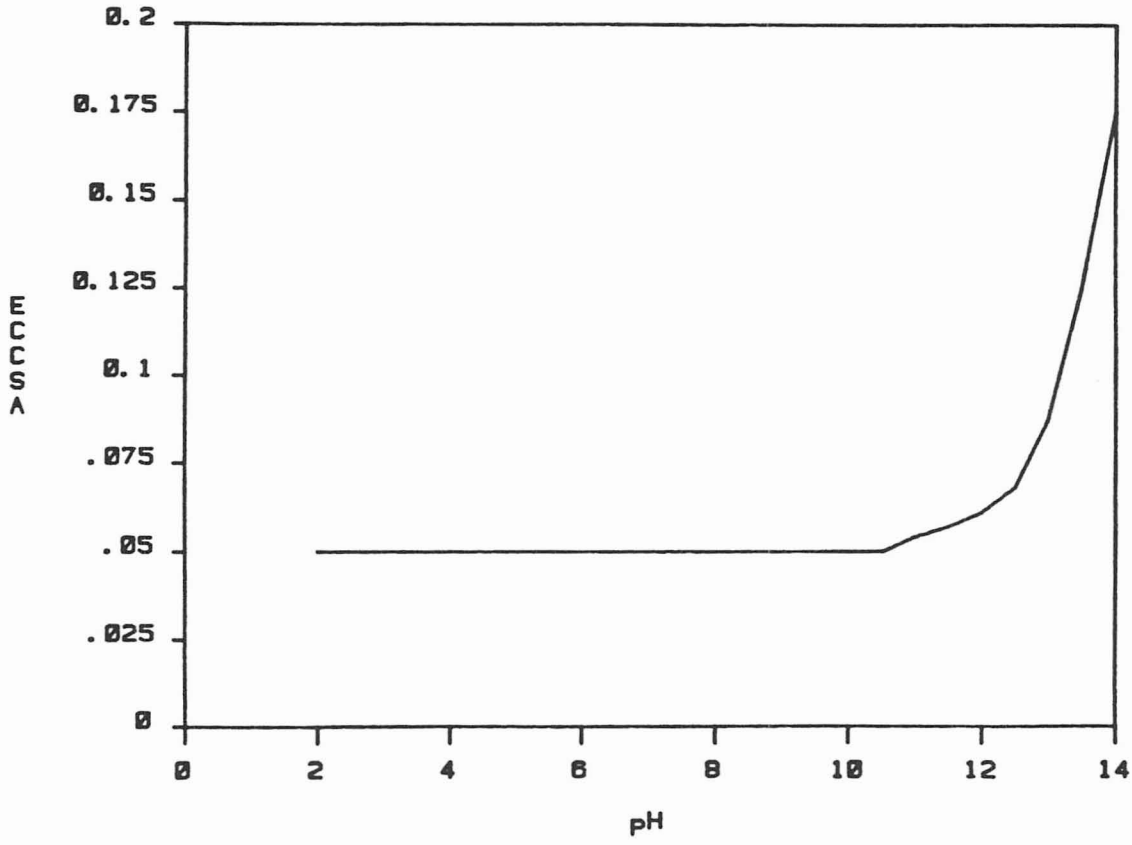

Figure 3.4. Change in ECCSA with pH for the tangential and radial directions in uncooked spruce wood (Hartler, 1962).

yield (Stone, 1957; Hartler, 1962).

Studies on the effect of temperature on diffusivity in wood show that the temperature dependence can be expressed as

$$D = k\, e^{(-Ea/RT)} \qquad \text{(Huang et al., 1977)}$$

or

$$D = k\, T^{1/2}\, e^{(-Ea/RT)} \qquad \text{(Christensen, 1951; McKibbins, 1960)}$$

In all these studies the value for the activation energy of diffusion in the transverse direction was found to be in the range of 4.0 to 5.0 Kcal/mole.

To estimate the diffusivity of alkali for use in the model, three relevant studies were used. The first is McKibbins's work (1960) in which he measured the diffusivity of sodium in kraft cooked chips. McKibbins measured the diffusivity by immersing the cooked chips in distilled water and then comparing the measured chip sodium concentration versus time curves to those predicted by unsteady state diffusion theory. This was done for a variety of temperatures and the results yielded Equation 3.22.

$$D = 3.4 \times 10^{-2}\, T^{1/2}\, e^{(-4870/RT)} \qquad (3.22)$$

where

D is the diffusivity [=] (sq cm/min)

T is the temperature [=] (K)

R is the gas constant [=] (cal/mole K)

Because McKibbins's work was done with cooked chips, Equation 3.22 needs to be corrected with respect to pH and lignin content. This correction was made with the results shown in Figures 3.3 and 3.4. It was assumed that the diffusivity of alkali varied with pH and yield as the ECCSA results in Figures 3.3 and 3.4. It was also assumed that the effect of pH and yield on the diffusivity is additive. The correction was simply made by fitting an equation to the curves in Figures 3.3 and 3.4, adding the equations, and multiplying the sum times the temperature dependence term. The corrected diffusivity is given in Equation 3.23.

$$D = 5.7\times10^{-2}\ T^{1/2}\ e^{(-4870/RT)}[-0.02\ L + 0.1299\ OH^{0.55} + 0.58] \qquad (3.23)$$

where

D is the diffusivity [=] (sq cm/min)

T is the temperature [=] (K)

L is the lignin content [=] (% on wood)

OH is the effective alkali concentration [=] (mole/l)

R is the gas constant [=] (cal/mole K)

The constant $5.7X10^{-2}$ was determined by requiring the diffusivities from Equations 3.22 and 3.23 to be equal when the alkali concentration and lignin content of the chips used in McKibbins's study are put into Equation 3.23.

CHAPTER 4

SOLUTION METHOD

The Equations 3.7 - 3.12 are highly non-linear, coupled, partial, differential equations. The solution to these equations, therefore, must be obtained numerically. In this chapter the numerical methods used are briefly discussed. The modifications to the model to simulate the multiple chip problem is also discussed.

4.1 Simulation of a single chip

To simulate the pulping of a single chip Equations 3.7 - 3.12 are solved with a modified version of Finlayson's program Reacol (Finlayson, 1980). Reacol uses the orthogonal collocation method to reduce the partial differential equation to a system of ordinary differential equations. The ordinary differential equations are then integrated numercially with the GEARB (Hindmarsh, 1974)

integration package.

The orthogonal collocation form of Equations 3.7, 3.9, and 3.11 are shown in Equations 4.1, 4.2, and 4.3, respectively.

$$dC_j/dt = \sum_{i=1}^{N+1} A_{ji}\alpha_i \sum_{i=1}^{N+1} A_{ji}C_i + \alpha_j \sum_{i=1}^{N+1} B_{ji}C_i - Ra_j \quad j = 1,..,N \tag{4.1}$$

$$\sum_{i=1}^{N+1} A_{N+1,i}C_i = Bw(C_{bulk} - C_{N+1}) \tag{4.2}$$

$$dOH_{bulk}/dt = -\alpha_{N+1} \sum_{i=1}^{N+1} A_{N+1,i}OH_i \ (V_c/V_b) \tag{4.3}$$

where

A_{ij} is the first derivative matrix

B_{ij} is the second derivative matrix

N is the number of collocation points

The boundary condition represented by Equation 3.8 is satisfied identically by the A and B matrices.

Equations 4.1 - 4.3 are solved for a single pulp chip with the

computer program PULPER. Solution times on a PDP 11/60 computer for PULPER are on the order of 10 seconds. A typical output from PULPER is shown in Appendix B.

4.2 Simulation of multiple chips

To simulate a cook that has a distribution of chip-thicknesses, the model needs to be expanded. Because the chips are coupled together through the bulk phase alkali concentration, the equations describing each chip must be solved simultaneously. In other words, Equations 4.1 and 4.2 for each chip must be simultaneously integrated in time. The bulk phase alkali concentration for a multiple chip simulation is calculated using Equation 4.4.

$$dOH/dt = \sum_{k=1}^{NC} f_k \left(- \alpha_{N+1} \sum_{i=1}^{N+1} A_{N+1,i} OH_i (V_c/V_b)\right)_k \qquad (4.4)$$

where

f_k is the weight fraction of the k-th chip

NC is the total number of chips

Equation 4.4 is simply the sum of the weighted fluxes of alkali into each chip.

For a simulation of 5 chips using 4 collocation points the number of ordinary differential equations to be integrated simultaneoulsy in time by GEARB is equal to the following:

5(chips) x 4(collocation points) x 3(chemical species)
+1(bulk phase alkali) = 61 ordinary differential equations

The solution time on a VAX 11/780 computer for the multiple chip problems varies from on the order of 1 minute for a 4 chip problem, to on the order of a day for an 80 chip problem. Methods of reducing the compution time for large problems are discussed in Section 7.2. The multiple chip simulator is called DPULPER and its output is virtually identical to the one shown in Appendix B for PULPER.

CHAPTER 5

VERIFICATION OF THE MODEL

The accuracy of the model is checked by comparing the model predictions with published literature data. In this chapter the verification of the kinetic equations is presented first; followed by a discussion of the model's predictions of the effect of chip-thickness on pulp properties and the proposal of a new method of predicting screen rejects. Finally, model predictions of the properties of a pulp produced from a known distribution of chip-thicknesses is discussed.

It should be emphasized that all the predictions are *a priori*, and that none of the data used to check the model were used in its derivation. Occasionally, however, the kinetic equations presented in Section 3.3.1 are slightly modified to accomodate differences in the pulping rates of different species. It will be noted in the discussion where these modifications have been made.

5.1 Verification of the kinetic equations

The accuracy of the kinetic equations was checked by comparing the model predictions with the data of Aurell and Hartler (1965) and Matthews (1974). These two studies were chosen because they both present the lignin content and carbohydrate content versus time curves for chips cooked under typical pulping conditions. Aurell and Hartler's data also include the alkali consumption.

The cooking conditions used by Aurell and Hartler are given in Table 5.1, and Figures 5.1 - 5.6 compare the model predictions with the experimental results. Case 1 corresponds to the 25 % effective alkali cook, and Case 2 the 15 % effective alkali cook. These two experiments are a good test for the model because the alkali concentrations are at the extremes used in commercial pulping. The comparison between the predicitions and data is seen to be very good.

To compare the model predictions with Matthews's data, the bulk phase carbohydrate reaction rate was adjusted to 0.20 x dL/dt. The value of 0.20 was derived by fitting a line through Matthews's bulk period lignin content vs. carbohydrate content data. The difference between Matthews's value of 0.20 and Rekunen's (1980) value 0.47 results from species differences in the two studies. The model predictions of Matthews's data are shown in Figure 5.7 and 5.8. The

	Case 1	Case 2
Effective alkali concentration	25 % on wood as NaOH	15.75 % on wood as NaOH
Sulfidity	25 %	25 %
Heating time	120 min.	120 min.
Cooking time	240 min.	240 min.
Liquor/Wood ratio	4 l/Kg	4 l/Kg
Cooking temperature	170 C	170 C
Lignin content	27.3 % on wood	27.3 % on wood
Carbohydrate content	67.7 % on wood	67.7 % on wood
Acetyl content	1.3 % on wood	1.3 % on wood
Species:	Pinus silvestris	
Chip-thickness	3 mm	

Table 5.1. Cooking conditions used by Aurell and Hartler (1965).

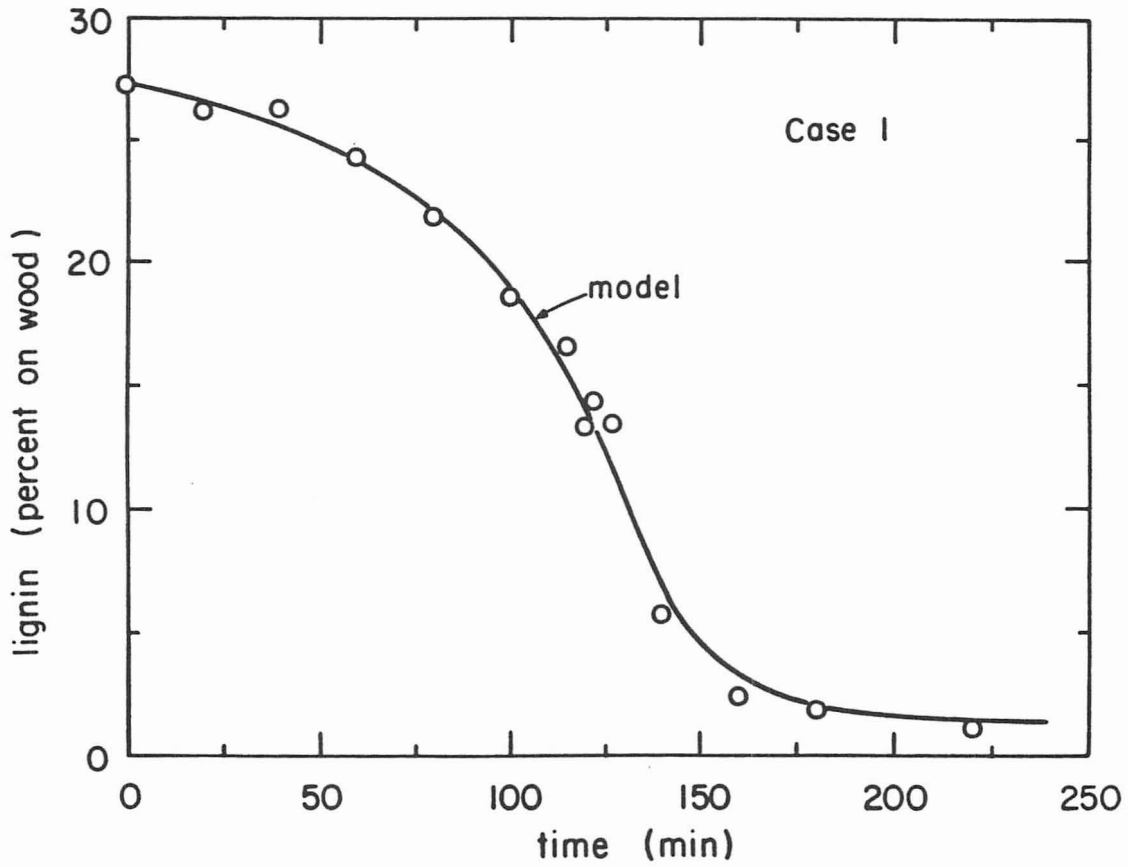

Figure 5.1. Model prediction and Aurell and Hartler's (1965) lignin content data.

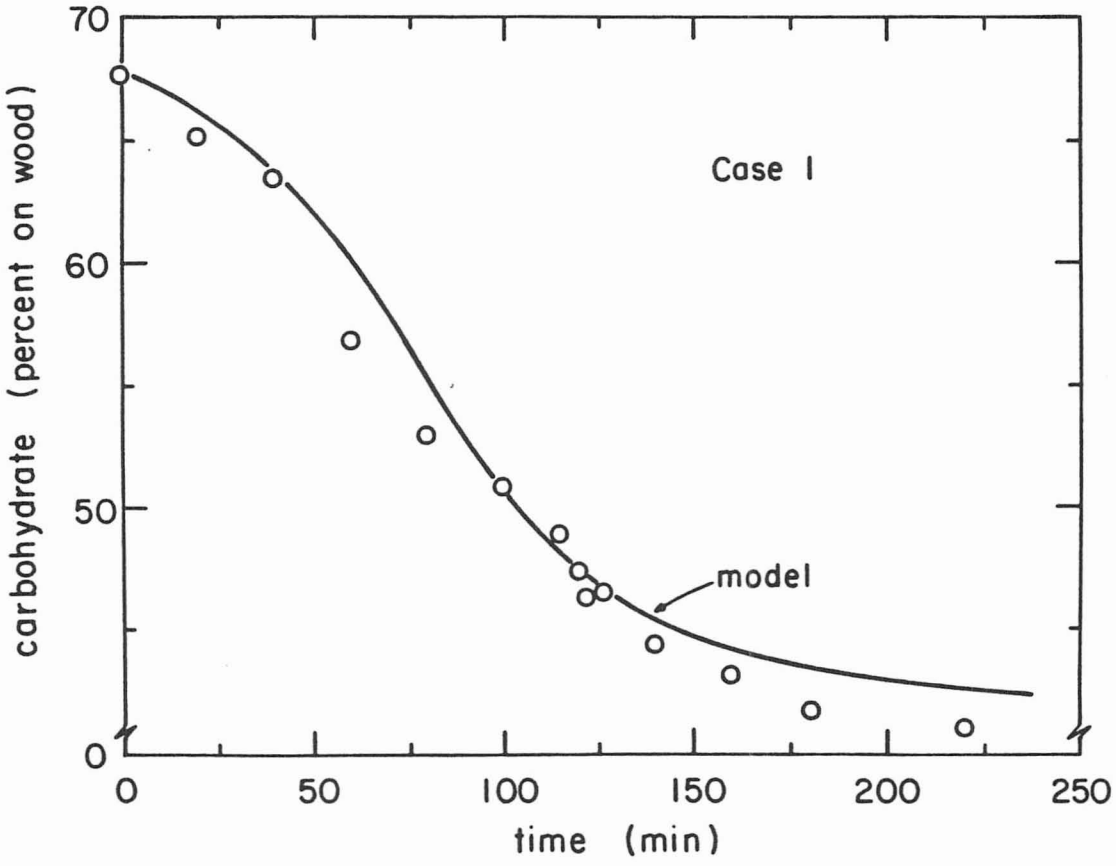

Figure 5.2. Model prediction and Aurell and Hartler's (1965) carbohydrate content data.

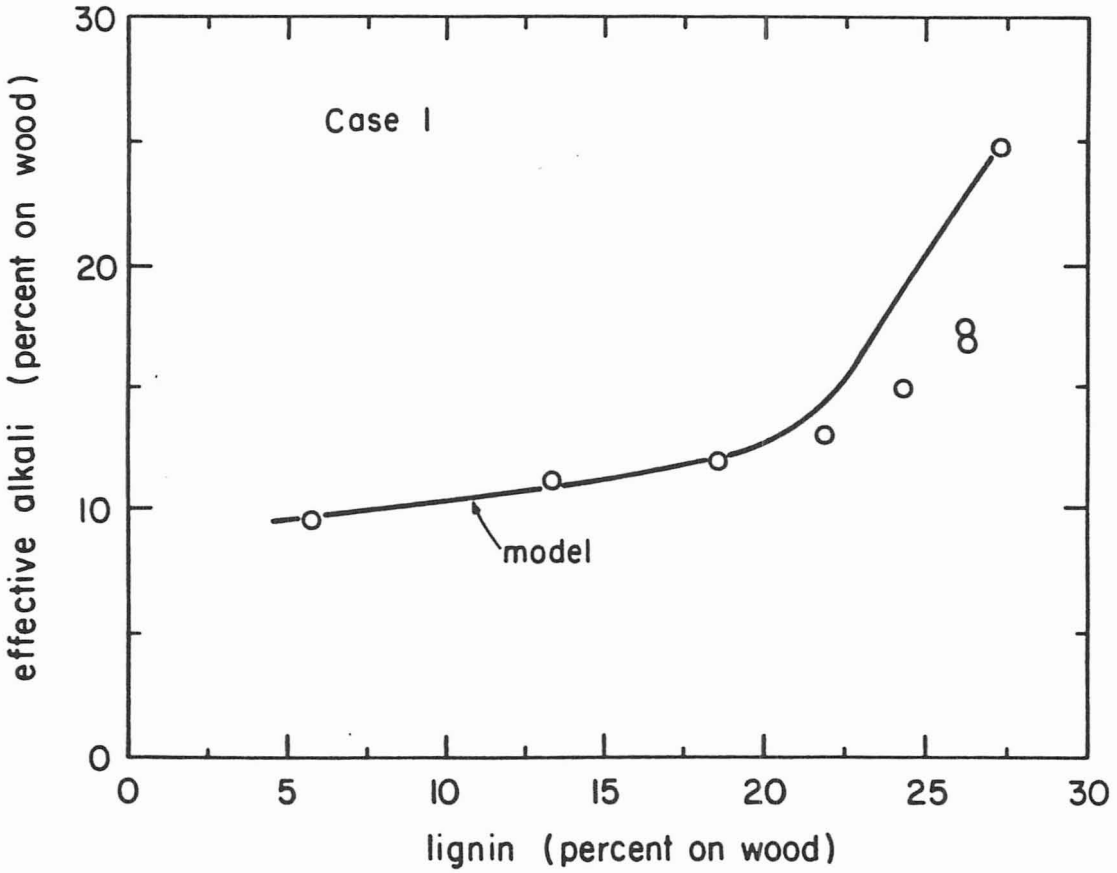

Figure 5.3. Model prediction and Aurell and Hartler's (1965) effective alkali concentration data.

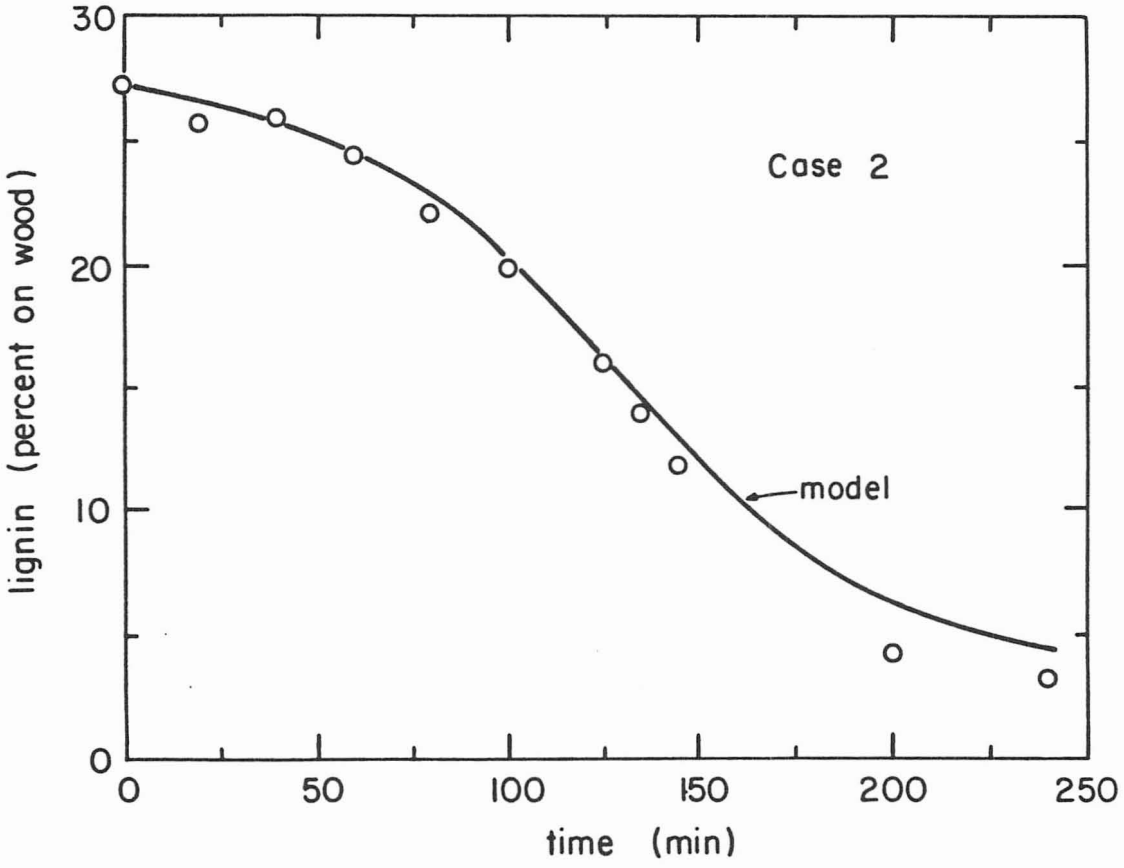

Figure 5.4. Model prediction and Aurell and Hartler's (1965) lignin content data.

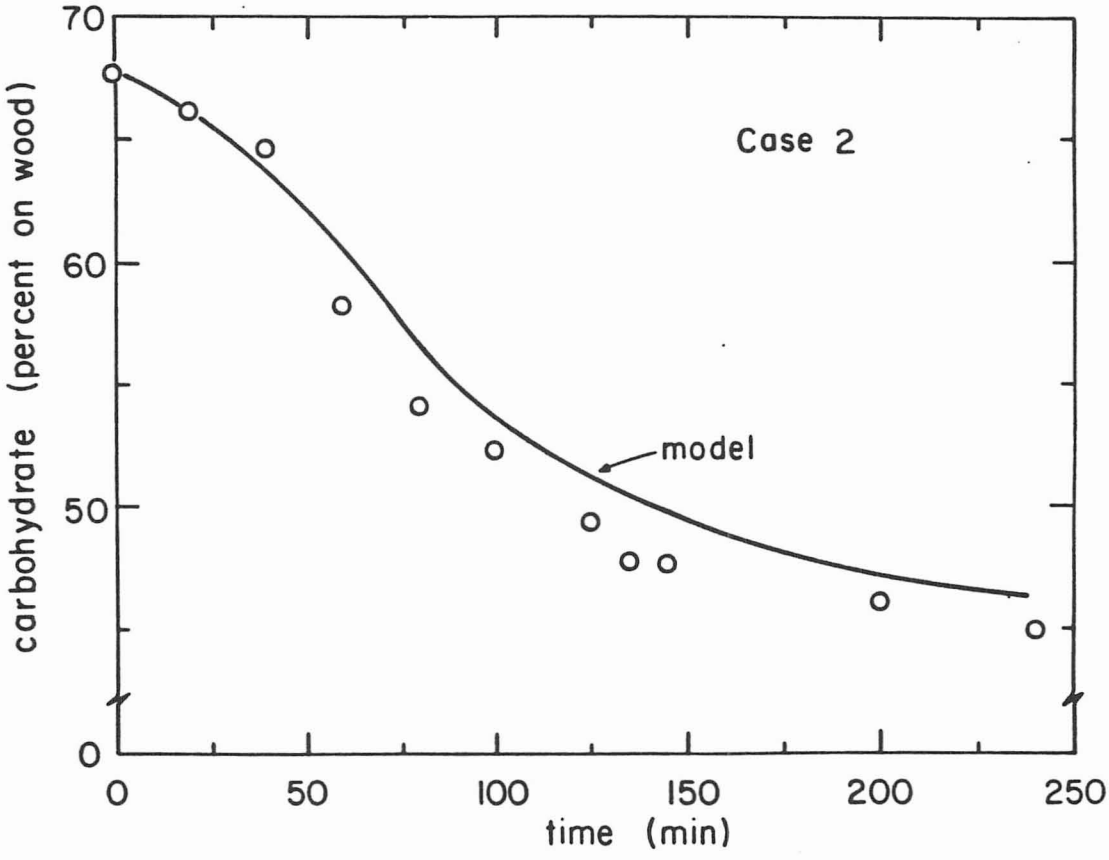

Figure 5.5. Model prediction and Aurell and Hartler's (1965) carbohydrate content data.

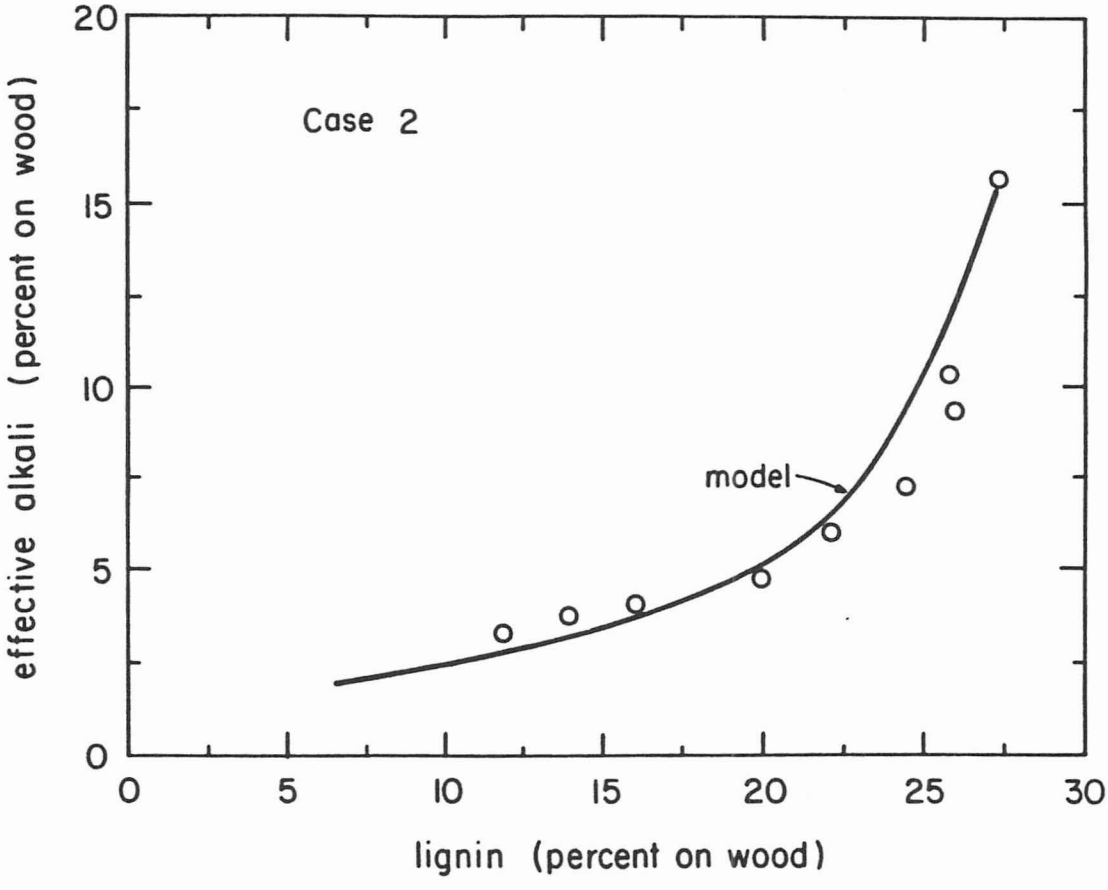

Figure 5.6. Model prediction and Aurell and Hartler's (1965) effective alkali data.

Effective alkali concentration	18.4 % on wood as NaOH
Sulfidity	22 %
Heating time	90 min.
Cooking time	180 min.
Liquor/Wood ratio	5 l/Kg
Cooking temperature	170 C
Lignin content	27.2 % on wood
Carbohydrate content	66.5 % on wood
Acetyl content	1.3 % on wood
Species:	Pinus elliottii
Chip-thickness	3 mm

Table 5.2. Cooking conditions used by Matthews (1974).

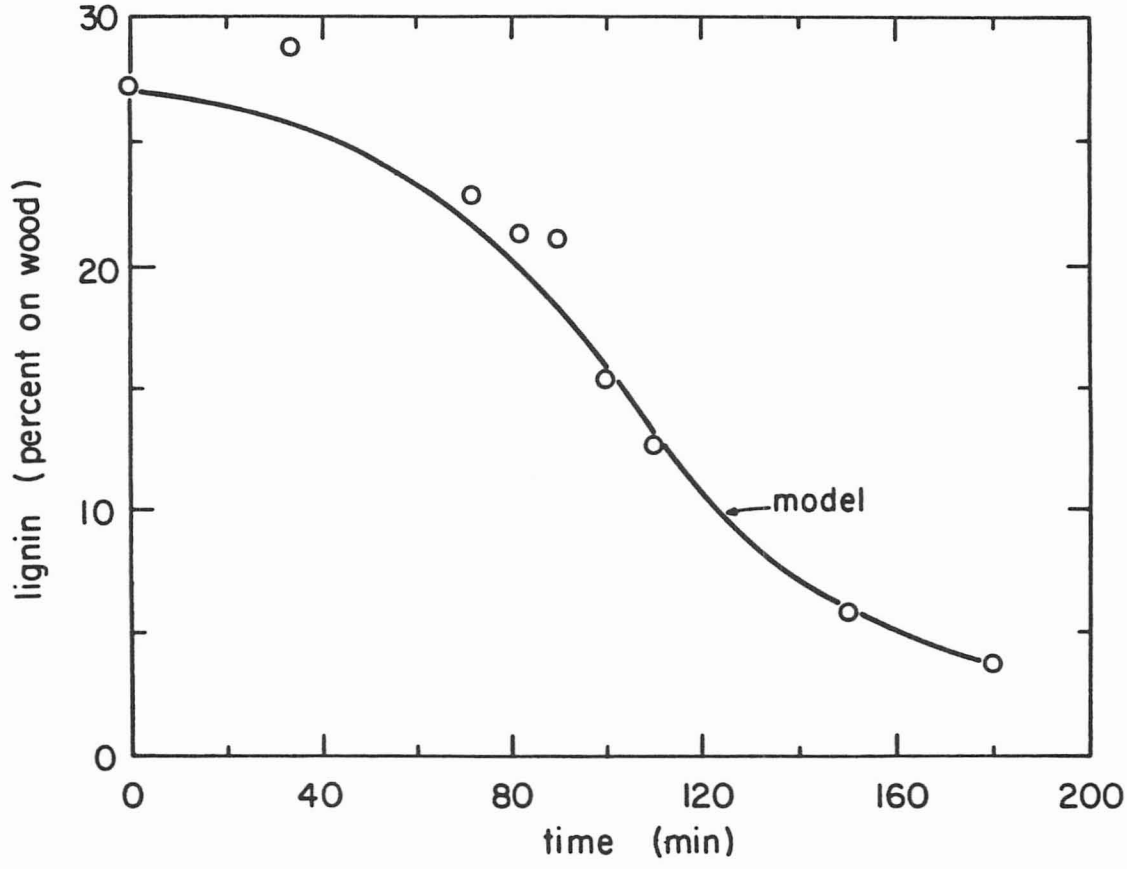

Figure 5.7. Model prediction and Matthews's (1974) lignin content data.

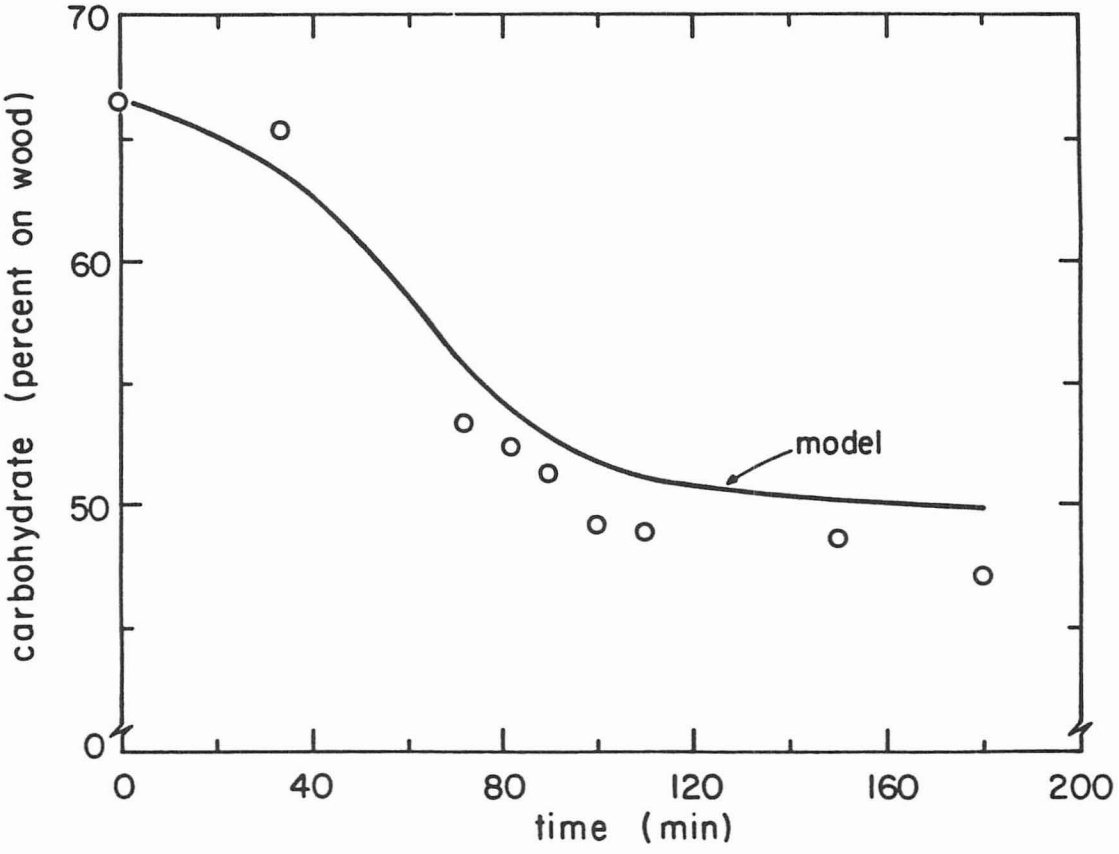

Figure 5.8. Model prediction and Matthews's (1974) carbohydrate content data.

cooking conditions used by Matthews are shown in Table 5.2. The comparison is again seen to be good.

Figures 5.1 - 5.8 illustrate the kinetic equations used in the model are very good; however, there are some differences between the model predictions and the experimental results that should be noted. In comparing the lignin versus time curves with the carbohydrate versus time curves, it can be seen that the lignin vs. time predictions are more accurate. This difference reflects the fact that the delignification kinetics have been more throughly studied and are therefore better understood than the carbohydrate kinetics. In Figures 5.3 and 5.6 it can be seen that the model predictions of the alkali concentration during the initial period is high. This discrepancy is unimportant because the initial period kinetics are slightly dependent on the alkali concentration.

5.2 Verification of the chip-thickness simulations

The model's ability to predict the effects of chip-thickness was tested next. For this test the data of Akhtaruzzaman and Virkola (1979, 1980) and the data of Hatton and Keays (1973) were used.

The cooking conditions used by Akhtaruzzaman and Virkola are given in Table 5.3. Figures 5.9 through 5.14 show the model

	Case 1	Case 2	Case 3
Effective alkali concentration	19 % on wood (NaOH)	22 % on wood (NaOH)	25 % on wood (NaOH)
Sulfidity	30 %	30 %	30 %
Heating time	60 min.	60 min.	60 min.
Cooking time	120, 211, 301 min.	120, 211, 301 min.	120, 211, 301 min.
Liquor/Wood ratio	4 l/Kg	4 l/Kg	4 l/Kg
Cooking temperature	170 C	170 C	170 C
Lignin content	27 % on wood	27 % on wood	27 % on wood
Carbohydrate content	67.7 % on wood	67.7 % on wood	67.7 % on wood
Acetyl content	1.3 % on wood	1.3 % on wood	1.3 % on wood
Species:	Pinus silvestris		

Table 5.3. Cooking conditions used by Akhtaruzzaman and Virkola (1979,1980).

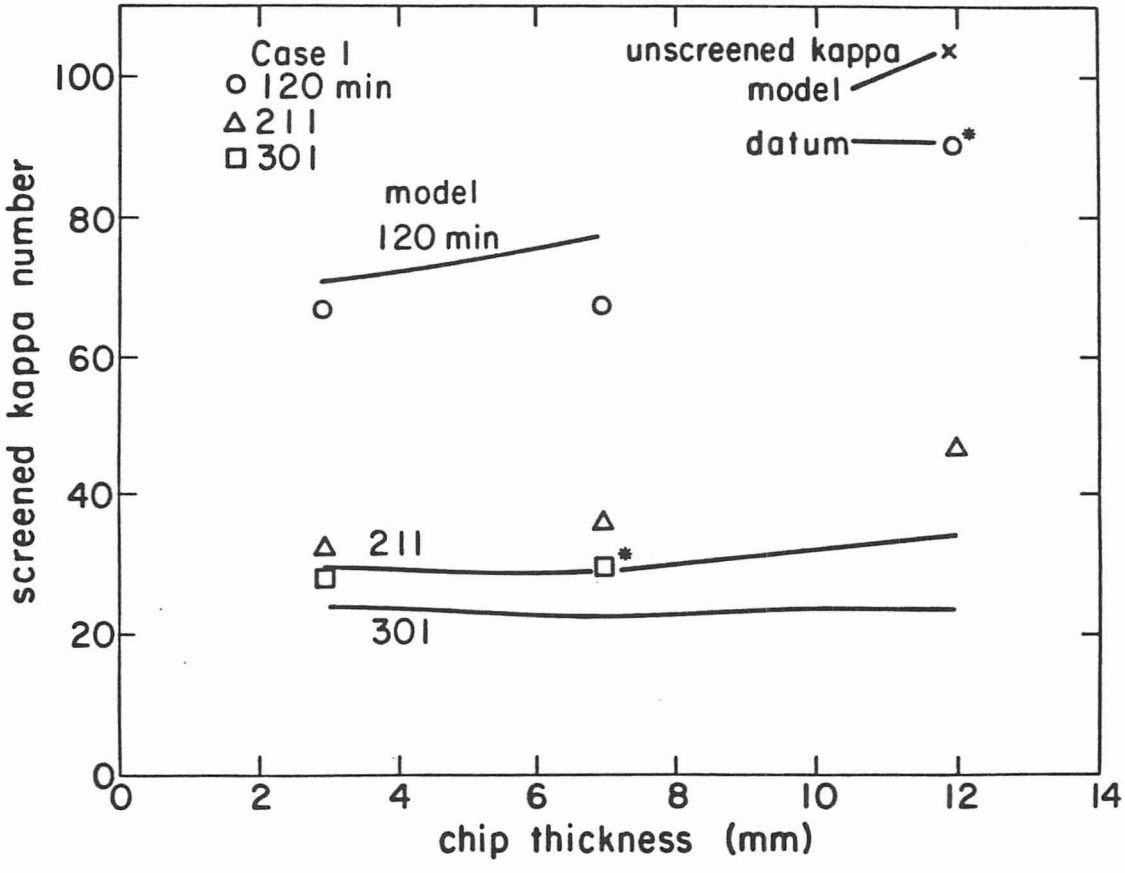

Figure 5.9. Model predictions and Akhtaruzzaman and Virkola's (1979, 1980) screened kappa data.

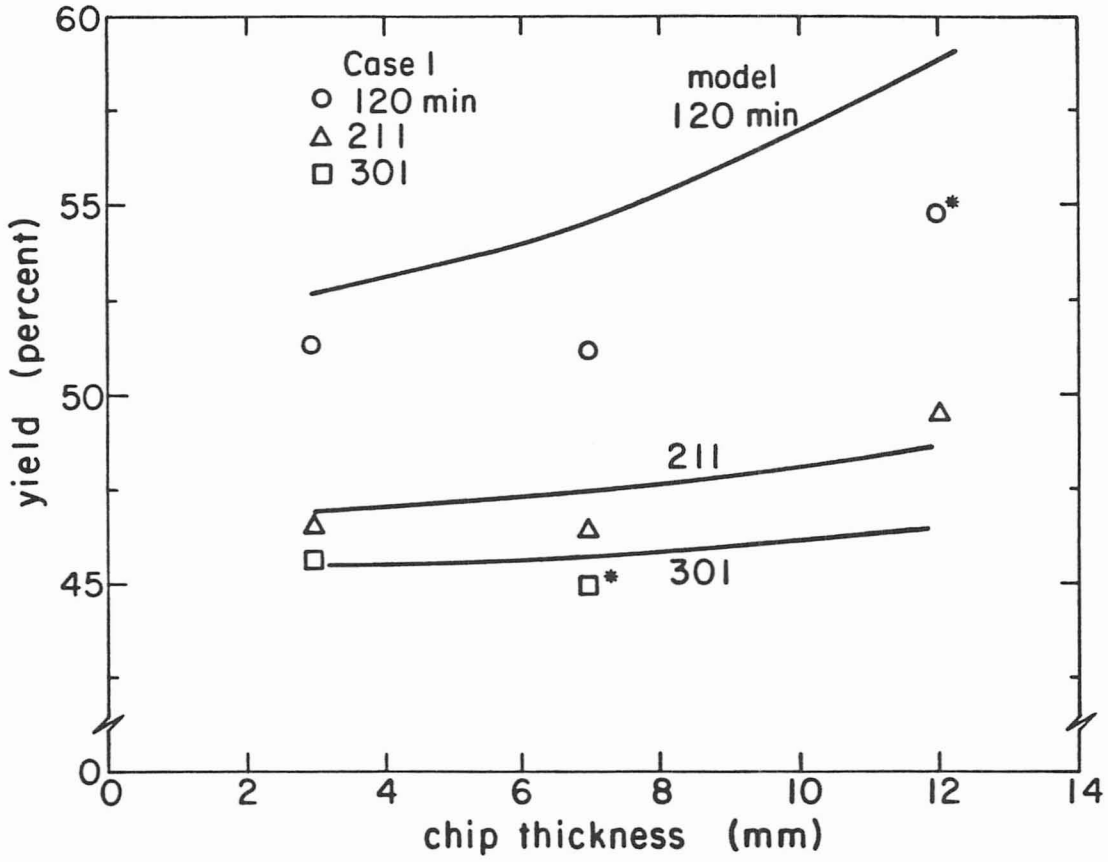

Figure 5.10. Model predictions and Akhtaruzzaman and Virkola's (1979, 1980) yield data.

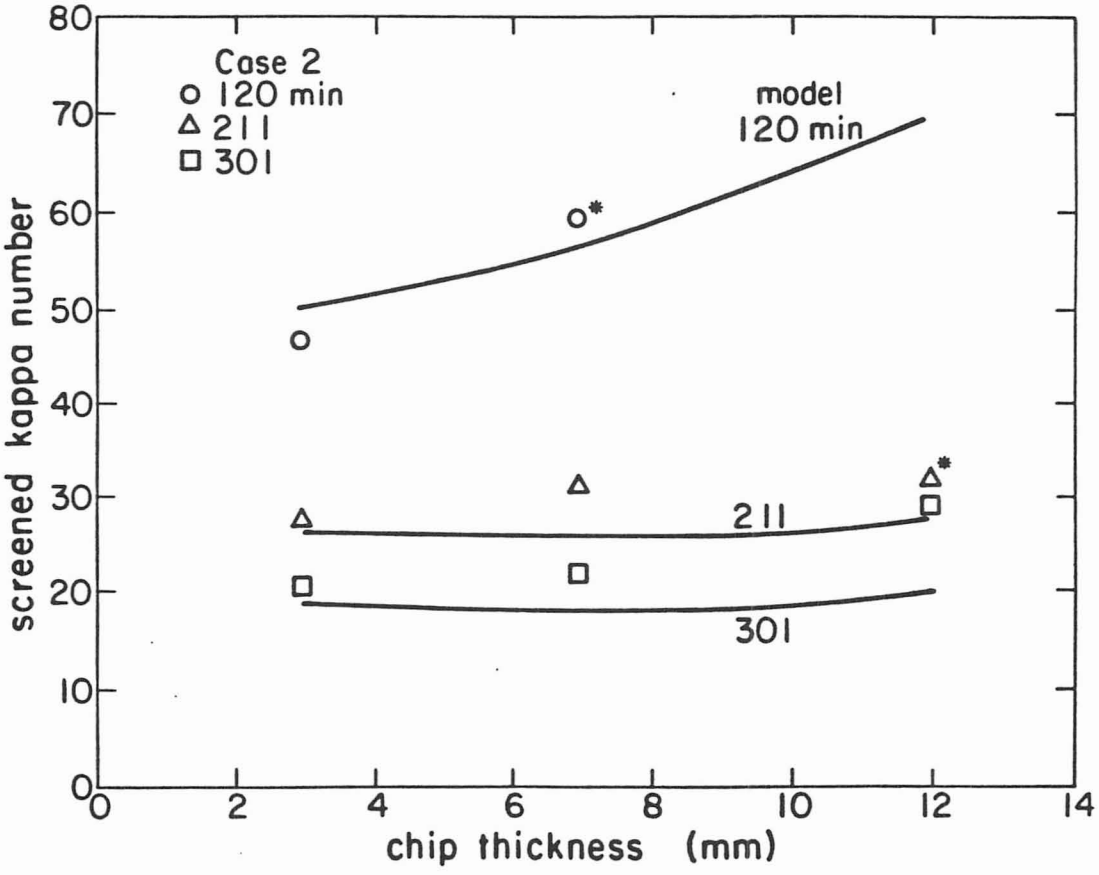

Figure 5.11. Model predictions and Akhtaruzzaman and Virkola's (1979, 1980) screened kappa data.

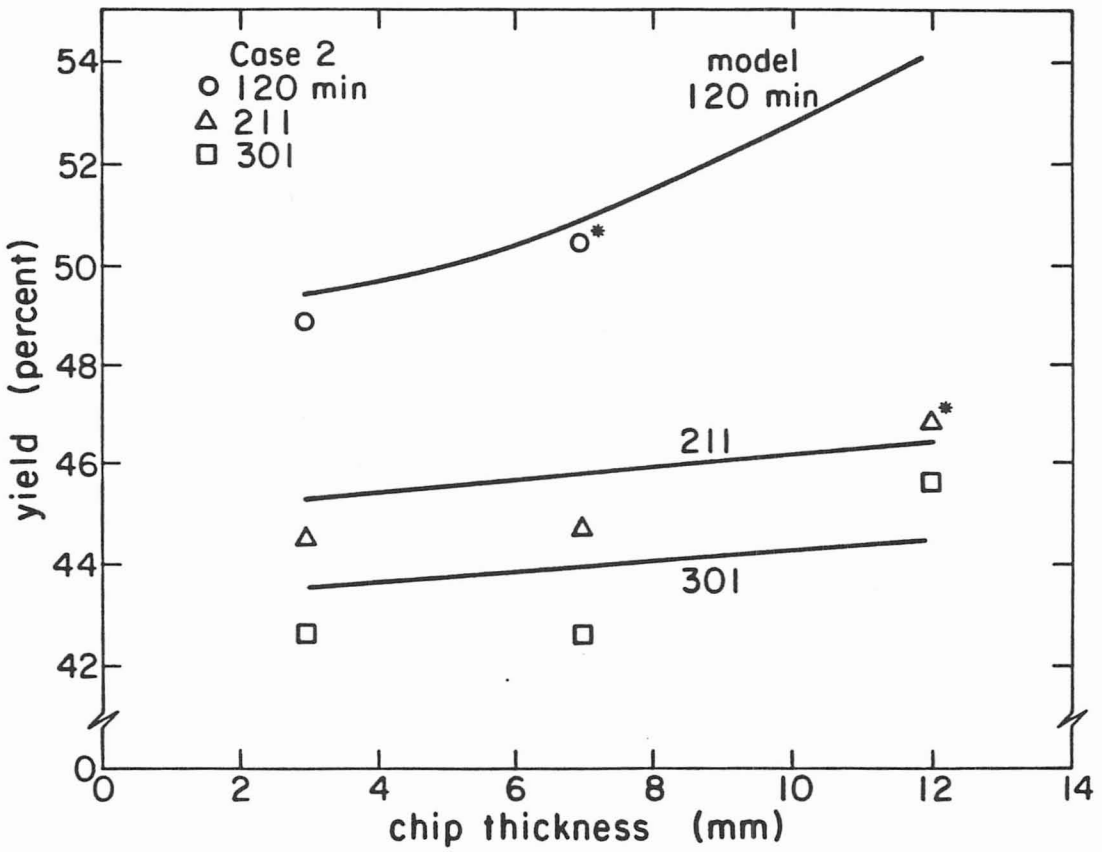

Figure 5.12. Model predictions and Akhtaruzzaman and Virkola's (1979, 1980) yield data.

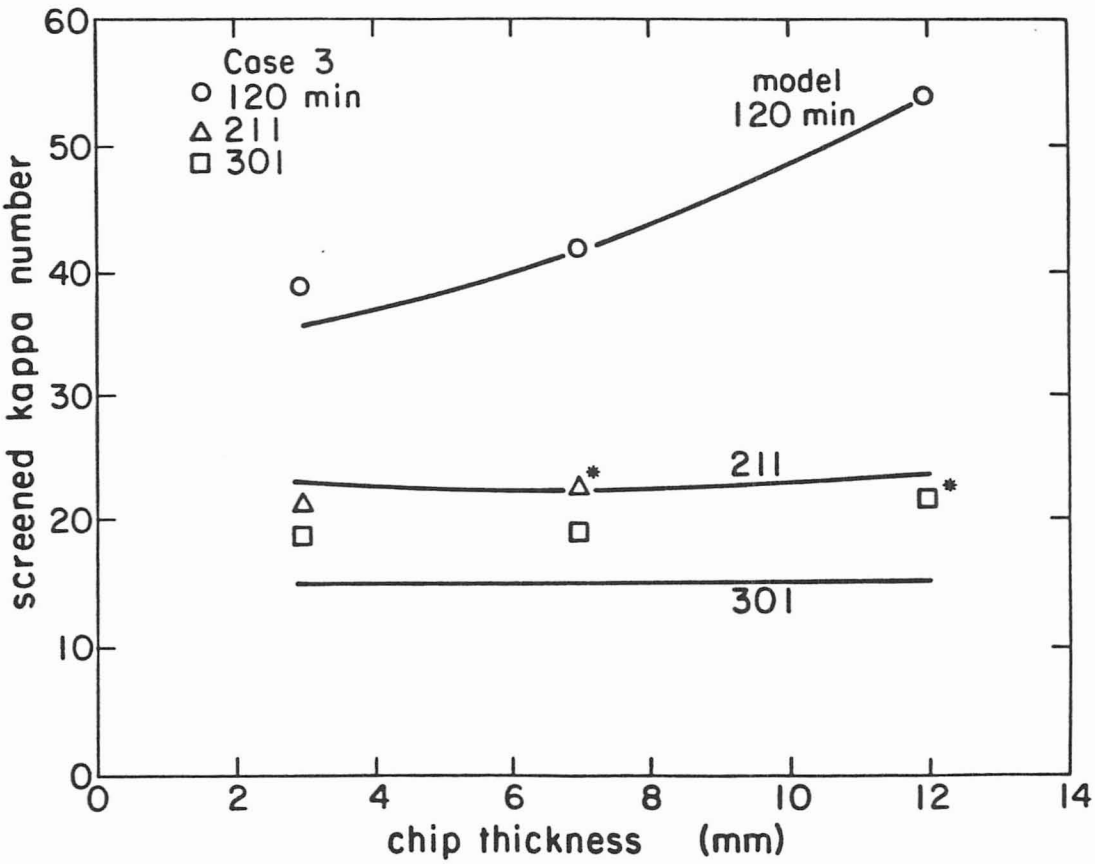

Figure 5.13. Model predictions and Akhtaruzzaman and Virkola's (1979, 1980) screened kappa data.

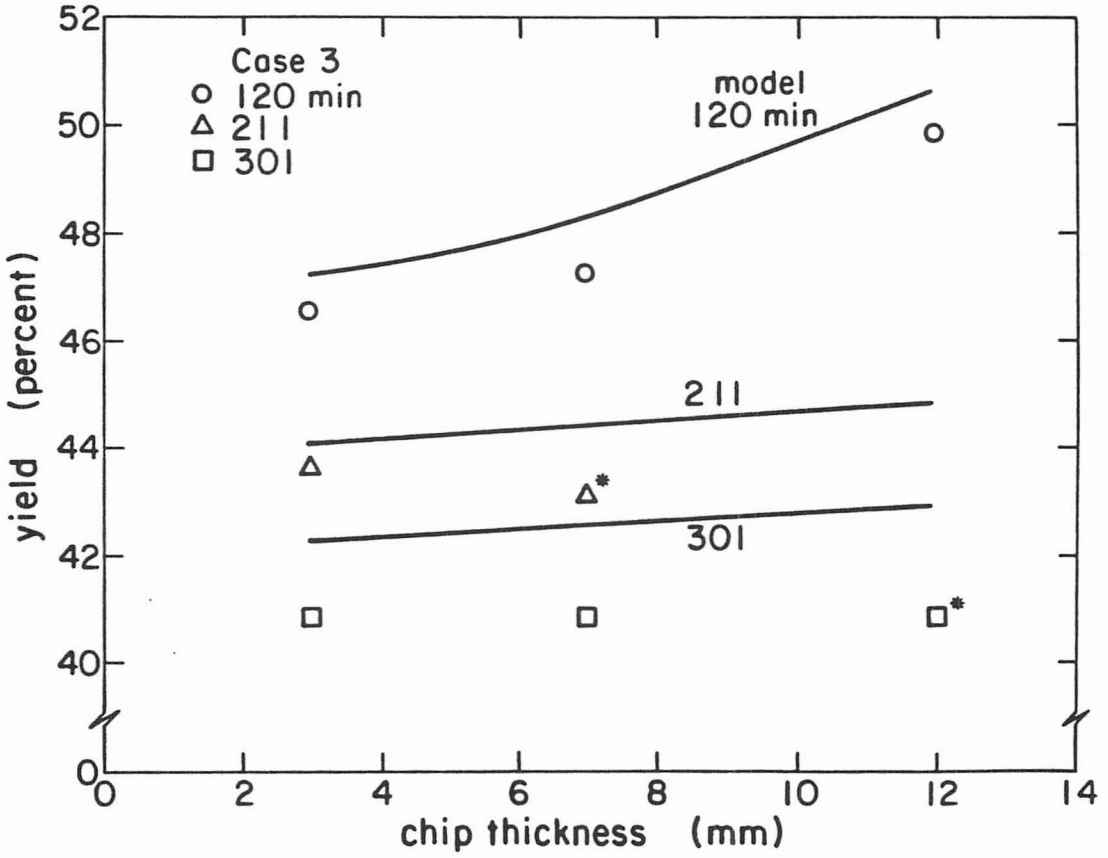

Figure 5.14. Model predictions and Akhtaruzzaman and Virkola's (1979, 1980) yield data.

predictions and data of screened kappa number vs. chip-thickness and of yield vs. chip-thickness for the three pulping conditions studied. The difference in these three pulping conditions is the effective alkali concentrations. The model was tested for all three cases to explore the limits of the model. Akhtaruzzaman and Virkola ran one other experiment on chips 12 mm thick and and 33 mm long with the pulping conditions shown in Table 5.3 except with a 28 % effective alkali charge. The results from this experiment are anomalous and are not consistent with their other experimental results, and therefore they were not used for checking the model. Comparison of the results from the 25 % effective alkali cook on 12 mm thick chips to the 28 % effective alkali cook show that the 28 % effective alkali cook produced 52 % more rejects and had a screened kappa of only 1 point less than the 25 % effective alkali cook; i.e., less pulping under more severe conditions was achieved. The stared (*) points are results of experiments with chips 33 mm in length corrected to 24 mm using the authors's correlation equations, which lower the kappa numbers by 2.8 and the yields by 0.69. The rest of the points are data for chips 24 mm in length. The model screened kappa numbers were calculated from the lignin content of the modeled 'chip' excluding the area in the center of the chip whose weight equals the experimental reject value. The kappa numbers were calculated by dividing the weight per cent of the lignin on the accept pulp by 0.15. It can be seen that the model generally predicts the experimental results well.

The model predicts that the effect of chip-thickness on kappa and yield is negligible at long cooking times, but the data show that this is not true for all pulping conditions (see Figures 5.9 - 5.12). There are two possible explanations for this difference. First, Akhtaruzzaman and Virkola state that the thicker chips have a higher percentage of knot wood than the thin chips, and they speculate that the thicker chips contain more tension and compression wood than the thin chips. These types of wood pulp slower than normal wood. It is not suprising, therefore, that the model, which assumes the chips are uniform, predicts kappa numbers and yields that are lower than the values measured in thick chips at long cooking times. Second, the conditions at the center of the thick chips are suitable for condensation reactions to take place. Work published by Hartler (1978) shows that lignin condenses when the cooking liquor lignin concentration is high and the alkali concentration is low.

High lignin concentration and low alkali concentration in the cooking liquor exist at the center of thick chips during pulping. For example, the model predicts that in 12 mm chips pulped in 19 % effective alkali liquor to an H factor of 540, the center effective alkali concentration is only 0.02 M while the concentration in the bulk phase is 0.68 M. At this same time all the initial period lignin has been solubilized, and because the diffusivity of lignin oligomers in wood is certainly low, we can expect the liquor lignin

concentration at the chip center to be high. The presence of condensed lignin will result in a higher lignin content than predicted by assuming all the delignification reactions are irreversible (Assumption 6).

The model does not predict the experimental result that the consumption of effective alkali is independent of chip-thickness (see Figure 5.15). (Only this result is shown because it is representative of those obtained from the simulation of the other experiments). This result experimental is surprising and is not substantiated by other studies on the effect of chip-thickness (Hatton and Keays, 1973; Colombo et al., 1960) (see Figure 5.18). Furthermore, Akhtaruzzaman and Virkola found that when chips of different dimensions are pulped together, higher rejects, higher yields, and lower screened kappa numbers are obtained than are predicted from the data obtained by pulping the chips individually. The authors explain this result, and I think correctly, by saying that when chips of different dimensions are pulped together, the smaller chips consume alkali at the expense of the larger chips. As a result, in mixtures, the small chips are over-cooked and the large chips are under-cooked as compared to what they would be if pulped individually. This consequence is inconsistent with the experimental result that the alkali consumption is independent of chip-thickness but is consistent with the model prediction shown if Figure 5.15. The difference between the prediction and the

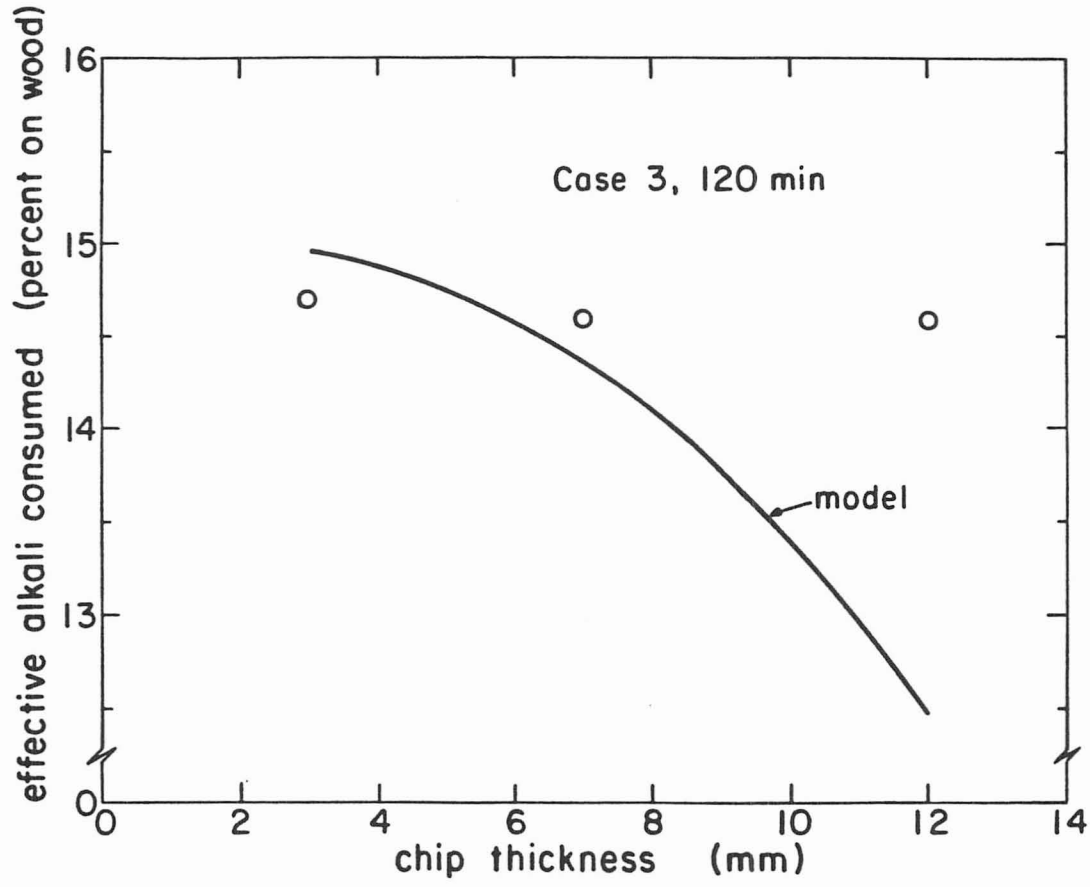

Figure 5.15. Model prediction and Akhtaruzzaman and Virkola's (1979, 1980) effective alkali concentration data.

experimental result shown in Figure 5.15 may be attributed to the difficulty in measuring the effective alkali concentration in kraft liquor mentioned in Section 3.3.2.

Hatton and Keays (1973) measured the effect of chip-thickness on hemlock and spruce pulp properties. To test the model on Hatton's data, an adjustment in the bulk delignification reaction rate was made. Hatton's data show that spruce and hemlock have equal reaction rates, and Kleinert's kinetic study (1966) on spruce shows that the bulk delignification reaction rate in spruce is greater than Equation 3.17 predicts. The adjustment, then, was simply to increase the bulk delignification reaction rate term, Equation 3.17, by 20 % so that it predicts Kleinert's data.

The cooking conditions used by Hatton are shown in Table 5.4. Figures 5.16 through 5.18 are plots of screened kappa, yield, and alkali consumption versus chip-thickness for the hemlock experiments. The experimental results are for chips 41.4 mm in length. In Figures 5.16 and 5.17 the actual data are presented. These data were obtained from Ludden's Ph.D. dissertation (1977). In Figure 5.18 Hatton's correlation of the data is shown. The correlation coefficient, R^2, for Hatton's regression is only 0.58, which reflects the difficulty in measuring alkalinities in the pulping liquor. Hatton's data is variable for thicker chips and is sometimes inexplicable. (For example, the three point drop in yield

Effective alkali concentration	22 % on wood as NaOH
Sulfidity	25 %
Heating time	135 min.
Cooking time	210 min.
Liquor/Wood ratio	4.6 l/Kg
Cooking temperature	170 C
Lignin content	27.8 % on wood
Carbohydrate content	70.0 % on wood
Acetyl content	1.0 % on wood
Species:	Tsuga heterophylla

Table 5.4. Cooking conditions used by Hatton and Keays (1973).

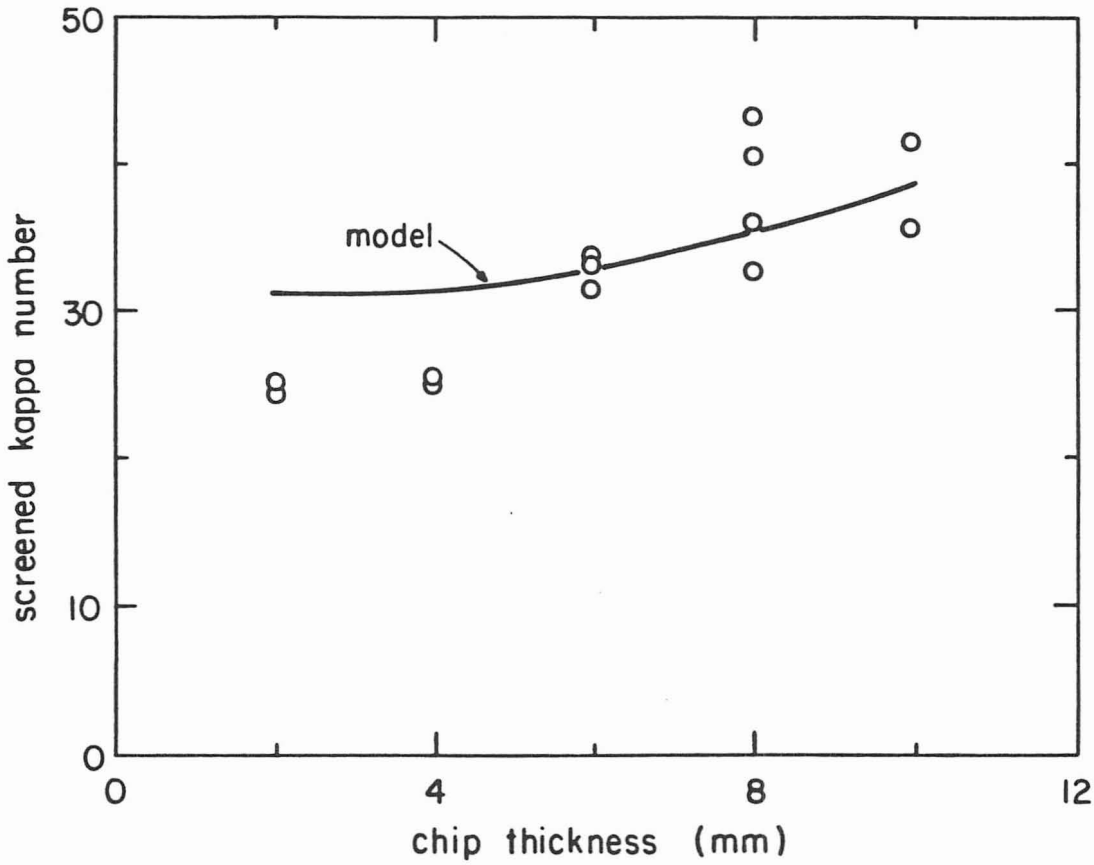

Figure 5.16. Model prediction and Hatton and Keays's (1973) screened kappa data.

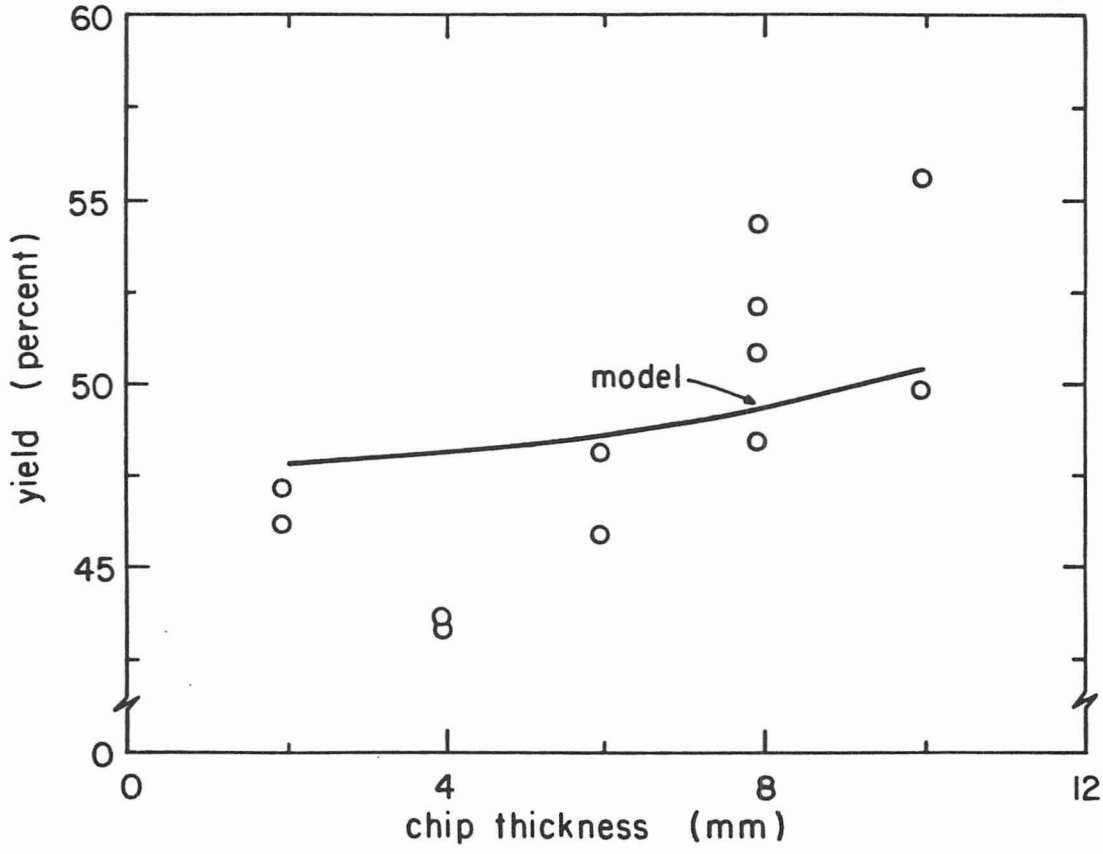

Figure 5.17. Model prediction and Hatton and Keays's (1973) yield data.

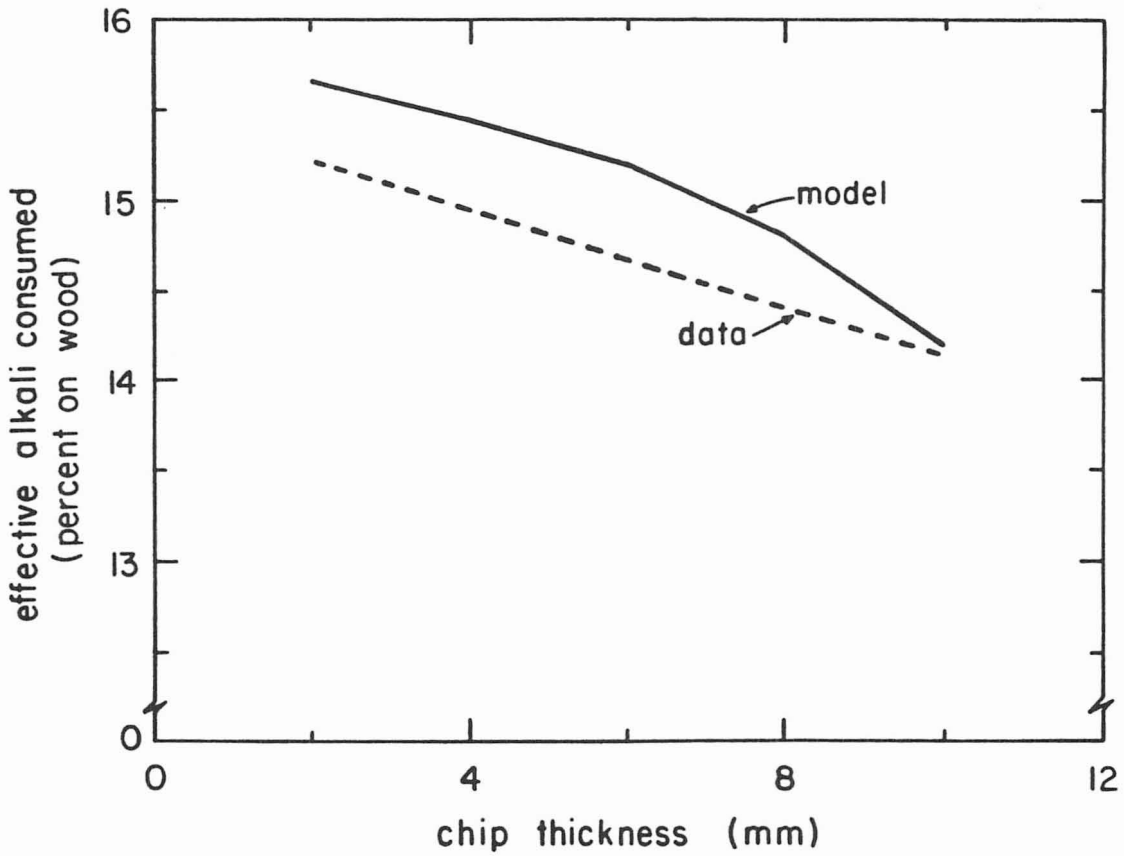

Figure 5.18. Model prediction and Hatton and Keays's (1973) effective alklai concentration data.

in going from a 2 mm to 4 mm thick chips shown in Figure 5.17). Therefore, there is considerable uncertainty in using those data to assess the accuracy of the model predictions. It can be seen from Figures 5.16 - 5.17 that the model predicts very close to or within the range of all the experimental data except for the 2 mm and 4 mm screened kappa data. And even here the difference between the experimental data and model predictions is only six points.

The model failed to predict Hatton and Keays's spruce results and this failure can be explained by reference to Table 5.5. The 10 mm, 8 mm , and 6 mm spruce chips pulps have much greater yields and reject values, at the equivalent kappa number, than the hemlock chip pulps. This means that the lignin profile in the spruce chips is very sharp.

The most reasonable explanation of Hatton's spruce data is that the impregnation of the chips was poor. The penetration in spruce wood has been shown to be slow (Stone, 1956). Futhermore, Hatton and Keays used laboratory cut chips, which have been shown to yield higher rejects than commercial chips (Colombo et al., 1964), presumably because of the enhanced penetration in the highly fissured commercial chips. The assumption of good impregnation incorporated in the model may not be appropriate for laboratory cut spruce chips.

	HEMLOCK			SPRUCE		
Chip-thick.(mm)	Screen kappa	Yield (%)	Screen Rejects(%)	Screen Kappa	Yield (%)	Screen Rejects(%)
2	24.3	46.65	0.2	23.0	47.4	0.1
4	24.35	43.55	0.3	30.3	49.4	1.0
6	31.67	47.3	3.6	35.0	54.0	10.3
8	37.03	51.28	9.15	37.0	58.4	19.0
10	37.25	52.55	12.3	39.0	61.1	22.8

Table 5.5. Pulping results of spruce and hemlock pulps, chip length of 41.4 mm, reported by Hatton and Keays (1973).

5.3 Rejects from oversized chip

In pulping of oversized chips it is generally believed that those fibers whose lignin content is above a critical level, called the fiber liberation point, will not be liberated from the chip and will form a screen reject. Values of the fiber liberation point are typically about 9 - 10 % on wood.

When simulating the data of Akhtaruzzaman and Virkola (1979,1980) and Hatton and Keays (1973), it was noted that the fiber liberation point was not constant. Figure 5.19 is a plot of reject values measured experimentally by Akhtaruzzaman and Virkola versus the fiber liberation point predicted by the model with the assumption that the reject is the area in the center of the chip whose weight equals the experimental reject value. It can be seen that the range of fiber liberation points is quite large and the values for the fiber liberation points are lower than expected. This same conclusion is evident in Tyler's (1981) predictions of screen rejects using a fiber liberation point of kappa 98.

It was suggested by N.L. Ricker (1981) that the normalized second moment (NSM) of the lignin profile in the chips might correlate with rejects. The NSM is defined as the following:

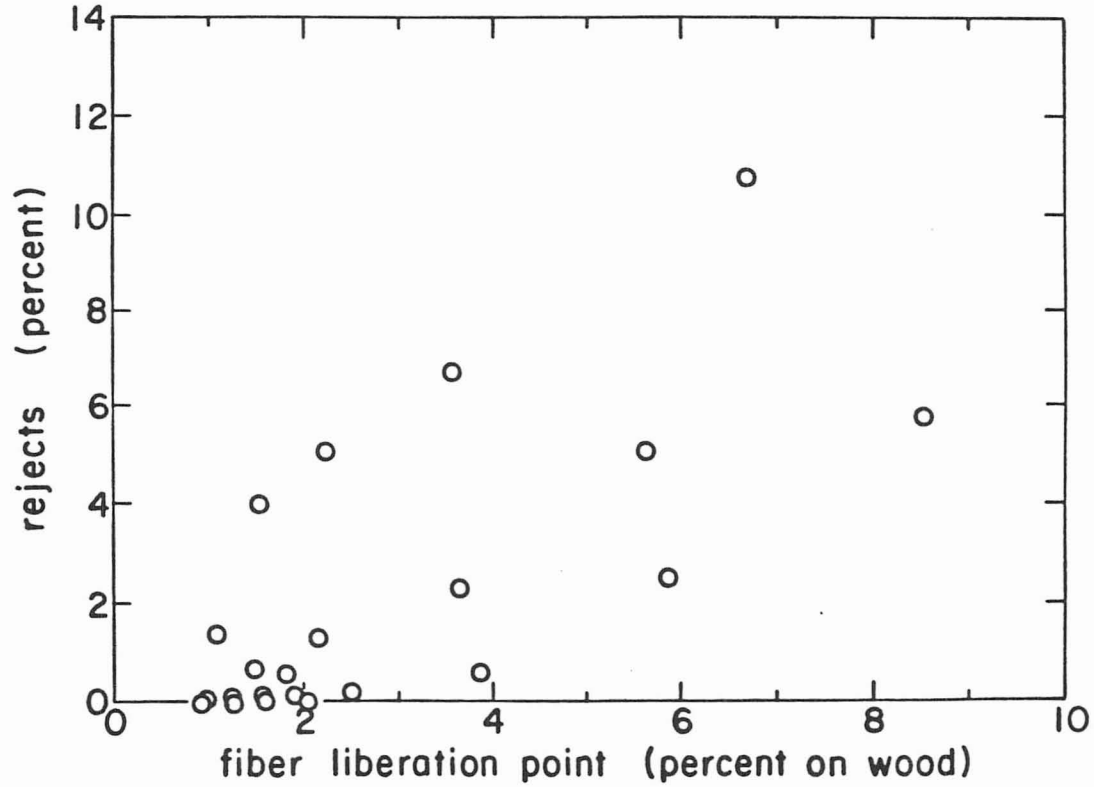

Figure 5.19. Correlation between the reject data of Akhtaruzzaman and Virkola (1979,1980) and the fiber liberation point predicted by the model.

$$\frac{\int_0^1 L\, x^2\, dx}{\int_0^1 L\, dx} \qquad (5.1)$$

where

L is the lignin content

x is the dimensionless distance from the chip center

The second moment of a distribution, which for a Gaussian distribution is the variance, is smaller the steeper the lignin profile. A plot of the lignin NSM versus the experimental reject levels measured by Akhtaruzzaman and Virkola is shown if Figure 5.20. It can be seen that the correlation is good., $R^2 = 0.90$. Hatton and Keays (1973) reject data gave similar results, as shown in Figure 5.21.

At first it seems strange that the reject levels depend not on the absolute value of the lignin content at the chip center, but on the profile of the lignin content in the chip. The physical explanation for the good correlation between the NSM and the reject levels may relate to the condensation reactions. Those chips with the lowest NSM, and thus the steepest lignin profiles, have had during the cook a time when the alkali concentration is low and the cooking liquor lignin concentration is high. Thus, it is those chips with the lowest NSM in which lignin has been condensing. The

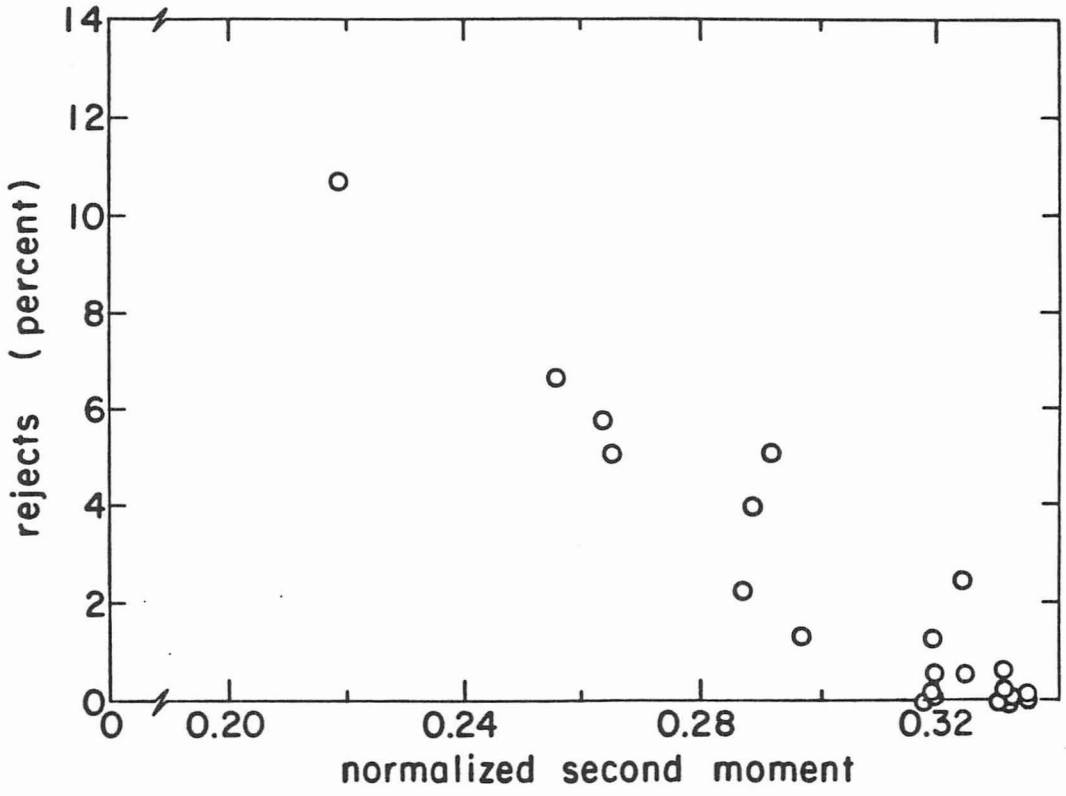

Figure 5.20. Correlation between the reject data of Akhtaruzzaman and Virkola (1979,1980) and the normalized second moment of the model.

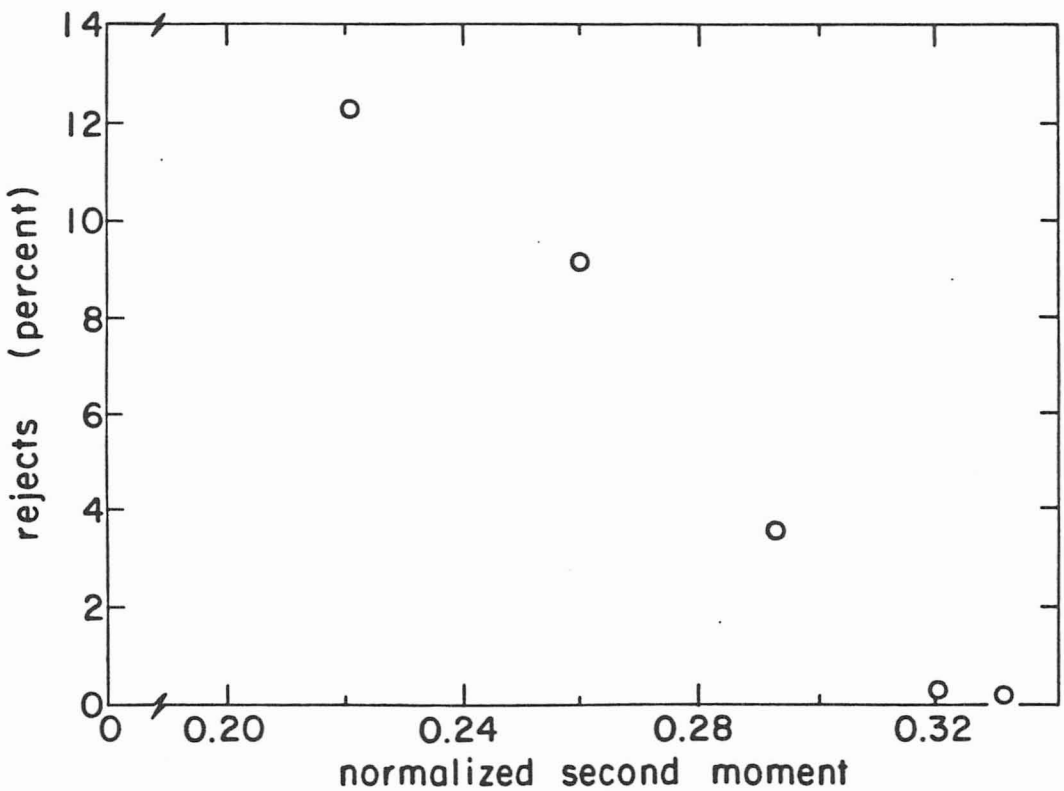

Figure 5.21. Correlation between the reject data of Hatton and Keays (1973) and the normalized second moment of the model.

condensing lignin may increase the bonding between fibers thus lowering the fiber liberation from that value observed in the absence of condensation reactions. Experiments need to be performed to confirm if the condensed lignin increases the fiber liberation point.

5.4 Verification of chip-thickness distribution simulations

To simulate commercial digesters the model must predict the properties of a pulp made from chips with a distribution of thicknesses. To check the model's ability to simulate a cook with a distribution of chip-thicknesses, the data of Akhtaruzzaman and Virkola (1979, 1980) were used. The cooking conditions they used for the chip-thickness distribution experiments, which are the same as for the individual chip experiments, are shown in Table 5.3. The thickness distribution of the chips Akhtaruzzaman and Virkola pulped is shown in Table 2.1. The length of these chips varies from 15 mm - 33 mm.

The model predictions of the experimental results are shown in Figures 5.22 - 5.23 and in Table 5.6. The screened kappa are calculated as in the single chip simulations, except that the reject values for the individual chips, which would be difficult to measure, are calculated from the normalized second moment

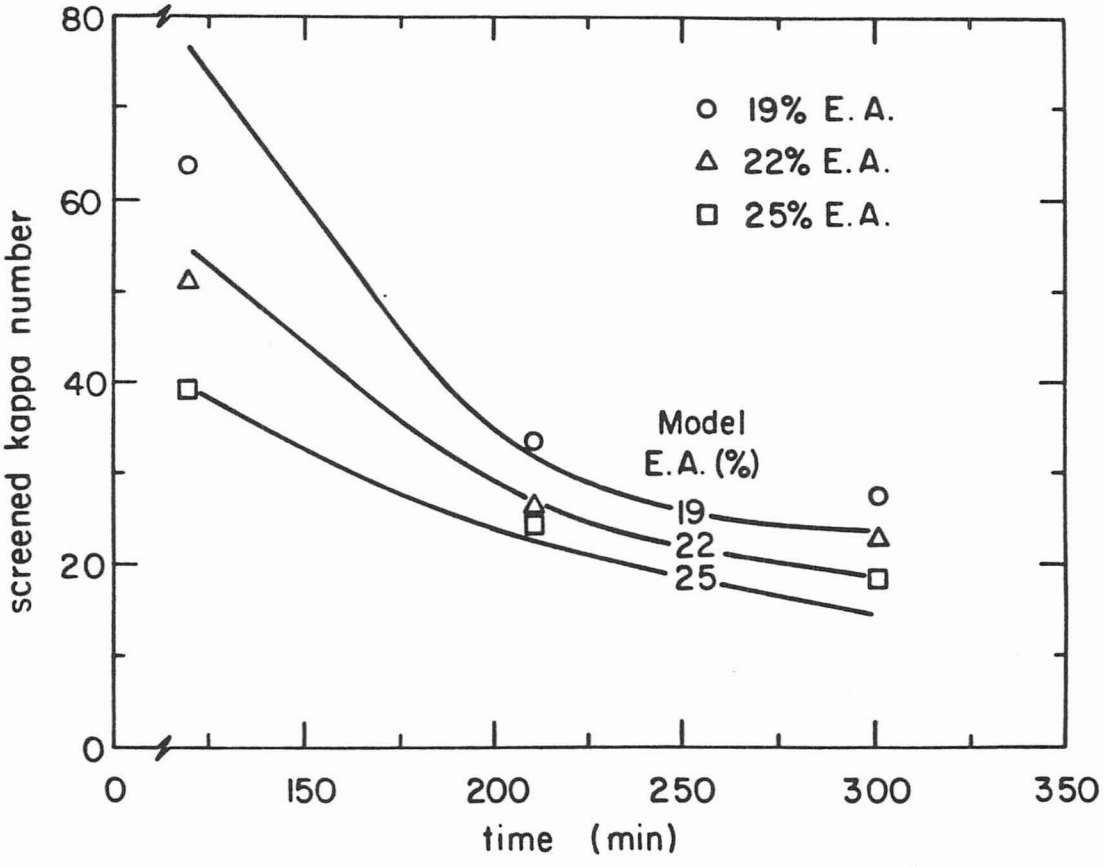

Figure 5.22. Model predictions and Akhtaruzzaman and Virkola's (1979, 1980) screened kappa data for a chip-thickness distribution.

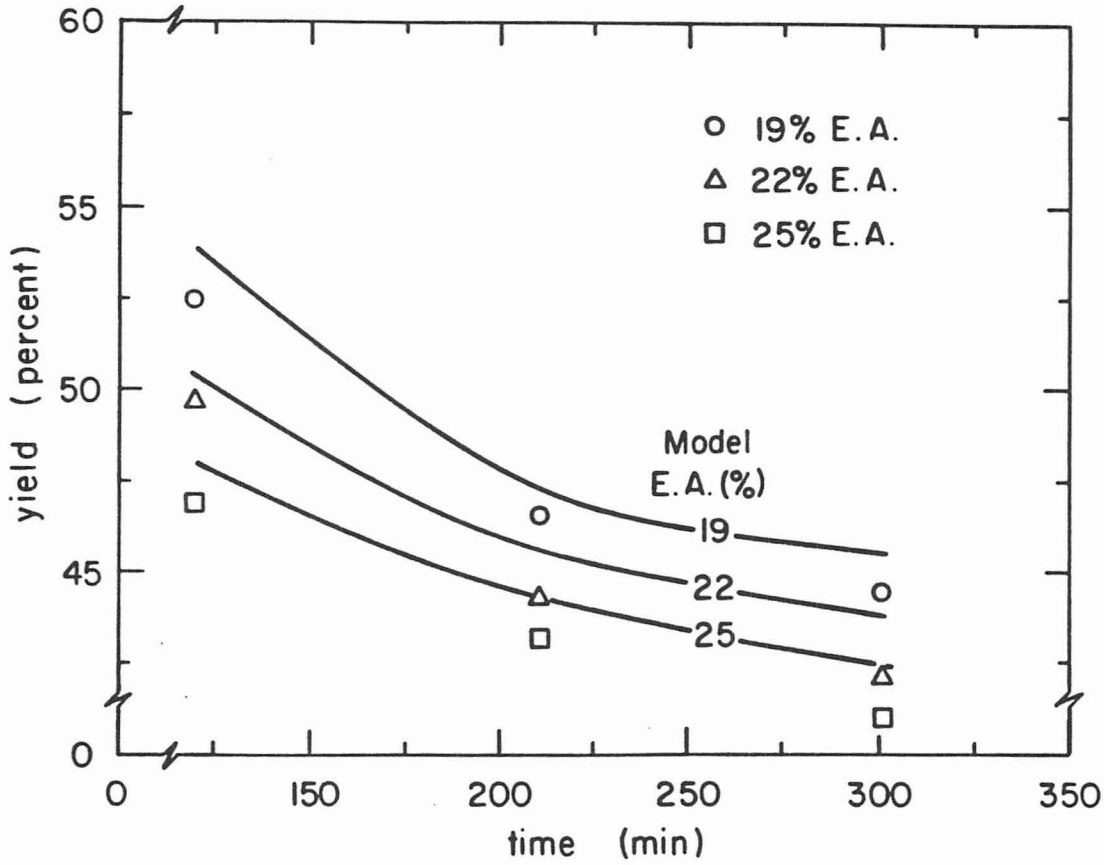

Figure 5.23. Model predictions and Akhtaruzzaman and Virkola's (1979, 1980) yield data for a chip-thickness distribution.

		MODEL			DATA		
Effective alkali (% on wood)	Cooking time (min.)	Screened kappa	Yield (%)	Screen rejects (%)	Screened kappa	Yield (%)	Screen rejects (%)
19	120	76.56	53.97	2.84	63.8	52.5	5.8
	211	30.95	47.33	1.20	33.4	46.6	1.1
	301	23.60	45.53	0.71	27.4	44.5	1.0
22	120	54.54	50.43	2.85	51.1	49.6	2.7
	211	26.09	45.60	0.58	26.2	44.3	0.6
	301	18.59	43.80	0.62	22.5	42.1	0.6
25	120	38.80	47.99	1.98	38.9	46.8	1.7
	211	22.24	44.26	0.5	24.0	43.1	0.4
	301	14.30	42.45	0.55	18.0	41.0	0.3

Table 5.6. **Model predictions of chip-thickness distribution experiments of Akhtaruzzaman and Virkola (1979,1980).**

predictions.

It can be seen from Figure 5.22 that the model accurately predicts the screened kappa numbers for all the experiments except for the 19 % effective alkali, 120 minute cook. (Even here the prediction is within 13 points of the experimental value). This discrepancy results from the model's under predicting the experimental screen reject value for this cook, see Table 5.6, and is discussed in detail below. The model predictions of the experimental yield results are also excellent (see Figure 5.23). The predictions are generally about 2 % above the experimental values, but the trends are correct.

It can be seen from Table 5.6 that the model predictions of the experimental screen reject values is very good except for, as mentioned above, the 19 % effective alkali, 120 minute cook. This result means that the NSM accurately predicts reject values only if the lignin content is below a critical level. At higher lignin contents, the absolute value of the lignin content will become the dominant variable in predicting rejects because a certain threshold must be reached before the wood may become defiberized (i.e. wood at 20 % lignin content does not fall apart regardless of the lignin profile). Once below this threshold lignin content other mechanisms, such as condensation reactions, may become influential in the formation of rejects. In the case of the 19 % effective

alkali, 120 minute cook, the lignin content at the center of the 12 mm and 9 mm chips are 17.8 % on wood and 13.5 % on wood respectively. At these values, the wood is still solid and will not break up without mechanical work.

To investigate the conclusion that the fiber liberation point is significant at higher lignin contents, the model screen rejects and screened kappas were calculated assuming a fiber liberation point of 9.45 % on wood (i.e. 65 % delignification). It was assumed that in those chips that have regions above a lignin content of 9.45 % the fiber liberation point is the best predictor of rejects, and in those chips that the lignin contents is less than 9.45 % on wood the NSM best predicts rejects. The results altered by calculating the rejects based on the fiber liberation point are the 19 % effective alkali, 120 minute cook, and the 22 % effective alkali, 120 minute cook. In the 19 % effective alkali, 120 minute cook, the model predictions of the rejects, using the fiber liberation point, is 6.74 % and the screened kappa is 72.24. Both of these predictions are closer to the experimental values then predicted by the NSM. In the 22 % effective alkali, 120 minute cook, the model predictions of the screen rejects, using the fiber liberation point, is 3.95 % and the screened kappa is 52.93. For this cook, therefore, the fiber liberation point and the NSM give similar results.

The results of these calculations support the hypothesis that different mechanisms control reject formation at different degrees of cooking. Again, experimental work is needed to verify and refine this conclusion.

CHAPTER 6

OPTIMAL OPERATION OF BATCH DIGESTERS

Commercial kraft pulp digesters are operated today in much the same way they were operated when the kraft pulping process was introduced about a century ago. Although good quality pulp is produced at a high rate, it is unlikely that the current operating conditions are optimal.

Little or no optimization work has been done with commercial digesters. This is not surprising considering the expense and difficulty of running experiments with production units and their limited range of operation. Several authors, however, have performed optimization studies with laboratory digesters (Bailey et al., 1969; Garceau et al., 1974a; Garceau et al., 1974b). The typical strategy is to run a large number of experiments to generate a response surface with respect to the variables of interest. The optimum operating conditions are then determined by interpolation

between discrete points on the surface. Disadvantages of this approach are the following:

1. generation of an accurate response surface requires many time consuming and expensive experiments,

2. the range of conditions that can be covered is limited by the experimental equipment used and it is possible that the optimum is beyond the allowable range,

3. it can be difficult to generalize from laboratory experiments to full scale operation.

An alternative approach is the use of a mathematical model of the process to generate the response surface. The advantages are that such experiments can be perfomed very quickly with a computer and the range of possible operating conditions is essentially limitless. For these reasons, model development and optimization can be a useful starting point in a process improvement project.

In the past, such optimization studies have been prevented by the lack of an accurate model of the kraft pulping process. Because the model developed in this work has a theoretical basis, and it predicts pulp properties over a wide range of operating conditions,

it is attractive for use in optimization studies.

In this chapter the development of the optimization program and the application of this program in two specific cases is discussed.

6.1 Description of optimization method

The kraft pulping model is coupled with a pattern search optimization method in a single computer program called OPTIM. The pattern search routine is the one developed by Nelder and Mead (1967). It was chosen because it is simple and is stable for most problems. Higher order methods, such as gradient searches, can be faster in some cases, but they are less stable and are more likely to fail, especially when the character of the response surface is unkown, as was the case here.

In all the studies described below, the goal was to determine the optimum conditions of temperature vs. time and bulk phase effective alkali concentration vs. time over the operating period of a batch cook. The Nelder-Mead and other search methods are designed to optimize discrete variables rather than variables that are functions of time. It was necessary, therefore, to specify in advance a functional form for the temperature and effective alkali histories (see, e.g., Equations 6.2 and 6.3). The Nelder-Mead

program then adjusts parameters in these functions (e.g., parameters x_1 to x_5 in Equations 6.2 and 6.3). This had the desired effect, although some trial and error was required to determine an appropriate functional form.

The Nelder-Mead optimizer and the pulping simulator work together as follows: the optimizer requires specification of an initial temperature history and effective alkali history. Given these cooking conditions, the simulator calculates the value of the "objective function," i.e., the goal of the optimization procedure. This is a well defined quantity, such as average productivity. Once the initial value of the objective function has been determined, the optimizer tries new cooking conditions, gradually moving toward the desired maximum (or minimum) in the objective function.

6.2 Results of optimization

6.2.1 Maximization of productivity of a pulp of kappa 35

The first use of the coupled optimizer-simulator was to determine the pulping conditions that maximized the net productivity for a pulp of kappa 35. Productivity is defined as follows:

Productivity =

Screened Yield/(Cooking Time + Turnover Time) (6.1)

where

Screened Yield [=] (%)

Cooking Time [=] (minutes)

Turnover Time [=] (minutes)

Productivity [=] (% / minute)

The turnover time between cooks was held constant at 30 minutes in all cases.

Initial optimization runs were made with the following functional forms for the temperature and effective alkali histories:

$$T = x_1 \left(1 - e^{-x_2 t} \right) + 293.15 \qquad (6.2)$$

$$[OH] = x_3 \left(1 - e^{-x_4 t} \right) + x_5 \qquad (6.3)$$

where

T is the cooking temperature [=] K

[OH] is the effective alkali concentration [=] M

x_i is the i-th optimized parameter

t is the cooking time [=] minutes

Equations 6.2 and 6.3 were choosen because they generate reasonable alkali and temperature histories with few parameters. The results show that the optimal temperature history is to heat up as fast as possible to as high a temperature as possible. This is surprising because higher temperatures favor the formation of rejects (Hartler and Onisko, 1962); therefore, a tradeoff was expected between higher rejects and shorter cooking times as the pulping temperature increased. The optimization results show, however, that the reduction of cooking time always outweighs the increase in rejects as the temperature increases.

It is important to note that this optimal temperature history and all other such results reflect the idealized digester simulated by the pulping model. A discussion of the limitations of the model and their effect on the optimization results is given in Section 6.3.

For all subsequent optimizations of the effective alkali history of the cook, the temperature history was set at that typically observed in a mill. The specific form chosen was the one used by Akhtaruzzaman and Virkola (1979,1980), i.e., a 60 minute

heating time from 20 C to 170 C followed by operation at 170 C for the remainder of the cook. In this way different effective alkali histories could be directly compared using the same temperature history. The main objective was to compare cooks in which there was a incremental addition of alkali vs. cooks in which all the alkali was added initially.

Various forms of the alkali history curve were tried. The form that gave the best results is shown in Figure 6.1. The four parameters in this history are the following:

x_1: the initial alkali concentration

x_2: the elapsed time during which the concentation is at x_1

x_3: the time required to change the alkali concentratin to x_4

x_4: the final alkali concentration

Optimal effective alkali histories were obtained for 2 mm, 5 mm, and 12 mm chip-thicknesses. The optimal history for the chip-thickness distribution used in the experiments of Akhtaruzzaman and Virkola (1979,1980), given in Table 2.1, was also determined. In the optimization procedure, the effective alkali concentration was not allowed to rise above 1.5 molar. This limit was set because there are insufficient data to determine whether the pulping model

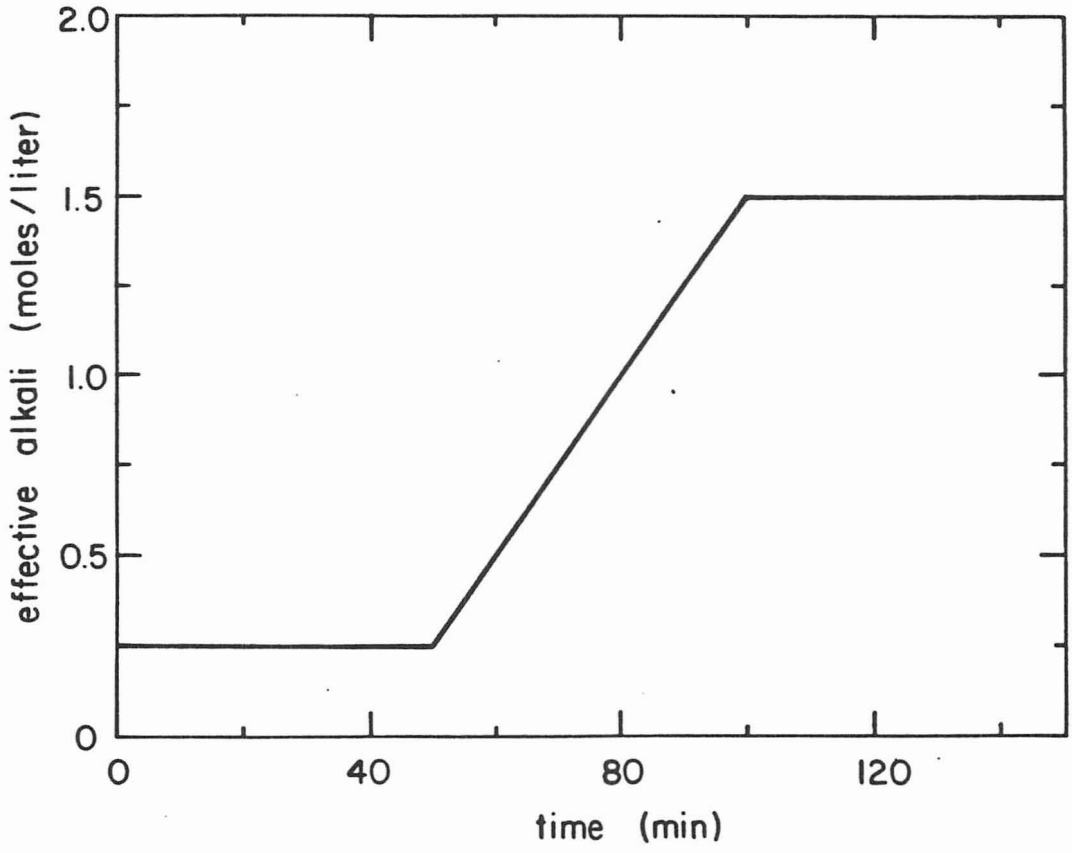

Figure 6.1. Optimum form of the effective alkali versus time curve.

is accurate at higher concentrations.

The calculated optimal histories are shown in Figure 6.2. In thin chips, where the reactions are kinetically controlled, the optimal operating policy is to keep the effective alkali concentration low initially and then quickly increase it to the maximum possible value (1.5 M) at about 45 minutes into the cook. This result is consistent with current knowledge of kraft pulping chemistry (Olm and Tistad, 1979). In the initial period, the delignification rate is independent of alkali concentration provided that the pH is above 12, but the carbohydrate degradation rate increases with increasing alkali concentration. A low alkali concentration in the initial period retards carbohydrate degradation, which results in higher yields than obtained from cooks with high initial alkali concentrations.

The sudden jump in the alkali concentration seen in Figure 6.2 signals the transition from the initial to the bulk delignification period. In the bulk period, the carbohydrate degradation rate is proportional to the delignification rate and the delignification rate is approximately first order in the effective alkali concentration. It is desirable, therefore, to maximize the alkali concentration during this period, as the optimization procedure indicates. Norden and Teder (11) have suggested an effective alkali history similar to that shown if Figure 6.2 for the 2 mm and 5 mm

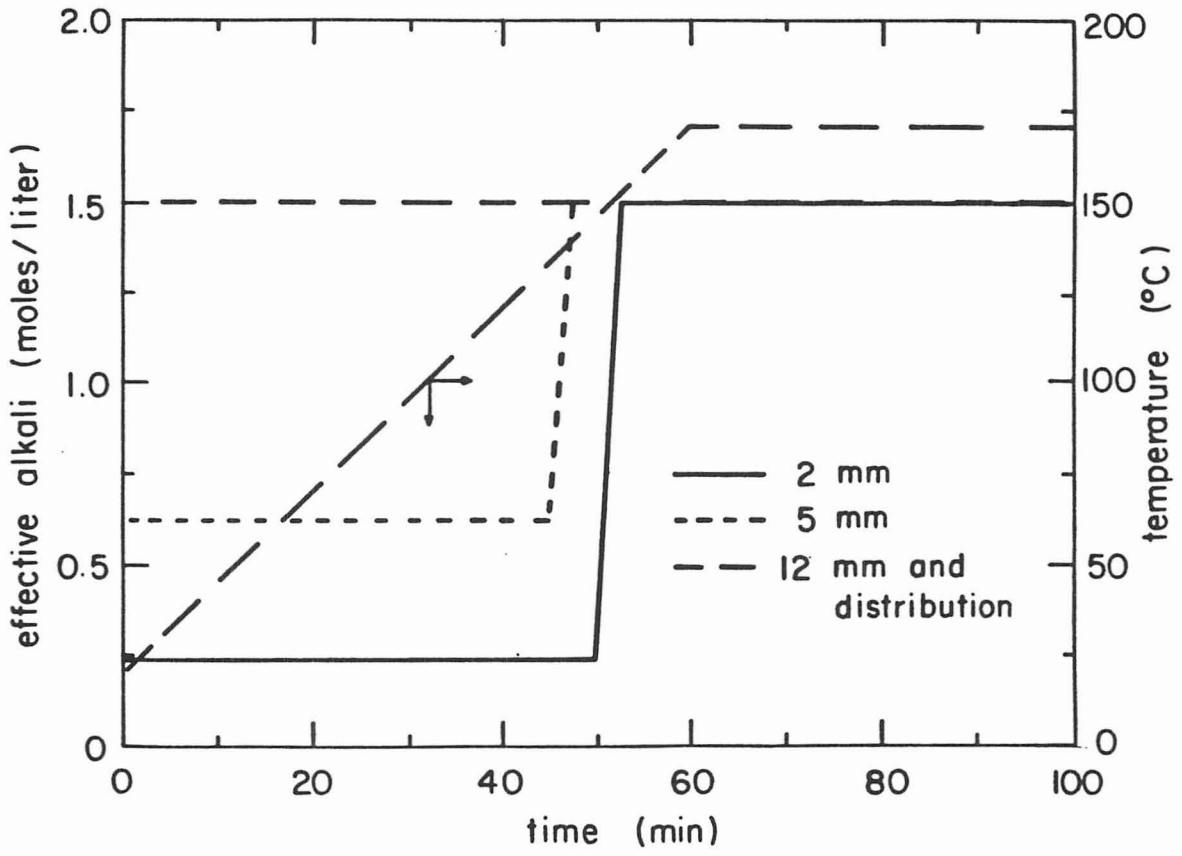

Figure 6.2. Optimal bulk phase effective alkali concentration history to maximize productivity of a pulp of kappa 35.

chips.

For the 12 mm chips and the chip-thickness distribution, the optimal policy is to maximize the effective alkali concentration throughout the cook. This is because reaction rates are partially mass transfer limited in the thicker chips. If the initial alkali concentration is low, the alkali in the center of the chip is quickly depleted, resulting in an undercooked chip center. Undercooking results in higher screen rejects and longer cooking times to achieve a given target kappa number. Both of these effects reduce the productivity.

The calculated maximum productivity for Akhtaruzzaman and Virkola's chip-thickness distribution is 0.33 %/min. In their actual experimental cooks, Akhtaruzzaman and Virkola used the same temperature history but the initial effective alkali concentration was 25 % on wood and no alkali was added during the cook. For these conditions, the simulator predicts a productivty of 0.278 %/min. The optimization procedure, therefore, increases the productivity by about 19 %. As shown in Figures 5.22 and 5.23, the simulator predicts Akhtaruzzaman and Virkola's experimental results with high accuracy; the extrapolation to the optimal conditions should be equally accurate.

6.2.2 Minimization of Rejects at a Specified Productivity

The second optimization study was to find the pulping conditions that minimize the formation of rejects in a pulp of kappa 35 and at a productivity of at least 0.25 %/min. This corresponds to maximization of pulp quality at a specified production rate (below the maximum possible productivity). A productivity of 0.25 %/min corresponds to a cooking time of about 150 minutes. Only the chip-thickness distribution shown in Table 2.1 was used.

Initial optimization runs showed that the effective alkali concentration should be held at the maximum possible value throughout the cook. Therefore, in further optimizations of the temperature history, the bulk phase effective alkali concentration was set at a constant value of 1.5 molar.

Many different forms for the temperature history were tested. In all cases, the optimum operating policy is to heat up as quickly as possible to the lowest temperature at which the specified productivity of 0.25 %/min can be achieved. Figure 6.3 shows the optimum temperature history, note the maximum cooking temperature is only 155 C. This is in line with experiments performed by Hartler and Onisko (1962), which show decreasing reject formation with decreasing cooking temperature (at a given kappa number). The use of rapid heating to minimize rejects may, however, run counter to

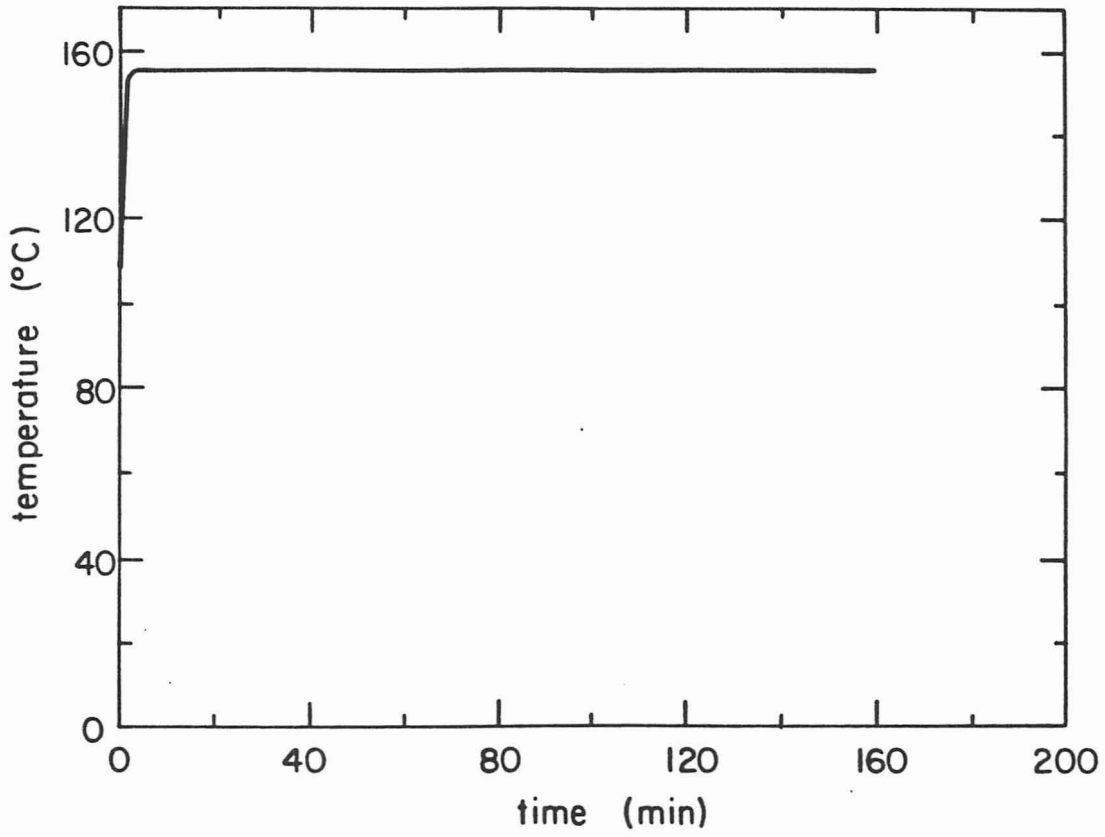

Figure 6.3. Optimal temperature history to minimize rejects of a pulp with kappa 35.

the expectations of pulping practitioners. This point is discussed further in the next section.

The calculated rejects for the temperature history shown in Figure 6.3 is 0.9 %. For the more conventional conditions used in the experiments of Akhtaruzzaman and Virkola (1979,1980) shown in Figure 6.2, the pulping simulator predicts 1.5 % rejects, which is within 4 % of the actual experimental value. Optimization thus decreases the rejects by about 40%.

6.3 Limitations of the Optimization Calculations

The optimization results are only as accurate as the model used and the data on which it is based. A key assumption in the model, as stated in Section 3.1, is that the chips are completely impregnated with cooking liquor before the temperature in the digester is high enough to cause significant reaction rates. At typical mill heating rates, this is a reasonable assumption (Hartler, 1962). For the very high heating rates shown in Figure 6.3, however, the assumption is invalid unless pre-impregnation were used. Pre-impregnation units are now available (Backlund, 1974), so it is possible to increase heating rates in such commercial units without increasing rejects because of incomplete penetration.

Optimization under conditions of imperfect impregnation is unlikely to be meaningful with the present model. Experiments and model development to include the effect of imperfect impregnation would allow one to determine whether pre-impregnation is really justified in a given situation. Temperature and concentration gradients in the digester, as well as other complicating factors that might be important in a specific case, have also been neglected. Such considerations could easily be incorporated in the calculations to model more closely the conditions in a specific digester. The main goal in the present work, however, is to demonstrate the potential for increased productivity and quality through optimization for a general case.

CHAPTER 7

MODELING OF A COMMERCIAL INDIRECT HEATED BATCH DIGESTER

To simulate conditions in a commercial indirect heated batch digeter the following modifications were made to the pulping model:

1. input of an appropriate value for the Biot number of a commercial digester to the model,

2. expansion of the model to simulate a non-isothermal digester.

In this chapter, we discuss the use of the modified model to investigate the effect of interchip mass transfer rates upon the overall reaction rates and the effect of digester temperature gradients on the properties of the pulp. The pulp properties examined are the average kappa number, yield, screen rejects, and

the distribution of the lignin content.

7.1 Effect of inter-chip mass transfer.

In laboratory cooks, which are well stirred, the mass transfer resistence between the bulk liquid phase and the chip phase is negligible. It is desirable to know if the same is true in commercial digesters, and if the inter-chip mass transfer rate is limiting the overall reaction rate, how much additional circulation is necessary to alleviate the problem.

In a commercial digester not all of the chips are submerged in the cooking liquor. It is necessary, therefore, to calculate two mass transfer coefficients, one for the submerged chips, and one for the chips above the liquor.

For the submerged chips, empirical equations developed for packed beds may be used to estimate the bulk liquid phase to chip phase mass transfer coefficient. Equations 7.1 and 7.2 are given by Sherwood et al. (1975) to calculate the mass transfer coefficient in a packed bed.

$$j_d = 1.17(d_p \times U_{ave} \times \rho / \mu)^{-0.415} \qquad (7.1)$$

$$k = j_d \times U_{ave} \times Sc^{-2/3} \qquad (7.2)$$

where

d_p is the diameter of a sphere having the same surface area of the packed particles

k is the solid to liquid mass transfer coefficient

Sc is the Schmidt number $[\mu/(\rho \times D)]$

U_{ave} is the superficial fluid velocity

ρ is the fluid density

μ is the fluid viscosity

D is the diffusivity in the fluid phase

Under typical commercial operating conditions the mass transfer coefficient in the submerged section of the digester is calculated from Equation 7.1 and 7.2, to be about 0.025 cm/sec. (See Appendix A for details of the calculation). With this value for k, a Biot number (Bw_i in Equation 3.9) of 70 is calculated for chips 3 mm thick. For thicker chips the Biot number is proportionally higher.

For the chips above the liquor, correlations for trickle bed reactors may be used to estimate the bulk phase to chip phase mass transfer coefficient. Such a correlation, given by Van Krevelen and Krekels (1948), is

$$Sh = 1.8 \times Re^{1/2} \times Sc^{1/3} \qquad (7.3)$$

where

Re is the Reynolds number $[(U_{ave} \times \rho)/(a \times \mu)]$

Sc is the Schmidt number $[\mu/(\rho \times D)]$

Sh is the Sherwood number $[k/(a \times D)]$

U_{ave} is the superficial velocity

D is the diffusivity in the fluid phase

a is the surface area of the contact per unit of volume

ρ is the fluid density

μ is the fluid viscosity

With Equation 7.3 the mass transfer coefficient at the top of a digester operating at typical conditions is calculated to be 0.041 cm/sec. (See Appendix A for details of the calculation). Using this value for k, a Biot number of 114 is calculated for chips 3 mm thick. For thicker chips the Biot number is proportionally higher.

A series of simulations were made with the pulping conditions shown in Table 7.1 to determine when the overall delignification rate is limited by the interchip mass transfer rate. The Biot numbers for the six simulations are 0.1, 1.0, 10., 100., 1000., and 10000. A plot of the lignin content vs cooking time for the six

Hydroxyl concentration	1.5 M
Sulfide concentration	0.26 M
Heating time	30 min.
Cooking time	100 min.
Liquor/Wood ratio	4 l/Kg
Cooking temperature	180 C

Table 7.1. Cooking conditions used for the simulations to study the effect of the Biot number on the delignification rate.

simulations is shown in Figure 7.1. From Figure 7.1 it can be seen that for the reaction rates encountered in kraft pulping, the Biot number is between 1 and 10 when the bulk to chip mass transfer rate begins to limit the overall reaction rate. Since the Biot numbers calculated for commercial digesters are on the order of 100, it can be concluded that the bulk to chip mass transfer resistence is negligible in indirect heated batch digesters. We anticipate this result because in commercial digesters the temperature dependence of the delignification rate is at a level typical for kinetically controlled reaction rates.

For all the simulations of commercial digesters the Biot number is set at 100.

7.2 Modeling a non-isothermal digester

Commercial batch digesters are not isothermal. Stephenson (1950) shows the temperature difference between the liquor inlet and outlet is significant while the digester is heating up, see Figure 7.2. Annergren et al. (1973) show that in digesters with channelling, the temperature gradients will be more severe than the liquor inlet and outlet temperatures indicate. For example, Annergren shows that the during heat-up the temperature difference between the digester inlet and oulet is 20 C, but the maximum

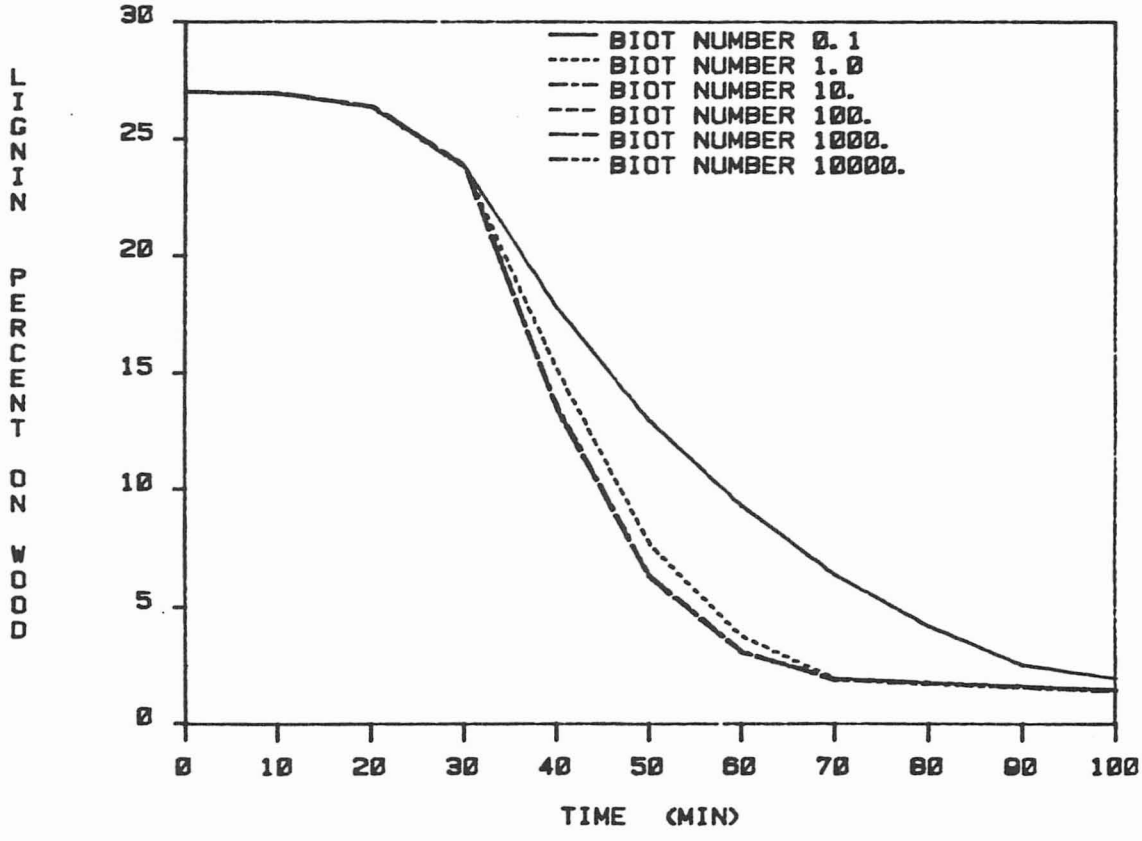

Figure 7.1. Effect of the Biot number on the overall delignification rate.

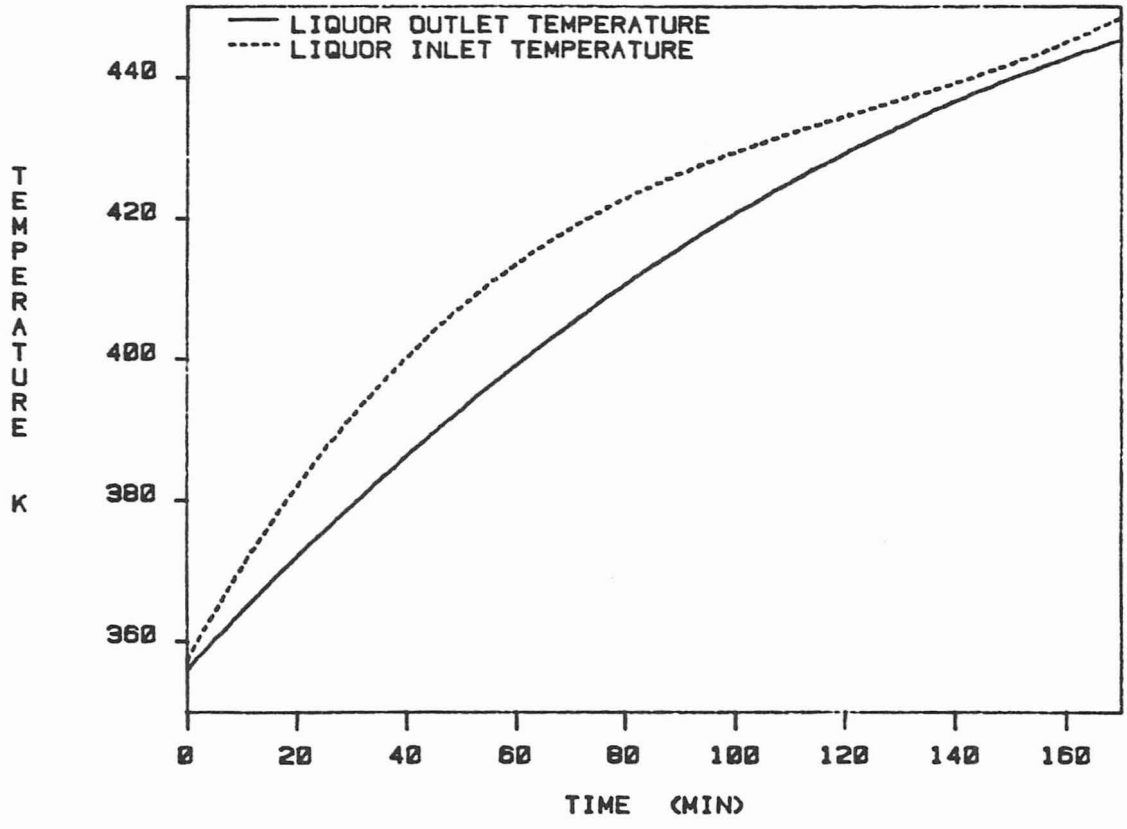

Figure 7.2. Liquor inlet and outlet temperatures in an indirect heated batch digester (Stephenson, 1950).

temperature difference in the digester is about 50 C.

The activation energy for delignification is about 32 Kcal/mole; therefore, a 10 degree temperature increase increases the delignification rate by a factor of 2 to 3. Clearly, then, the degree of delignification observed in different regions of a non-isothermal digester will be significantly different. The results of temperature gradients will be a pulp with a broad kappa and yield distribution. It is well known that pulps with broad kappa distributions are more difficult to bleach uniformly and have inferior paper making properties.

To understand better the effect of digester temperature gradients on the properties of a pulp, the model is expanded to simulate a non-isothermal digester. Because the liquor is continually recycled and because the bulk phase alkali concentration changes slowly, it may be assumed that the digester is well mixed with respect to alkali.

To simulate the temperature gradients, the digester is divided into a series of mixing cells. Each mixing cell has a unique temperature history and chip-thickness distribution, both of which are input to the model. By dividing the digester longitudinally, it is assumed that there are no radial temperature gradients. This is probably not a good assumption, but there are no data available to

check the assumptions validity. By ignoring the radial temperature gradients, the pulp property distributions predicted by the model will probably be less than the property distributions observed in a pulp produced in a commercial non-isothermal digester.

The program DPULPER simulates the non-isothermal digester. The modifications made in the computer code to model the non-isothermal digester are the same as those made in expanding the model to accomodate a chip-thickness distribution, see Section 4.2. The result of the modifications is that the integrator has to solve simultaneously the ordinary differential equations for each chemical species at each collocation point for each chip-thickness in a given mixing cell, plus the equation for the bulk phase alkali concentration. For example, 193 ordinary differential equations are simultaneously integrated to simulate a digester with 4 temperature zones with each containing 4 chip-thicknesses using 4 collocation points. Solution times for such a simulation are on order of 90 minutes on a VAX computer.

To predict accurately the lignin content distribution, it was found that the digester needs to be divided into 10 temperature zones with each zone containing 8 chip-thicknesses. This results in 961 ordinary differential equations. The solution time for this problem was about 1500 minutes when the program was aborted at eight-tenths of the way through the solution. Such solution times

make the model impractical and expensive. To improve the solution time, the number of equations to be integrated simultaneously must be reduced. The differential equations describing each chip are coupled only by the bulk phase alkali concentration. If the bulk phase alkali concentration history of a cook can be predicted accurately, the solution for each chip can be determined consecutively, significantly reducing the compution time.

Figure 7.3 is a plot of the effective alkali concentration versus the cooking time for three simulations. Table 7.2 gives the cooking conditions simulated. Curve 1 is from the simulation of 8 chip-thicknesses in 10 temperature zones, curve 2 is from the simulation of 4 chip-thicknesses in 3 temperature zones, and curve 3 is from the simulation of 4 chip-thicknesses in an isothermal digester. The temperature histories for all three simulations are derived from the digester temperature data presented by Stephenson (1950), see Figure 7.2. The 8 chip-thickness distribution is shown in Table 7.3, the 4 chip-thickness distribution is shown in Table 7.4. It can be seen from Figure 7.3 that the bulk phase alkali history for the complex simulation is accurately predicted by a simpler and hence quicker simulation. (The solution time for the 4 chip-thicknesses in an isothermal digester is only 1.5 minutes). This result is explained by noting that at a given initial alkali concentration, for a given chip-thickness distribution, the rate of delignification, and thus the rate of alkali consumption, is

Hydroxyl concentration	1.375 M
Sulfide concentration	0.243 M
Liquor/Wood ratio	4 l/Kg
Cooking time	170 min.

Table 7.2. Cooking conditions used for the simulation of non-isothermal digesters.

Chip-thickness (mm)	Weight fraction
2.00	0.2149
3.42	0.2645
4.86	0.2516
6.28	0.1613
7.74	0.0452
9.14	0.0194
10.58	0.0194
12.00	0.0194

Table 7.3. Chip-thickness distribution with 8 chip-thicknesses.

Chip-thickness (mm)	Weight fraction
3.0	0.4101
5.0	0.3847
7.0	0.1152
11.18	0.0900

Table 7.4. Chip-thickness distribution with 4 chip-thicknesses.

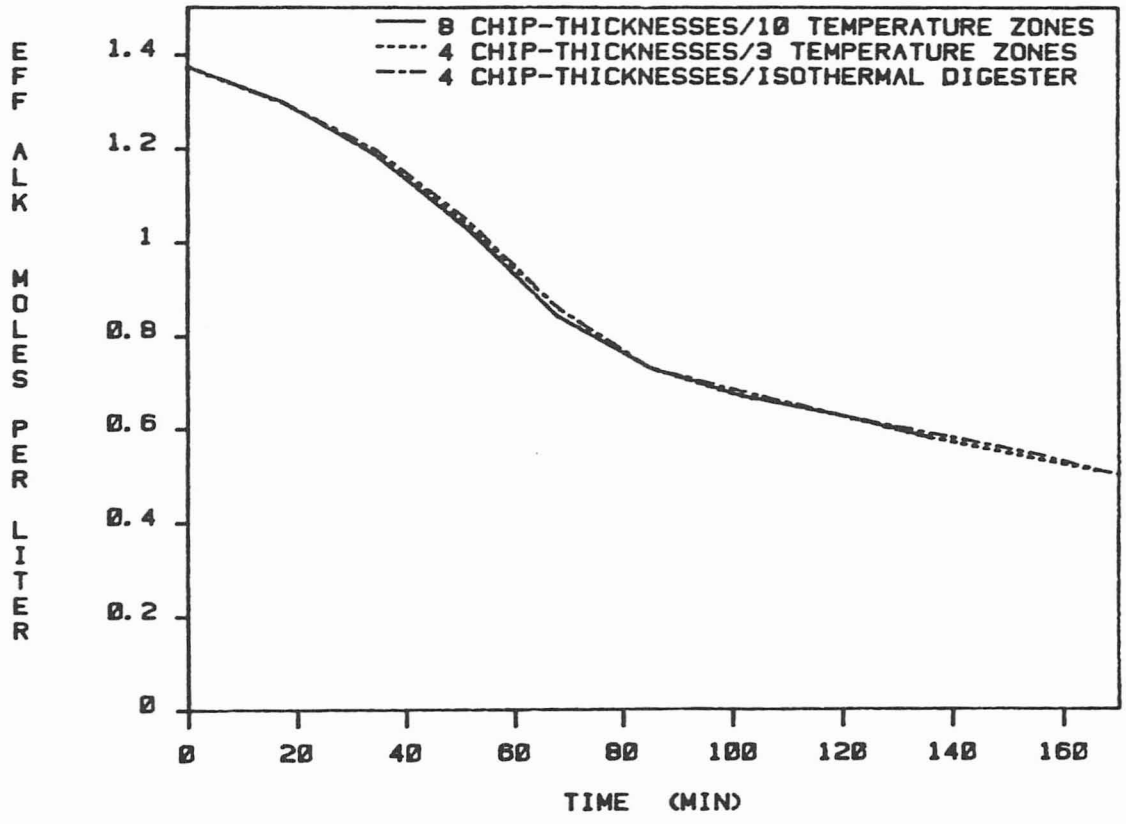

Figure 7.3. Effective alkali concentrations during a kraft cook from three simulations of varying complexity.

controlled primarily by the temperature history of the cook. If the temperature history of the isothermal digester is a good average of the non-isothermal temperature history, the alkali consumption rate for both should be nearly identical.

To confirm this hypothesis, a simulation was made using the pathological temperature history measured by Annergren et al. (1973) shown if Figure 7.4. Figure 7.5 is a plot of the bulk phase effective alkali concentration versus the cooking time for the simulation of 4 chip-thicknesses, see Table 7.4, in 4 cooking zones, and the alkali concentration versus the cooking time for the same chip-thickness distribution in an isothermal digester whose temperature history is an average of the other 4 zones. It can be seen from Figure 7.5 that even with bizzare digester temperature profiles, the bulk phase alkali concentration is accurately predicted by a smaller, isothermal digster simulation.

To simulate a digester with many temperature zones, a simulation is first made, using DPULPER, of an isothermal digester with the same chip-thickness distribution or a similar chip-thickness distribution as in the large problem. The alkali concentration history of the isothermal digester is fit with a polynomial. With that alkali history, each chip in each temperature zone is simulated consecutively with the program SPULP. The results of each simulation are then combined to calculate the average kappa,

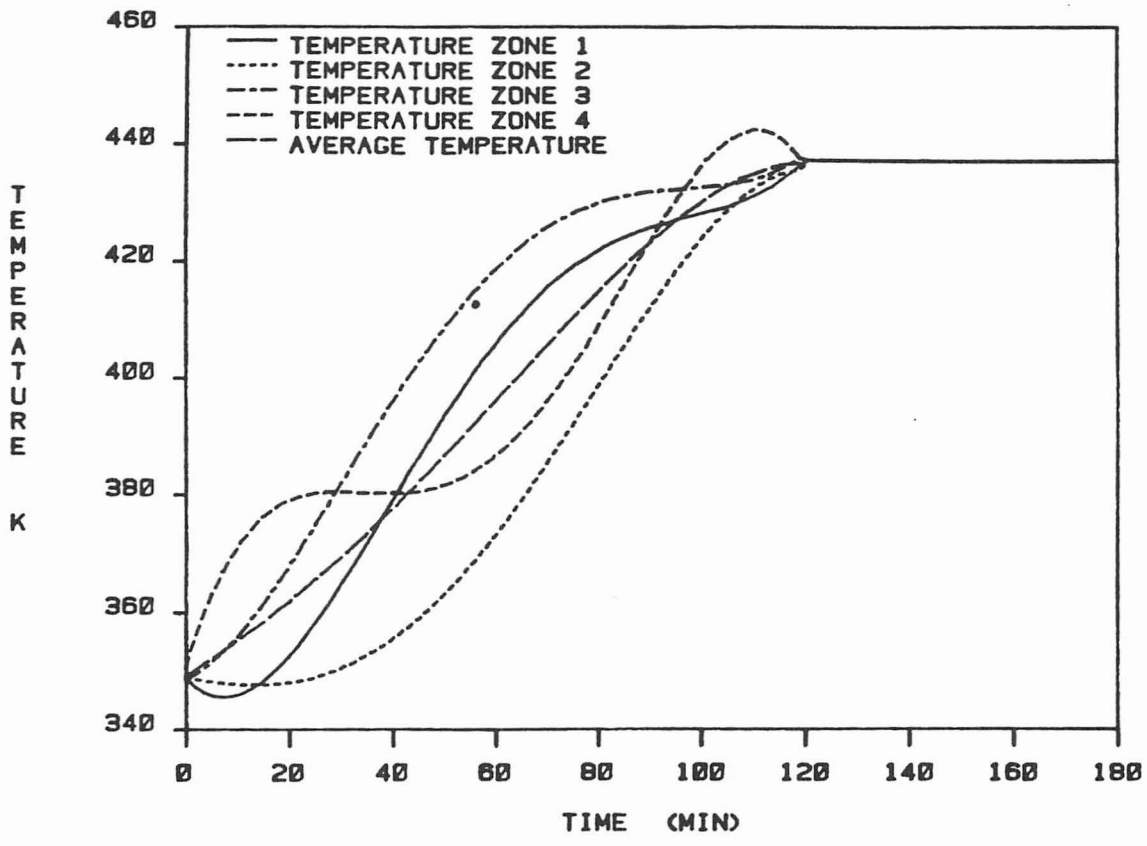

Figure 7.4. Temperature history within 4 different zones of a batch digester (Annergren et al., 1973), and the average temperature history.

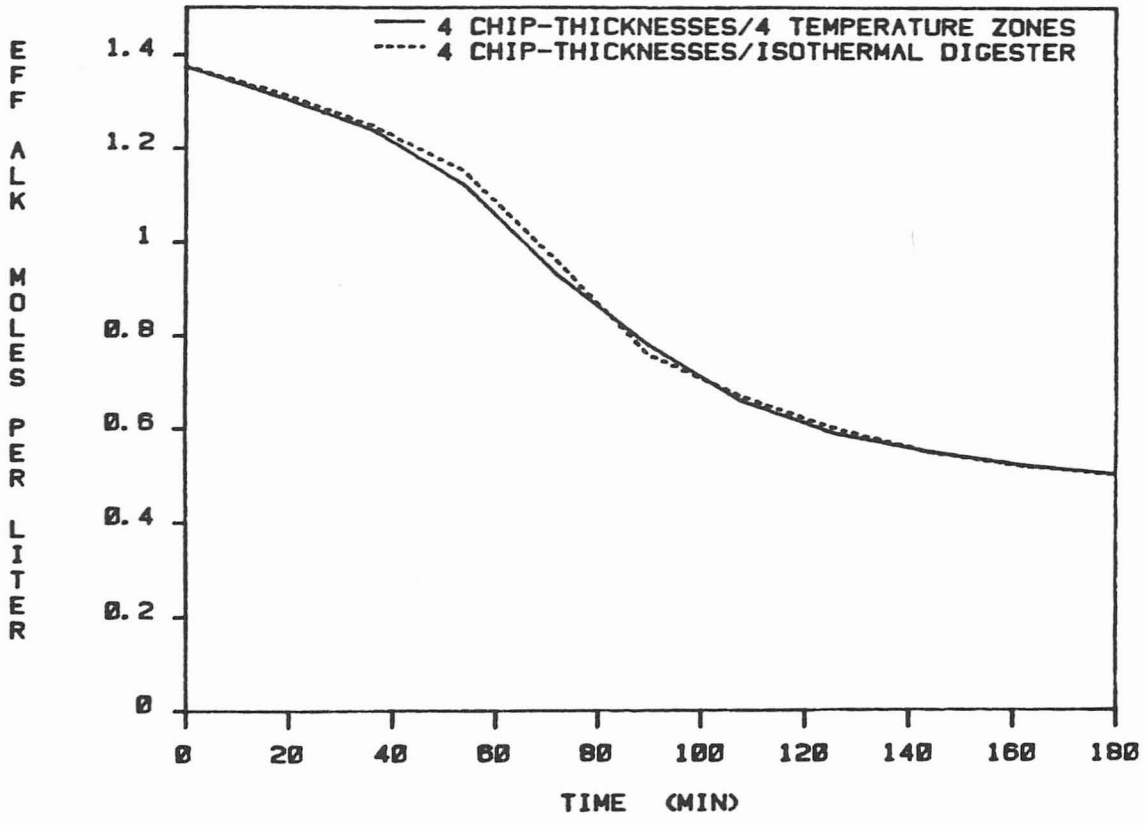

Figure 7.5. Alkali concentration during non-isothermal and isothermal simulations using Annergren's et al. (1973) temperature history.

yield, and rejects, and to calculate the lignin content distribution of the pulp. The solution time for the 8 chip-thicknesses in 10 temperature zone simulation mentioned earlier was reduced a 1000 fold by solving the problem consecutively.

7.3 Generation of lignin content profiles.

The range of lignin contents, or kappa numbers, of a pulp is an important physical characteristic. If the range is broad, more bleaching is required to lower the lignin content of all fibers to an acceptable level. It is also more difficult to make paper from fibers that have a broad lignin content distribution because the mechanical properties of the fibers are a strong function of the lignin content.

To generate a lignin content distribution, it is necessary to solve for the weight fraction of fibers that have a lignin content within a specied range. This can be calculated with Equations 7.4 and 7.5.

$$W_L = \left(\sum_{i=1}^{NC} W_{L_i}\right)/Y_T \qquad (7.4)$$

$$W_{L_i} = f_i \times \Delta L \times dx/dL_L \times Y_L \qquad (7.5)$$

where

f_i is the weight fraction of chip i

ΔL is the lignin interval over which the weight fraction is to be calculated, set equal to 0.002.

NC is the number of chips

W_L is the weight fraction of fibers with lignin content L

W_{L_i} is the weight fraction of fibers in chip i that have a lignin content of L

Y_L is the yield in the chip at lignin content L

Y_T is the total yield of the cook

dx/dL_L is the inverse of the slope of the lignin profile within a wood chip at lignin content L

W_L is calculated from the intrachip lignin content and carbohydrate content distribution with the computer program FRAC in the following manner: Starting at the edge of the chip, where the lignin content is Lo, the value of W_{Lo_i} is calculated and stored, the program then steps to the location within the chip where the lignin content is $L + \Delta L$ and calculates $W_{Lo + \Delta L_i}$. The values of the weight fractions for each lignin content within each chip, W_{L_i}, are then summed over all the chips to get the total weight fraction of fibers that have a given lignin content.

The lignin content distributions generated as described above are discontinuous because the simulation is done using discrete chip sizes and discrete temperature zones. In reality, both of these vary continuously and, therefore, the lignin content distribution should also be continuous. To smooth the computer generated distributions the weight fractions, W_L, are averaged in groups of 500. A histogram generated as described above is shown in Figure 7.6.

7.4 Results of non-isothermal digester simulation.

To investigate the effect of digester temperature gradients on pulp properties, the temperature data of Stephenson (1950) were used. Stephenson presents the liquor inlet and outlet temperatures as a function of cooking time. Figure 7.2 is a plot of Stephenson's data. To model the non-isothermal case, the digester was divided into ten mixing cells with heating schedules such that the temperature drop along the digester is linear. The 8 chip-thickness distribution shown in Table 7.3 was used. The 8 chip-thickness distribution is very similar to the 5 chip-thickness distribution published by Akhtartuzzaman and Virkola (1979,1980). The other cooking conditions used in the simulation are given in Table 7.2. For comparison an isothermal digester with the same chip-thickness was simulated. The heating schedule for the isothermal digester is

intermediate to the heating schedules at the liquor inlet and outlet presented by Stephenson.

The effect of stratifying the chips by thickness within the digester was also investigated. With the same chip-thickness distribution as in the previous two cases, a simulation was made by placing the thickest chips in the hottest zone of the digester with the chips becoming progressively thinner in the cooler sections. By stratifying the chips the difference in the extent of delignification between the thick chips, which pulp slower, and the thin chips will be reduced; creating a narrower lignin content distribution.

Table 7.5 shows the average kappa number, yield, and screen rejects for the three simulations. As expected, because the temperature histories of the three simulations are similar, the average kappa numbers and average yields are about equal. It is surprising, however, that the stratified chip cook did not have less screen rejects than the non-isothermal cook, because as the thicker chips are more delignified in the hotter zones the rejects will drop. This result is explained by observing, as stated in Section 6.3, that pulping at higher temperatures leads to higher rejects at a given average lignin content. By placing the thick chips, those responsible for the formation of rejects, in hotter zones, the rejects are not reduced because the benefit in increased

	Kappa number	Yield (%)	Rejects (%)
10 temperature zone simulation	62.94	51.06	0.87
Isothermal simulation	68.42	51.76	0.80
Stratified chip simulation	62.97	51.22	0.95

Table 7.5. Average pulping results predicted by the model for the simulation of a non-isothermal, isothermal, and stratified digester.

delignification is nullified by pulping at higher temperatures.

Figures 7.6 - 7.8 show the lignin content distribution, generated as discussed in Section 7.3, for the three simulations. Because the distributions are not regularly shaped, a standard deviation of them is meaningless; however, qualitative information on the extent of dispersion of the lignin content may be obtained by examining the figures. It can be seen from Figure 7.6 and Figure 7.7 that the extent of dispersion of the lignin content can be dramatically reduced by completely eliminating the temperature gradients in the digester. In comparing Figure 7.6 with 7.8 it can be seen that the reduction in the width of the lignin content distribution obtained by stratifying the chips is also significant. In the stratified case, the largest weight fraction, at a given lignin content, contains about 50 % of the pulp, but in the non-isothermal digester the largest weight fraction at any lignin content is about 30 %.

Both chip stratification and reducing the temperature gradients are possible with existing technology. Chip screens that classify on the basis of thickness are available, and sequentially loading chips into a digester to take advantage of the temperature gradients is simple. Digester temperature gradients may be reduced by increasing the liquor circulation rate or by reducing the liquor path in the digester. The former may be accomplished by increasing

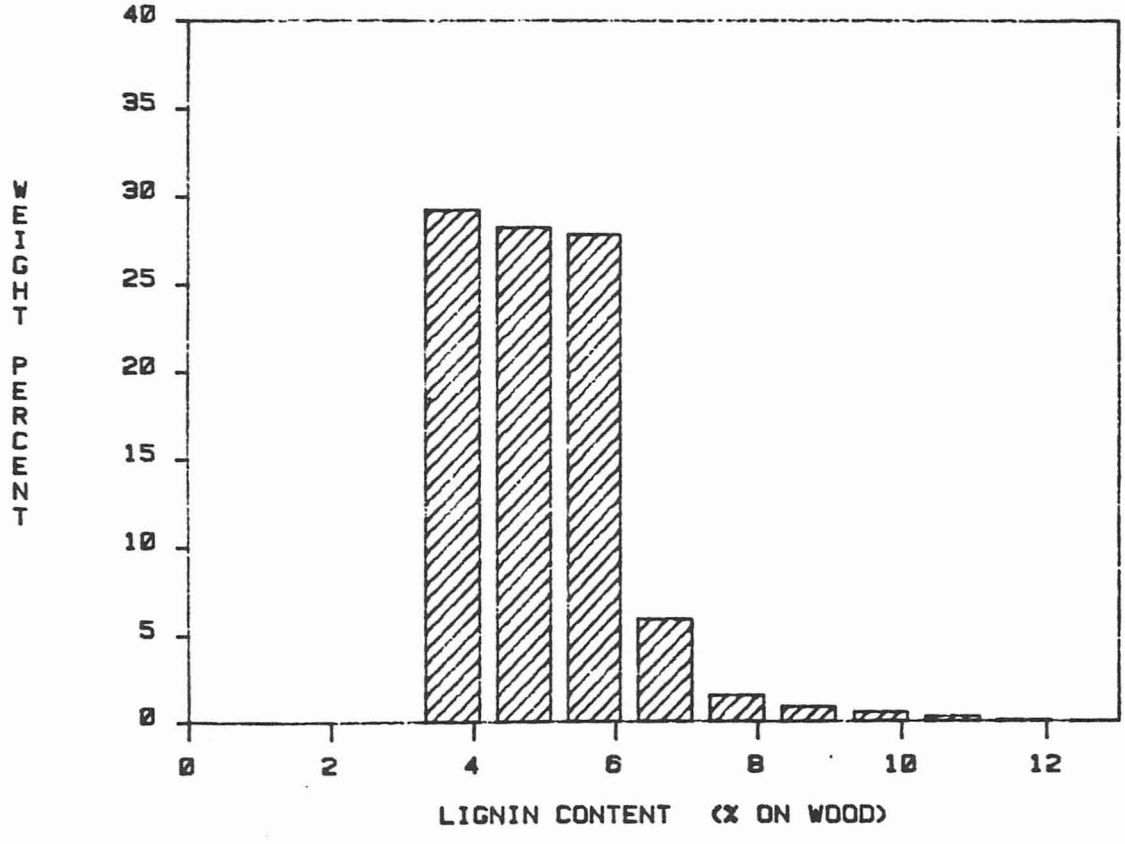

Figure 7.6. Lignin content distribution from a non-isothermal digester simulation.

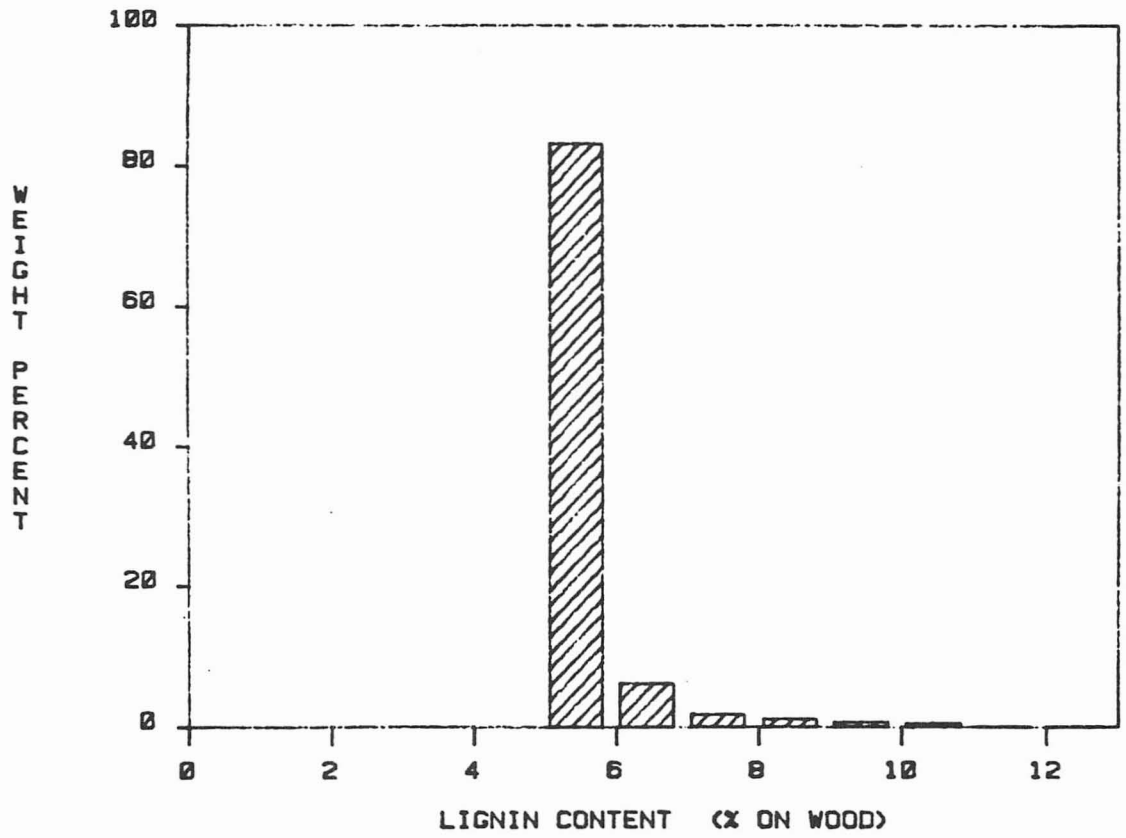

Figure 7.7. Lignin content distribution from an isothermal digester simulation.

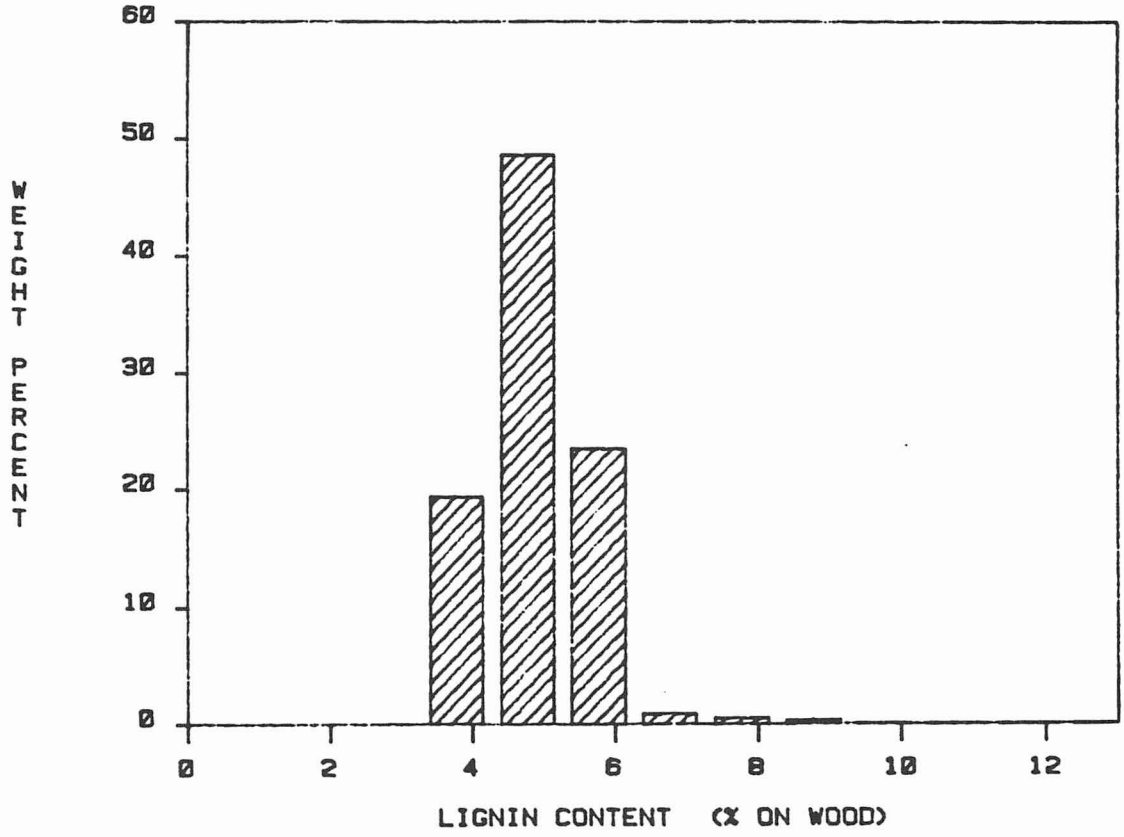

Figure 7.8. Lignin content distribution from a stratified digester simulation.

the pumping and piping capacity, the later may be accomplished by increasing the number of liquor inlets and outlets.

CHAPTER 8

CONCLUSIONS AND RECOMMENDATIONS

8.1 Summary and Conclusions

A theoretical model of a batch kraft pulp digester has been developed. The model predicts a priori the lignin content distribution, the carbohydrate content distribution, and the effective alkali concentration distribution within pulp chips as a function of cooking time. From this information the kappa number, yield, screen rejects, and kappa distribution of a cook may be calculated. The model also predicts the bulk phase effective alkali concentration as a function of cooking time. The accuracy of the simulator is verified by comparing model predictions with data from pulping experiments in which the reaction rates are kinetically controlled and with experiments in which the diffusion rate restricts the overall reaction rates. In both cases the comparison

is good.

The model predictions of the lignin content at the center of thick chips show that the fiber liberation point cannot be used to predict screen rejects. It was found, however, that the normalized second moment (NSM) of the lignin content correlates well with experimental screen rejects. The good correlation between the NSM and screen rejects is suggested to be a consequence of condensation reactions at the center of thick chips.

The potential value of an accurate kraft pulping simulator coupled with a pattern search optimization of pulping conditions is demonstrated. In two specific optimization studies, significant improvements over pulps cooked in a conventional manner were obtained. For example, an increase in productivity of 19 % was obtained by optimizing the bulk phase effective alkali concentration in a cook to a kappa number of 35. Because the accuracy of the pulping simulator has been demonstrated over a wide range of operating conditions, the optimization results obtained suggest likely strategies for improvements in mill operations.

Finally, simulations of a non-isothermal, indirect heated, commercial, batch kraft pulp digester were made to determine the effect of chip to bulk mass transfer rates on the overall delignification rate, and the effect of temperature gradients on

pulp properties. It was found that the bulk to chip phase mass transfer resistence is negligible.

Digester temperature gradients were found to have a negligible effect on the rejects of a pulp, but a large effect on the lignin content distribution of the pulp. Stratifying the chips by thickness (i.e., placing thicker chips in the hot regions) was found to reduce the lignin content distribution but has no effect on screen reject levels. Two methods of reducing temperature gradients are suggested.

8.2 Recommendations

Like most research, this project has uncovered many questions. Both experimental and theoretical work may be done as an extension of this work. The following are those projects the author believes should have top priority.

8.2.1 Experimental

1. Complete the work currently being done by on the diffusivity of alkali in wood (McKean, 1982). The diffusivities in various wood species should be known quantitatively as a function of pH, yield, and temperature.

To model condensation reactions, the diffusivity of the lignin degradation products must also be measured.

2. Continue experimental work on penetration of kraft liquor into pulp chips. Variables that control the rate of penetration need to be better understood. Under what conditions the good penetration assumption is valid also needs to investigated. (Theoretical work on penetration is discussed in the next section).

3. Experimental work to confirm if condensation reactions cause rejects needs doing. It would also be useful to have condensation reaction kinetics to input to the pulping model.

4. Run experiments to confirm optimization results.

8.2.2 Theoretical

1. Modify the existing kraft pulping simulator to incorporate a better equation for the diffusivitiy of alkali (McKean, 1982) and an improved intial delignification equation (Sarkanen, 1982) when the equations are available. Test the model with these modifications.

2. If penetration experiments show that for some cases of interest the good impregnation assumption is invalid, then the model should be modified to include incomplete penetration. This should be done in two parts. First, derive a penetration model that predicts laboratory penetration data. Second, use the penetration model in the pulping model to simulate the poor impregnation case.

3. If the condensation kinetics and lignin diffusion data are available, input them to the model to investigate condensation reactions at the center of thick chips

4. Modify the pulping model to simulate the continuous digester.

REFERENCES

Akhtaruzzaman, A.F.M.; Virkola,N-E. Paperi ja Puu, 1979, 61, 578, 629, 737, 805.

Akhtaruzzaman, A.F.M.; Virkola,N-E. Paperi ja Puu, 1980, 62, 15, 70, 297.

Annergren, G.E.; Backlund, S.O.E.; Wiik, K.I. Svensk Papperstid., 1973, 76, 324.

Aurell, R.; Hartler, N. Svensk Papperstid., 1965, 68,59.

Backlund, E.A. U.S. pat. 3,802,956 (April 9, 1974).

Bailey, R.N.; Maldonado, P.; McKibbins, S.W.; Tarver, M.-G. Tappi 1969, 52, 1272.

Bailey, R.N.; Yawn, Y.P Tappi, 1969, 52, 1696.

Behr, E.A.; Briggs, D.R.; Kaufert, F.H. J. Phys. Chem., 1953, 57, 476.

Borlew, P.B.; Miller, R.L. Tappi, 1970, 53, 2107.

Brauns, F.E.; Grimes, W.S. Paper Trade Journal, 1939, 108, 40.

Burr, H.K.; Stamm, A.J. J. Phys. Chem., 1947 51, 240.

Christensen, G.N. Aus. J. of Appl. Sci., 1951, 2, 430.

Colombo, P.; Corbetta, D.; Pirotta, A.; Ruffini, G. Svensk Papperstid., 1960, 63, 457.

Colombo, P.; Corbetta, D.; Pirotta, A.; Ruffini, G. Svensk Papperstid., 1964, 67, 505.

Daleski, E.J. Tappi, 1965, 48, 325.

Eriksson, O.; Goring, D.A.I.; Lindgren, B.O. Wood Sci. Technol., 1980, 14, 267.

Farkas, J. Papir Celuloza, 1965, 20, 11.

Finlayson, B.A. "Nonlinear Analysis in Chemical Engineering", McGraw Hill: New York, 1980; chapter 5.

Garceau, J.J.; Goel, K.N.; Ayroud, A.M. Tappi, 1974a, 57, 137.

Garceau, J.J.; Goel, K.N.; Ayroud, A.M. Tappi, 1974b, 57, 121.

Gierer, J. Wood Sci. Technol., 1980, 14, 241.

Hartler, N. Paperi ja Puu, 1962, 44, 365.

Hartler, N. Svensk Papperstid., 1978, 81, 457.

Hartler, N.; Onisko, W. Svensk Papperstid., 1962, 65, 905.

Hartler, N.; Ostberg, K. Svensk Papperstid., 1959, 62, 524.

Hatton, J.V. Tappi, 1973, 56, 97.

Hatton, J.V.; Keays, J.L. Pulp Pap. Mag. Can., 1973, 74, 79.

Huang, H.I.; Sarkanen, K.V.; Johanson, L.N. Wood Sci. Technol., 1977 11, 225.

Helberg, B.E.; Neuberger, E.D.; Simmons, W.B. Tappi Alkaline Pulping Conference, Williamsburg Virginia, (1975).

Hindmarsh A.C. "GEAR..Ordinary Differential Equation System Solver", UCID-30001, Rev. 3, Lawrence Livermore Laboratory, December, 1974.

"International Critical Tables", McGraw Hill: New York, 1929; p. 5-66

Johnsson, L. Acta Polytech. Scand. Math. Comput. Mach. Ser., 1971, No. 22, 1.

Kerr, A.J. Appita, 1970, 24, 180.

Kerr, A.J.; Uprichard, J.M. Appita, 1976, 30, 48.

Kleinert, T.N. Tappi, 1966, 49, 53.

Kleppe, P.J. Tappi, 1970, 53, 35.

Lemon, S.; Teder, A. Svensk Papperstid., 1973, 76, 407.

Lightfoot, R.G.; Premont, P. Pulp Pap. Mag. Can., 1962, 63, T141.

Ludden, J. Ph.D. Thesis, University of Washington, 1977.

Luner, P. Pulp Pap. Mag. Can., 1956, 57, 216.

Matthews, C.H. Svensk Papperstid., 1974, 77, 629.

McKean, W.T. Ph.D. Thesis, University of Washington, 1968.

McKean, W.T. Personal Communication, 1982.

McKibbins, S.W. Tappi, 1960, 43, 801.

Nelder, J.A.; Mead, R. Computer J., 1967, 7, 736.

Norden, S.; Teder, A. Tappi, 1979, 62, 49.

Olm, L.; Tistad, G. Svensk Papperstid., 1979, 82, 458.

Pulp and Paper International, 1982, 24, 27.

Reid, R.C.; Prausnitz, J.M.; Sherwood, T.K. " The Properties of Gases and Liquids", McGraw Hill: New York, 1977; p. 630.

Rekunen, S., Jutila, E.; Lahteenmaki, E.; Lonnberg, B.; Virkola, N.-E. Paperi ja Puu, 1980, 62, 80.

Ricker, N.L. Personal Communication, 1981.

Rydholm, S. "Pulping Processes", Wiley: New York, 1965a; p. 584.

Rydholm, S. "Pulping Processes", Wiley: New York, 1965b; p. 603.

Rydholm, S. "Pulping Processes", Wiley: New York, 1965c; p. 603.

Rydholm, S. "Pulping Processes", Wiley: New York, 1965d; p. 586.

Rydholm, S. "Pulping Processes", Wiley: New York, 1965e; p. 334.

Rydholm, S. "Pulping Processes", Wiley: New York, 1965f; p. 90.

Sarkanen, K.V. Personal Communication, 1982.

Sherwood, T.K.; Pigford, R.L.; Wilke, C.R. "Mass Transfer", McGraw Hill: New York, 1975, p. 242.

Smith, C.C., Ph.D. Thesis, Purdue University, 1975.

Stephenson, J. "Pulp and Paper Manufacture, Vol I", McGraw Hill: New York, 1950; p. 450.

Stone, J.E. Pulp Pap. Mag. Can., 1956, 57, 139.

Stone, J.E. Tappi, 1957, 40, 539.

Teder, A.; Tormund, D. Svensk Papperstid., 1973, 76, 607.

Tyler, D.B., M.S. Thesis, University of Idaho, 1981.

Van Krevelen, D.W.; Krekels, J.T.C. Rev. Trav. Chim., 1948, 67, 512.

Vroom, K.E. Pulp Pap. Mag. Can., 1957, 58, 228.

Wahlman, M. Paperi ja Puu, 1967, 49, 107.

Wilder, H.D.; Daleski, E.J. Tappi, 1965, 48, 293.

Yllner,S.; Ostberg, K.; Stockman, L. Svensk Papperstid., 1957, 60, 795.

APPENDIX A

CALCULATION OF BIOT NUMBERS

Estimation of the mass transfer cofficient in an in direct heated batch digester at 180 C.

To calculate the mass transfer coefficient in the packed portion of the digester from Equations 7.1 and 7.2, we need values for d_p, U_{ave}, ρ , μ , and D. A pulp chip has a surface area of about 12.9 cm^2 therefore the diameter of a sphere of the same surface, d_p, is $(12.9/\pi)^{1/2}$ or 2.03 cm. The superficial velocity, U_{ave}, is calculated with equation A-1

$$U_{ave} = V/(A \times \varepsilon) \qquad (A-1)$$

where

A is the digester cross-sectional area

ε is the digester void fraction

V is the volumetric flow rate of the liquor

For a typical digester 3.81 m in diameter, with a flow rate of 126 l/sec, and a void fraction of 0.69 (Rydholm, 1965e);

$$U_{ave} = 126{,}000/(\pi \times (381/2)^2 \times 0.69) = 1.6 \text{ cm/sec}$$

The density and viscosity of the liquor is assumed to be equal to that of water. The viscosity is calculated with the equation in Reid et al. (1977) to be 0.001343 p, and the density taken from the steam tables is 0.89 g/cm^3. Equation 7.1 yields

$$j_d = 1.17(2.03 \times 1.6 \times 0.89/0.001343)^{-0.415} = 0.048$$

To calculate k from equation 7.2 the, Schmidt number is needed. To calculate Sc, the diffusivity of alkali in water at 180 C is needed. With data from the International Critical Tables (1929), equation A-2 is derived for the temperature dependence of the diffusivity of alkali in water.

$$\ln(D) = -2468/T - 2.76 \qquad \text{(A-2)}$$

where

D is the diffusivity [=] (cm^2/sec)

T is the temperature [=] (K)

At 180 C, D is calculated to be 2.729×10^{-4} cm^2/sec, and the Schmidt number is,

$$Sc = 0.001343/(0.89 \times 2.729 \times 10^{-4}) = 5.5$$

Using Equation 7.2;

$$k = 0.048 \times 1.6 \times 5.53^{-2/3} = 0.025 \text{ cm/sec.}$$

The Biot number is,

$$Bw = k\ CT/D_c \qquad \text{(A-3)}$$

where

CT is one-half the chip-thickness

D_c is the diffusivity in the chip phase.

From McKibbins's (1960) equation for the diffusivity of alkali in the chip phase, the Biot number in a 3 mm thick chip is,

$$Bw = 0.025 \times 0.15/5.376 \times 10^{-5} = 69.75.$$

For the trickle bed portion, Equation 7.3 is used to calculate k. To calculate the Reynolds number for equation 7.3 the surface to volume ratio of the digester, a, is calculated with equation (A-4).

$$a = (1 - \varepsilon)/CT \qquad \text{(A-4)}$$

For an ε of 0.69, and CT of 0.15 cm, a is equal to 2.07 cm^{-1} and the Reynolds number is,

$$Re = 1.6 \times 0.89/(2.07 \times 0.001343) = 512.33$$

The Sherwood number calculated from equation 7.3 is,

$$Sh = 1.8 \times 512.33^{1/2} \times 5.53^{1/3} = 72.04$$

and k is,

$$k = Sh \times a \times D = 72.04 \times 2.07 \times 2.729 \times 10^{-4} = 0.041 \text{ cm/sec}$$

The Biot number, calculated as before, is,

$$Bw = 0.041 \times 0.15/5.376 \times 10^{-5} = 114.4$$

```
POSITION =       0.500   Z

CONCENTRATIONS
  0.2204596E+00  0.3000477E+00  0.3766595E+00  0.4224719E+00  0.4334596E+00  COP(1,1) COP(2,1) COP(3,1) COP(4,1) COP(5,1)
  0.9309430E+01  0.4866917E+01  0.2400202E+01  0.2073480E+01  0.2068980E+01  COP(1,2)    .        .        .
  0.5027101E+02  0.4773146E+02  0.4569143E+02  0.4452520E+02  0.4443719E+02  COP(1,3)    .        .        .      COP(5,3)

REACTION RATES AND EFFECTIVENESS FACTORS

  0.7736E+00  1.0000  0.1640E+01  1.0000  0.3074E+00  1.0000  RA(1,1) ETA(1,1)  RA(1,2) ETA(1,2)  RA(1,3) ETA(1,3)
  0.4911E+00  1.0000  0.1041E+01  1.0000  0.1951E+00  1.0000  RA(2,1) ETA(2,1)     .        .        .
  0.5205E+00  1.0000  0.1175E+00  1.0000  0.1027E+00  1.0000  RA(3,1) ETA(3,1)     .        .
  0.4877E+00  1.0000  0.1101E+00  1.0000  0.9620E-01  1.0000  RA(4,1) ETA(4,1)     .     RA(4,3) ETA(4,3)

AVERAGE CONCENTRATIONS
  0.3006123E+00  0.5719551E+01  0.4787428E+02  CAOP(1) CAOP(2) CAOP(3)

REJECTS (%)=       12.86202

YIELD=       53.59383 SCREENED YIELD=       40.73182 KAPPA=       71.14723

CENTER CONCENTRATIONS
  0.2065362E+00  0.1044526E+02  0.5081023E+02  CCOP(1) CCOP(2) CCOP(3)

WALL FLUX (POSITIVE OUT)
 -0.2307825E+00  0.0000000E+00  0.0000000E+00

AL=  1.77898  2.17843  2.40391  2.44841  2.45343  AL(1,1)     .        .        .      AL(5,1)

[OH] BULK = 0.4334871

TEMP= 443.15

LAST STEP SIZE USED =  0.340E-02 FOR    2 -TH  ORDER METHOD  HUSED     NQUSED
NUMBER OF STEPS =          70                               NSTEP
NUMBER OF FUNCTION EVALUATIONS =         373                NFE
NUMBER OF JACOBIAN EVALUATIONS =          18                NJE
```

The following is a description of the variables noted on the sample output shown on the previous page.

Variable	Description
Z	Dimensionless cooking time
COP(I,1)	Alkali concentration at the I-th collocation point
COP(I,2)	Lignin concentration at the I-th collocation point
COP(I,3)	Carbohydrate concentration at the I-th collocation point
RA(I,1)	Alkali reaction rate at the I-th collocation point
RA(I,2)	Lignin reaction rate at the I-th collocation point
RA(I,3)	Carbohydrate reaction rate at the I-th collocation point
ETA(I,J)	All the effectiveness factors are set at 1.0
CAOP(1)	Average alkali concentration in the chip
CAOP(2)	Average lignin concentration
CAOP(3)	Average carbohydrate concentration
CCOP(1)	Center alkali concentration
CCOP(2)	Center lignin concentration
CCOP(3)	Center carbohydrate concentration
AL(I,1)	Dimensionless diffusivity of the alkali at the I-th collocation point

HUSED, NQUSED, NSTEP, NFE, and NJE, are variables from GEARB